upna
Universidad Pública de Navarra
Nafarroako Unibertsitate Publikoa

Universidad Pública de Navarra

Departamento de Ingeniería Eléctrica, Electrónica y de Comunicación

MATERIALS FOR THE FABRICATION OF OPTICAL FIBER REFRACTOMETERS BASED ON LOSSY MODE RESONANCE

PhD dissertation by

Aritz Ozcariz Celaya

Advisors:

Dr. Carlos Ruiz Zamarreño

Prof. Francisco Javier Arregui San Martín

Pamplona, May 2020

upna
Universidad Pública de Navarra
Nafarroako Unibertsitate Publikoa

A mi familia
y amigos

upna
Universidad Pública de Navarra
Nafarroako Unibertsitate Publikoa

ACKNOWLEDGEMENTS

Several institutions have made possible the realization of this PhD thesis. I would like to thank the Spanish Ministry of Universities (FPU15/05663 grant), as well as the Ministry of Economy, Industry and Competitiveness (TEC2016-78047-R) and the Government of Navarra (Bioptsens Avanza) for their financial support.

A special thanks to the Public University of Navarra (UPNA), where most of the work presented here was done, and the research group of Dr. Cicero Martelli at the Federal University of Technology, Paraná (UTFPR) in Curitiba, Brazil, where a research stay was made.

upna
Universidad Pública de Navarra
Nafarroako Unibertsitate Publikoa

AGRADECIMIENTOS

Ahora que ha llegado el momento de finalizar una etapa tan importante es un buen momento para agradecer a todas aquellas personas que me han permitido llegar hasta aquí. Son muchas las personas que han colaborado de una manera o de otra para que esta tesis sea una realidad.

En primer lugar, me gustaría agradecer por apoyarme siempre a toda mi familia, incluyendo tíos, primos y abuelos, que considero tan amplia que no puedo nombrar a todos. Muy especialmente a mi hermana Nerea y a mis padres, Raquel y José Luis, que me proporcionaron una buena educación para llegar hasta aquí. También debo agradecer a Iñaki su inestimable apoyo, sin el cual muy probablemente no podría haber acabado esta tesis.

También debo agradecer la inestimable ayuda de mis directores de tesis, Carlos Ruiz y Patxi Arregui, que han sacado tiempo de donde parecía imposible para resolver cualquier duda y proporcionar orientación. También debo reconocer la ayuda de todo el grupo de Sensores, tanto de profesores como compañeros investigadores, que siempre han estado ahí para ayudar en cualquier tarea y con quienes he compartido muy buenos momentos. Reconocimiento que me gustaría extender a otros compañeros de otros grupos que también he conocido en estos cuatro años.

Finalmente me gustaría agradecer a Cícero Martelli y a Jean C. C. da Silva por haberme acogido en su grupo en la Universidade Tecnológica Federal do Paraná (UTFPR), así como a todos los integrantes del mismo, que me proporcionaron incalculables lecciones y me hicieron sentir como en casa.

Muchas gracias a todos.

upna
Universidad Pública de Navarra
Nafarroako Unibertsitate Publikoa

ABSTRACT

Lossy mode resonances (LMR) have been studied as an exceptional phenomenon for the development of optical fiber refractometers. These sensors rely on the interaction of the light propagating through the waveguide with a thin-film fabricated onto it. The properties of such film will determine the sensitivity of the LMR to surrounding refractive index variations. The nature of the film will also play an important role on the possibilities to develop sensing applications.

This thesis analyzes the use of four different materials (tin oxide, aluminum-doped zinc oxide, indium-gallium-zinc oxide and copper oxide) for the development of LMR-based refractometers. First, the optimization on the fabrication process of tin oxide coatings is described, with the purpose of maximizing the sensitivity in a refractive index range close of the fused silica (1.44). Then, materials based on zinc oxide are presented for the first time for the fabrication of LMR-based sensors: aluminum-doped zinc oxide (AZO) and indium-gallium-zinc oxide (IGZO), leading to the development of several sensors working in the visible and near-infrared wavelength range. The last material analyzed in this work is copper oxide, which presents a refractive index considerably larger than the previously studied materials. Such feature is suggested to provide a greater sensitivity of the LMR to SRI variations, promising a better performance than the one achieved with different thin-films.

upna
Universidad Pública de Navarra
Nafarroako Unibertsitate Publikoa

TABLE OF CONTENTS

Chapter 1

Introduction

1.1. Motivation and Objectives

Lossy mode resonances (LMR) have been studied as the basis for the fabrication of refractometers on optical fibers for several years now. This technique has allowed to develop sensors in a number of fields such as, industry [1–3] of biomedicine [4–6].

The use of LMR for the fabrication of sensors relies on the propagation of light through a waveguide coated with certain thin-films. The interaction of light in the waveguide-coating interface causes the generation of a resonance (LMR). In order to be able to support LMR generation, a thin-film must have a permittivity such that its real part is positive and greater (in magnitude) than its imaginary part, and also greater than the real part of the permittivity of the medium surrounding the film [7]. If those conditions are matched, analyzing the spectrum of the transmitted light, one or several peaks of absorbance will be observed at certain wavelengths, corresponding to LMRs. The wavelength at which a LMR is observed depends on the optical properties of the film, its thickness, and the refractive index of the media surrounding the waveguide. For instance, provided the film properties and thickness are stable, the wavelength of the LMR will depend on the surrounding media refractive index (SRI), making possible to establish a direct relationship between central wavelength of the LMR and SRI, which can be used as the basis for the development of refractometers.

Optical fibers are an ideal medium for the fabrication of these kind of sensors. Several configurations based on multimode [8–11], single mode [12] or side-polished (D-shaped) [4,6,13,14] fibers, for instance, have been successfully employed in the design of LMR-based sensors. One of the key elements that are responsible for the results provided by the sensor, is the film fabricated on the waveguide to support the LMR. The nature and the optical properties of such coating will determine the response of the resonances [15].

A review of the published literature revealed that several materials have been considered for this purpose. However, it was also suggested that the study of some materials (such as tin oxide) could still need an optimization to maximize their performance, and also other coatings (like aluminum-doped zinc oxide, for instance) were only theoretically proposed, lacking some experimental research. It was also observed that there were some materials, not previously studied in this field, which possess distinctive optical properties that could maximize the sensitivity of the LMR-based sensors.

Following such consideration, the aim of this thesis is to study new coating materials for the development of LMR-based sensors with the objective to optimize their performance and widen their possibilities of fabrication. For that purpose, this thesis will:

- Identify materials potentially capable to support LMRs with a high sensitivity and the fabrication techniques that could be applied.

- Study the fabrication process of the chosen coating materials, determine the optimal fabrication parameters, and analyze the optical properties of the films fabricated on the laboratory.

- Apply the coatings on an optical fiber setup and corroborate their capacity to support LMRs.

- Analyze the behavior of such LMRs and characterize their response to SRI variations. This information will allow to evaluate the performance of the coatings in the optimization of LMR-based sensors.

1.2. Organization

This thesis has been organized in chapters as follows. First of all, Chapter 2 presents the state of the art on the fabrication of coatings for LMR-based optical fiber refractometers. This chapter introduces the basic concepts related to LMR, different possible configurations for the design of the sensors, and a brief description of techniques for thin-films fabrication. Then, the chapter details the different coating materials employed by several authors to develop LMR-based sensors and the results they achieved.

The next chapters describe the experimental work performed for this thesis, testing several coating materials for the development of LMR-based sensors. Chapter 3 describes the experimental optimization of tin oxide thin-films aiming to achieve a maximum sensitivity in the SRI range close to the refractive index of fused silica (1.44). This work is performed on a D-shaped fiber setup making use of polarized light in order to get very narrow and sensitive resonances to enhance the performance of the sensor.

The following chapters introduce materials that had not been previously used for the purpose of LMR generation. In chapter 4 it is presented the first experimental use of aluminum-doped zinc oxide (AZO) thin-films for this purpose. It describes the study of the fabrication process and the analysis of the film characteristics prior to its use on optical fibers. Then, cladding-removed multimode optical fibers (CRMOF) are used as basis for the fabrication of refractometers. Finally, the fabricated devices are characterized and the performance of several LMRs of different order is compared. This chapter also presents a color-based device that makes use of the color change in the propagated light due to the resonance shift induced by the SRI variation.

The use of a different zinc oxide based material, indium-gallium-zinc oxide (IGZO) is presented in chapter 5. Like in the previous case, the fabrication process and the optical properties of the IGZO film are studied as a first step. The analysis continues with the fabrication and characterization of devices based on a CRMOF configuration. Next, IGZO thin-films are applied on D-shaped fibers with the purpose of optimize the performance demonstrated on the multimode fibers. Here, the impact of the polishing degree (the distance of the polished surface to the fiber core) is analyzed by depositing IGZO coatings on D-shaped fibers with different polishing depths.

The last material analyzed in this thesis is copper oxide on Chapter 6. Copper oxide presents a refractive index comparatively larger than the rest of the coating materials tested previously, which is expected to generate more sensitive LMRs. This chapter analyzes the optical properties of the copper oxide thin-films fabricated on the lab and presents the use of this material for the development of LMR-based refractometers for the first time. The deposition of copper oxide thin-films on CRMOF and D-shaped fiber configuration is described in this chapter and their performance as refractometer devices is compared with the results yielded by other materials.

Finally, Chapter 7 makes a comparison between the different materials presented here, taken into consideration the effect of the wavelength and SRI range present for the sensitivity of the LMRs, as well as the order of the resonances.

Chapter 8 summarizes the principal results introduced in this thesis, presenting the main conclusions that can be extracted from this study.

Bibliography

1. Sanchez, P.; Zamarreno, C. R.; Arregui, F. J.; Matias, I. R. LMR-Based Optical Fiber Refractometers for Oil Degradation Sensing Applications in Synthetic Lubricant Oils. *J. Light. Technol.* **2016**, *34*, 4537–4542, doi:10.1109/JLT.2016.2562701.

2. Usha, S. P.; Mishra, S. K.; Gupta, B. D. Zinc oxide thin film/nanorods based lossy mode resonance hydrogen sulphide gas sensor. *Mater. Res. Express* **2015**, *2*, 095003, doi:10.1088/2053-1591.

3. Tiwari, D.; Mullaney, K.; Korposh, S.; James, S. W.; Lee, S.-W.; Tatam, R. P. An ammonia sensor based on Lossy Mode Resonances on a tapered optical fibre coated with porphyrin-incorporated titanium dioxide. *Sensors Actuators B Chem.* **2017**, *242*, 645–652, doi:10.1016/j.snb.2016.11.092.

4. Chiavaioli, F.; Zubiate, P.; Del Villar, I.; Zamarreño, C. R.; Giannetti, A.; Tombelli, S.; Trono, C.; Arregui, F. J.; Matias, I. R.; Baldini, F. Femtomolar Detection by Nanocoated Fiber Label-Free Biosensors. *ACS Sensors* **2018**, *3*, 936–943, doi:10.1021/acssensors.7b00918.

5. Zubiate, P.; Urrutia, A.; Zamarreño, C. R.; Egea-Urra, J.; Fernández-Irigoyen, J.; Giannetti, A.; Baldini, F.; Díaz, S.; Matias, I. R.; Arregui, F. J.; Santamaría, E.; Chiavaioli, F.; Del Villar, I. Fiber-based early diagnosis of venous thromboembolic disease by label-free D-dimer detection. *Biosens. Bioelectron. X* **2019**, *2*, 100026, doi:10.1016/j.biosx.2019.100026.

6. Zubiate, P.; Zamarreño, C. R.; Sánchez, P.; Matias, I. R.; Arregui, F. J. High sensitive and selective C-reactive protein detection by means of lossy mode resonance based optical fiber devices. *Biosens. Bioelectron.* **2017**, *93*, 176–181, doi:10.1016/j.bios.2016.09.020.

7. Del Villar, I.; Arregui, F. J.; Zamarreño, C. R.; Corres, J. M.;

Bariain, C.; Goicoechea, J.; Elosua, C.; Hernaez, M.; Rivero, P. J.; Socorro, A. B.; Urrutia, A.; Sanchez, P.; Zubiate, P.; Lopez, D.; De Acha, N.; Ascorbe, J.; Matias, I. R. *Optical sensors based on lossy-mode resonances*; Elsevier B.V., 2017; Vol. 240, pp. 174–185;.

8. Hernaez, M.; Mayes, A.; Melendi-Espina, S. Graphene Oxide in Lossy Mode Resonance-Based Optical Fiber Sensors for Ethanol Detection. *Sensors* **2017**, *18*, 58, doi:10.3390/s18010058.

9. Sanchez, P.; Zamarreño, C. R.; Hernaez, M.; Del Villar, I.; Fernandez-Valdivielso, C.; Matias, I. R.; Arregui, F. J. Lossy mode resonances toward the fabrication of optical fiber humidity sensors. *Meas. Sci. Technol.* **2012**, *23*, 014002, doi:10.1088/0957-0233/23/1/014002.

10. Kosiel, K.; Koba, M.; Masiewicz, M.; Śmietana, M. Tailoring properties of lossy-mode resonance optical fiber sensors with atomic layer deposition technique. *Opt. Laser Technol.* **2018**, *102*, 213–221, doi:10.1016/j.optlastec.2018.01.002.

11. Usha, S. P.; Gupta, B. D. Performance analysis of zinc oxide-implemented lossy mode resonance-based optical fiber refractive index sensor utilizing thin film/nanostructure. *Appl. Opt.* **2017**, *56*, 5716, doi:10.1364/AO.56.005716.

12. Ascorbe, J.; Corres, J. M.; Matias, I. R.; Arregui, F. . High sensitivity humidity sensor based on cladding-etched optical fiber and lossy mode resonances. *Sensors Actuators B Chem.* **2016**, *233*, 7–16, doi:10.1016/j.snb.2016.04.045.

13. Zubiate, P.; Zamarreño, C. R.; Villar, I. Del; Matias, I. R.; Arregui, F. J. J.; Del Villar, I.; Matias, I. R.; Arregui, F. J. J. High sensitive refractometers based on lossy mode resonances (LMRs) supported by ITO coated D-shaped optical fibers. *Opt. Express* **2015**, *23*.

14. Del Villar, I.; Zubiate, P.; Zamarreño, C. R.; Arregui, F. J.; Matias, I. R. Optimization in nanocoated D-shaped optical fiber sensors. *Opt. Express* **2017**, *25*, 10743,

doi:10.1364/OE.25.010743.

15. Del Villar, I.; Hernaez, M.; Zamarreño, C. R.; Sánchez, P.; Fernández-Valdivielso, C.; Arregui, F. J.; Matias, I. R. Design rules for lossy mode resonance based sensors. *Appl. Opt.* **2012**, *51*, 4298, doi:10.1364/AO.51.004298.

Chapter 2

Materials for the fabrication of optical fiber refractometers based on Lossy Mode Resonances: State of the art

Lossy mode resonances based sensors have been extensively studied in the last years. The versatility of this phenomenon has led to the development of sensors based on different configurations that make use of a wide number of materials. The coating material is one of the key elements in the performance of the refractometer. This chapter provides the state of the art of the LMR-based optical fiber sensors focusing on the relevance of the coatings materials. It also intends to provide an overview of the different setups and coating procedures that can be employed for the development of such sensors.

The contents of this chapter have been partially published under the title "*A Comprehensive Review: Materials for the Fabrication of Optical Fiber Refractometers Based on Lossy Mode Resonance*" in Sensors vol. 20 (7), 1972 (2020).

2.1. Introduction

Sensors have acquired an unprecedented presence in the modern society. In industry, medicine and even at our own homes, we are increasingly relying on a number of sensors to get a safer environment and a healthier and more comfortable life [1–4]. As this field evolves, new mechanisms and configurations are researched, which facilitate the development of better sensors and new applications.

The versatility and practicality of optical fibers make them a great base for the fabrication of sensors. In fact, there is a wide range of mechanisms that allow the fabrication of optical fiber sensors. Amongst all of them, this chapter will discuss about one that has already been proved to be capable of achieving astonishing sensitivities, the lossy modes resonances (LMR). LMRs occur due to the interaction of the light propagating through a waveguide coated with a film of appropriate optical properties [5]. If the conditions match, the waveguide modes are coupled to the coating modes generating lossy modes. This effect causes an absorption peak at the wavelength at which the conditions are fulfilled. These resonances should not be confused with the Surface Plasmon Resonances (SPR), which can also be observed in waveguides with certain coatings, since they are two separate phenomena. SPRs are generated on a metal/dielectric interface which is typically obtained with conductive thin films, such as gold [6], whereas the LMR conditions enable the use of a larger range of materials [7]. LMRs can be supported by the fabrication of films made of different materials such as ITO [8], zinc oxide [9], polymers [10] or silicon nitride [11], only to mention a few of them

Lossy mode resonances are sensitive to a variation in the properties of the LMR supporting film, or the optical properties (refractive index) of the surrounding media, meaning that they are essentially, a good mechanism for the development of refractometers. This mechanism can be used as the basis for the design of multiple kind of physical and chemical sensors. An external coating whose optical

properties rely on a given parameter that is desired to measure, could be fabricated on top of a LMR based refractometer, and the variation of such variable could be measured by monitoring the LMR wavelength shift. It should be noted that the development of such sensors does not rely solely on the fabrication of a functionalizing overlay. Given the number of materials capable to support LMR, the right choice for the composition of this coating can facilitate the fabrication of many different kind of sensors. For instance, an ITO (indium tin oxide) nanoparticles coating was used for the fabrication of a hydrogen gas sensor [8], while zinc oxide nanorods were used in the fabrication of a coating whose LMR is sensitive to sulfide gas (H_2S) [12]. On a different note, polymeric coatings of PAH/PAA (polyallylamine hydrochloride and polyacrylic acid) were used to fabricate LMR based pH [13] and relative humidity [10] sensors.

This review chapter presents a state of the art of the different coating possibilities available for the design and fabrication of lossy mode resonances based sensors. The basic concepts of LMR are explained, as well as different setup configurations that have been developed. Finally, the wide range of reported coating materials for the development of LMR sensors are explained in detail and the results obtained are discussed.

2.2. Basic concepts

Optical fibers are typically composed of a cylindrical core surrounded by a layer known as cladding. The lower refractive index of the cladding with respect to the core and the physical properties of both core and cladding allow the light to propagate trough the fiber with a really low attenuation and practically insensitive to the external conditions out of the fiber, making it the ideal mechanism for long distance transmission of optical signals. If the cladding (or a part of it) is removed in a segment of the fiber, and substituted by a different material, the propagation of the light might be affected. Depending on the optical properties of the applied coating, different resonances might be excited.

One of the most known resonances generated this way is the surface plasmon resonance (SPR), which occurs when the coating permittivity real part is negative and greater in magnitude than both its imaginary part and the real part of the external medium permittivity [5]. A conductor, such as gold, is the typical material used for the fabrication of SPR supporting thin films. Another type of resonance that can be generated with materials of different optical properties is the lossy mode resonance (LMR). In order to obtain a LMR, the coating must have a positive permittivity real part, which must also be greater in magnitude than both its imaginary part and the real part of the external medium permittivity. In terms of refractive index, this means that the chosen coating must have a relatively high real part (n), and a comparatively low (but non zero) imaginary part, k (see fig. 2.1). Such characteristics are shared by several materials such as metal oxides, compounds or polymers, which widens the possibilities for potential sensing applications. Another important difference is the fact that SPR requires the use of polarized light, as it is only observed on TM (transverse magnetic) mode of propagation, while LMR occurs in both TM and TE (transverse electric) modes, and no polarization is needed. There is also a difference in the angle of incidence of light that excites these resonances. SPR is typically seen on angles between 40º and 70º, while LMR is seen on angles close to 90º. That behavior must be taken into account for the design of the appropriate setup for exciting each resonance. One more typical characteristic of LMRs is the fact that a growth in the thickness of the resonance supporting coating may induce the generation of more LMRs of higher orders. It is possible to observe several LMRs simultaneously at different wavelengths.

LMR and SPR generation conditions

TYPE OF RESONANCE	$\hat{\varepsilon}$ CONDITIONS	n,k CONDITIONS $\forall\, n>0, k>0$
SPR Surface Plasmon Resonance	$\varepsilon_2' < 0$ $\lvert\varepsilon_2'\rvert > \lvert\varepsilon_2''\rvert$ $\lvert\varepsilon_2'\rvert > \lvert\varepsilon_3'\rvert$	$k_2 > (\sqrt{2}+1)n_2$ $k_2^2 - n_2^2 > 1.45^2$
LMR Lossy Mode Resonance	$\varepsilon_2' > 0$ $\lvert\varepsilon_2'\rvert > \lvert\varepsilon_2''\rvert$ $\lvert\varepsilon_2'\rvert > \lvert\varepsilon_3'\rvert$	$k_2 < (\sqrt{2}-1)n_2$ $n_2^2 - k_2^2 > 1.45^2$

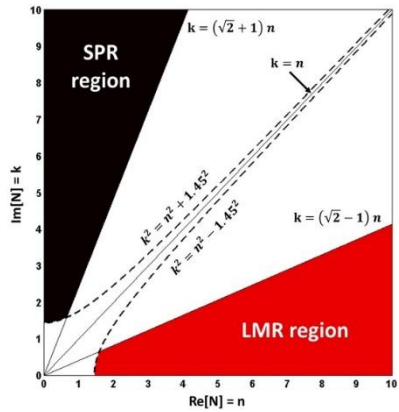

Figure 2.1: *Optical parameters for the generation of surface plasmon resonances and lossy mode resonances. Reprinted from* [5] *with permission from Elsevier.*

As mentioned above, the excitation of these resonances requires the incidence of light at certain angle. This can be done in setups involving a prism to couple and reflect the light at a variable angle of incidence (Kretschmann configuration), but optical fibers also permit the light to reflect at the appropriate angles to generate and observe the resonances. The most common configurations will be explained in detail in the next section. When a LMR is generated in an optical fiber, this phenomenon can be observed as an absorption peak at a given wavelength in the transmission spectra. The location of this resonance in the spectra depends on the optical properties (refractive index) of the LMR supporting film, its thickness, and the surrounding refractive index (SRI) [5]. Therefore, a variation in the SRI or in the film (either its thickness or its refractive index) will induce a shift in the wavelength of the LMR that can be measured, and is the basis for the fabrication of a number of sensors.

Fig. 2.2 shows an example of the spectra of a LMR sensor measuring different SRI values. The peak of the LMR shifts to longer wavelengths as the SRI increases. Hence, the LMR wavelength peak or LMR resonance wavelength can be tracked, establishing a direct

relation between the LMR position and the SRI value. Here, it is important to note that the sensitivity to SRI (measured as the wavelength shift in nanometers per refractive index unit) is not a constant, since it increases for higher SRI values [7]. Besides, it can be observed that an increase in the coating thickness causes a shift on the LMRs to longer wavelength, which also causes an increase in sensitivity. It should also be noted that, as the thickness increases, more LMRs of higher order appear at shorter wavelengths, and these new resonances are consecutively less sensitive than the previous one. Another factor to consider regarding the sensitivity of the LMR is the refractive index of the coating. A coating with higher refractive index will generate a more sensitive resonance. It can be easily inferred that the appropriate choice of this material will have a direct impact on the performance of the sensor.

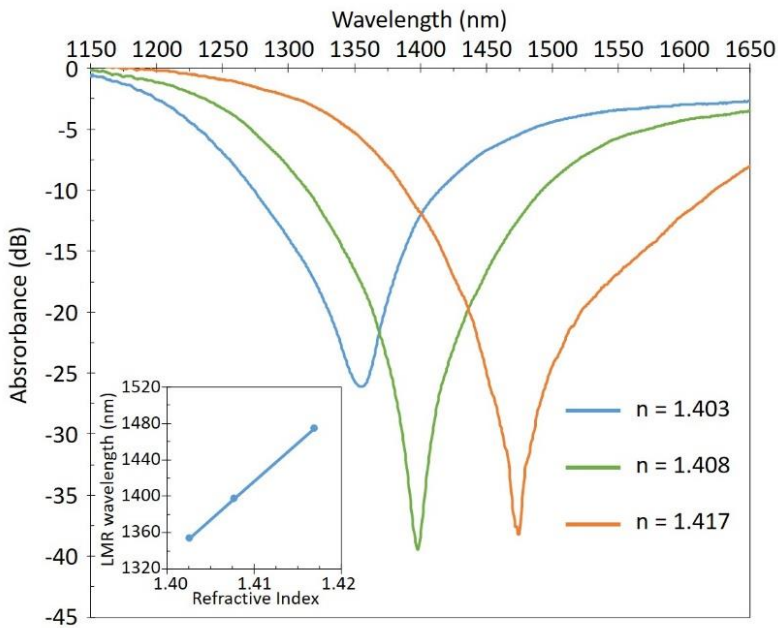

Figure 2.2: *Example of the evolution of a LMR for different SRI values. The peak of the LMR shifts to longer wavelength as the SRI increases.*

It is possible to observe LMRs in a number of configurations, as explained previously. The next section will explain in more detail the different setup possibilities for designing LMR-based sensors and their main characteristics.

2.2.1 Setup configurations

A relevant aspect to take into consideration is the architecture or setup designed for the sensor. It is important to remark that LMR, unlike SPR, occurs in both transverse electric (TE) and transverse magnetic (TM) modes. This way, the study of SPR requires the use of polarized light so that only the TM mode is propagated, which allows to observe the full amplitude of the resonance. On the contrary, LMR can occur simultaneously in both modes of propagation, and provides a greater flexibility in the experimental setups, as no polarization of light is needed in principle. Therefore, a basic probe configuration for LMR sensor fabrication consists of a segment of cladding removed multimode optical fiber (CRMOF), on top of which a high refractive index thin film is deposited [7]. The coated CRMOF is then connected on one end to a broadband light source and on the other end to an optical spectrum analyzer (OSA) or a spectrometer, in order to study the transmitted spectra (see fig. 2.3).

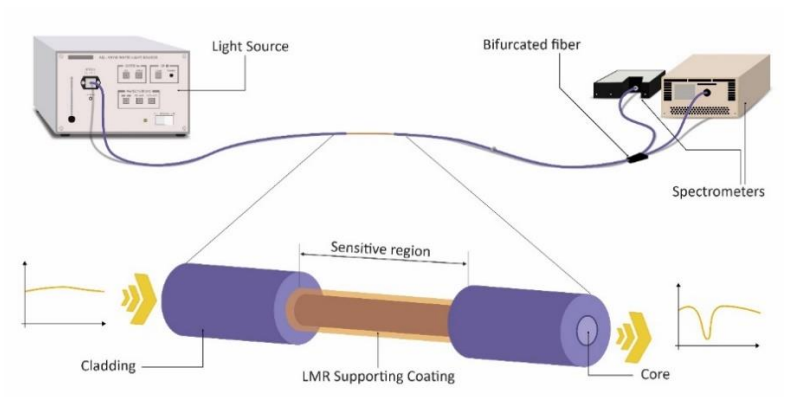

Figure 2.3: *Typical setup involving a CRMOF for the fabrication of a LMR based refractometer. In this case, a bifurcated fiber was included to observe a broader VIS-NIR spectrum using two refractometers.*

A similar approach using single mode fiber (SMF) would require applying an etching process to the fiber in order to reduce the diameter of the cladding so that the evanescent mode in the fiber could reach the later deposited LMR supporting coating. This process is necessary in standard SMF because the small diameter of the core in such fibers makes very difficult the complete removal of the cladding. In contrast, there are commercially available multimode fibers (MMF) with a large core diameter and an easily removable cladding that do not require the etching process.

It was mentioned earlier that LMR is generated in both TE and TM propagation modes and a setup with radial symmetry as the one described above does not allow to separate the contribution of each mode. However, it may be of interest to observe these polarizations separately, as it can maximize the performance (in terms of sensitivity) of the device. A more complex setup, with the purpose of separating the propagation modes, involves the use of polarized light and a D-shaped fiber. This kind of fiber presents a segment where a polishing process has been performed. This procedure modifies the geometry of the fiber, whose section acquires a capital 'D' shape (hence its name). This asymmetric configuration, in combination with the use of polarized light, permits the effective separation of LMRs generated at different polarization modes. As an example, fig. 2.4 presents the simulation of two propagation modes in an ITO coated D-shaped fiber [14]. In fig. 2.4, the cladding mode $TE_{1,1}$ is confined in the cladding at a wavelength of 1690 nm and it is transformed into a TE mode on the ITO layer as the wavelength decreases. Fig. 2.4 also shows how the $HE_{1,1}$ is confined in the core for all the simulated wavelength, with an exception at 1420 nm, where it can be observed how part of the energy couples to the ITO coating due to the LMR.

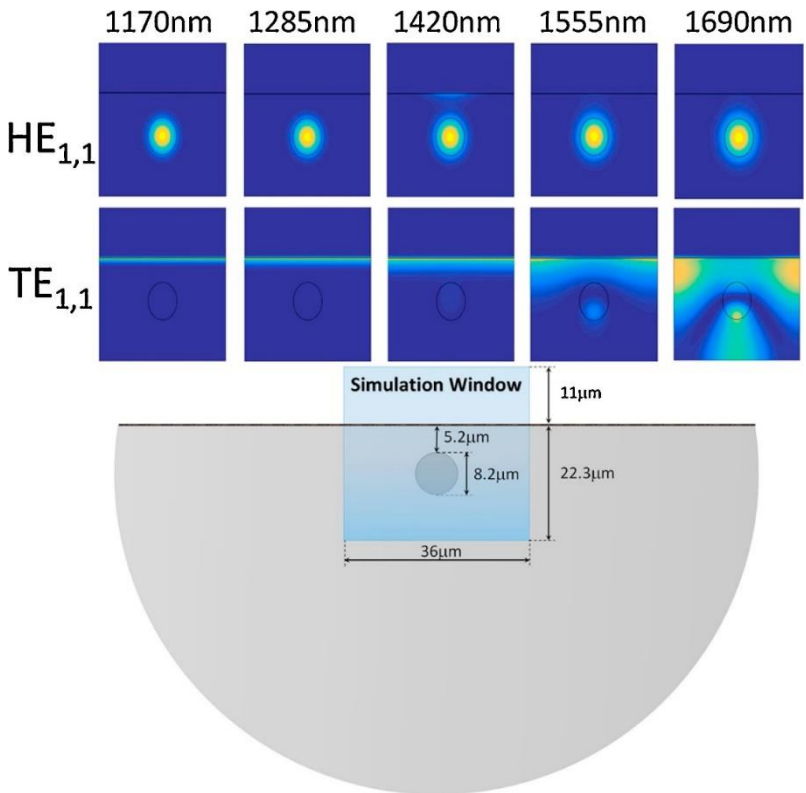

Figure 2.4: *Schematic and simulation results of the electric field intensity in a ITO coated D-shaped fiber for the $TE_{1,1}$ and $HE_{1,1}$ modes. Reproduced from* [14] *with permission from Elsevier.*

Another setup to consider, since it is the standard for SPR based systems, is the Kretschmann configuration (fig. 2.5). This design involves the use of polarized light directed to a coated prism at different incident angles, monitoring the reflectance power at the corresponding angle. In this case, the resonance will typically be observed as a dip at a given angle, and the SRI variations will be measured as a shift in the angle at which said dip is measured. Alternatively, a broadband light source can be used in the same setup in order to monitor the spectra, like in the setups explained previously.

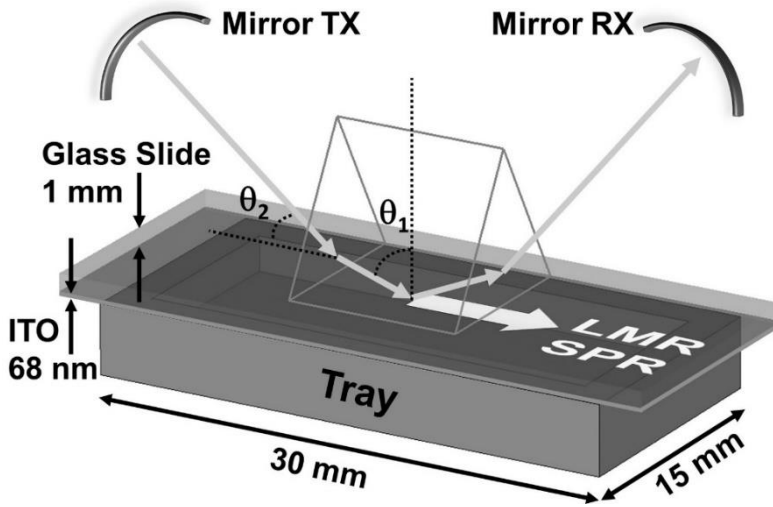

Figure 2.5: *Example of a Kretschmann configuration for the analysis of SPRs and LMRs. In this case, the polarized light coming from Mirror TX is coupled through a prism to a coated glass slide, so the light beam is reflected in the interface at the desired angle θ_1. The coated side is facing a sample tray containing the media whose refractive index is being measured. The reflected beam is collected by Mirror RX. Reprinted from* [15] *with permission from AIP Publishing.*

In contrast to SPR, for which there are only a few coating materials considered appropriate for the resonance generation (being gold the standard), several materials have been successfully studied for LMR generation. Given the optical parameters required for a coating material to be able to support LMR generation, most of the research has been focused on metal oxides such as SnO_2, TiO_2 or ZnO, for example, but also other materials such as graphene oxide or polymer based films have been tested as will be described in section 2.4. The choice of the coating material will directly affect the performance and the validity of the sensor for the target application. Accordingly, a thorough study of the different materials used for this purpose is presented, indicating the main characteristics of each coating and some of the most relevant sensors developed with them.

2.3. Deposition techniques

Before discussing the different choices for coating materials, it is important to consider the available methods for thin-film fabrication on optical fibers [16,17]. The properties of the coating determine the behavior and performance of the LMRs, and such properties will be directly conditioned by the fabrication process. Several thin-film deposition techniques are widely used in industry and research fields, but not all of them are suitable for the fabrication of LMR-based sensors on optical fibers. The application of these procedures on optical fibers implies some limitations in the process. For instance, since optical fiber does not handle well the high temperatures (it becomes quite fragile), some methods that require (or cause) a high substrate temperature should be avoided. Other limitations are imposed by the composition of the coating materials, since not every method is available for the fabrication of all kind of coatings. The opposite case can also occur, and one could find a number of different technologies for the fabrication of a thin-film of a given material. This situation should be thoroughly assessed because maybe not all of them provide an optimal result, as different deposition methods may produce differences in crystalline structure, porosity, purity, strength, etc., which directly affect its optical properties. Factors such as cost, equipment, deposition time, and thickness control, amongst others, must be taken into consideration. The possibility of monitoring the transmission optical spectra during the deposition process is also of great interest in the fabrication of LMR-based sensors. There have been a number of deposition techniques reported for this purpose, and the most relevant methods for the fabrication of thin-films are described in this section.

2.3.1. Dip Coating Techniques

In this section several methods are presented that involve the dipping of the substrate (optical fiber, in this case) in one or more liquid solutions, in order to fabricate a coating onto them. In comparison with other techniques described below, the dip-coating

methods usually require less and not so complex equipment, making them potentially more economical. There is a number of mechanisms that are capable to deposit a coating on a substrate based on such premise. In the fabrication of LMR-based sensors, the coatings fabricated this way are most recurrently based on two techniques: sol-gel process and Layer-by-Layer method.

2.3.1.1. Sol-Gel Method

The sol-gel method has been used, for instance, in the fabrication of ITO and indium oxide coatings for LMR-based humidity sensors [18]. The name of this technique refers to the nature of the precursors used for the fabrication of the films. A sol is a dispersion of colloidal particles (diameter of 1-100 nm), while the term gel refers to a rigid interconnected network of polymeric chains longer than 1 μm in average with pores of submicrometer dimensions [19]. The sol precursor is employed for the creation of a gel layer on a substrate, which will form the solid film after a heating/drying process. In other words, in the simplest form, the substrate (optical fiber in this case) is immersed in a sol, and extracted at a controlled speed. As result part of the dispersed material on the sol will remain attached to the fiber, and a gel will form on its surface. After a drying or heating process, a solid film will be obtained [20]. The dipping of the substrate can be repeated subsequently in order to increase the thickness of the film. Another aspect that will affect the thickness and the end result is the withdrawal speed. It is important to maintain a steady pace and a controlled speed to assure uniformity on the coatings.

2.3.1.2. Layer-by-Layer Nano-assembly Technique

The Layer-by-layer (LbL) nano-assembly method has been recurrently used for the fabrication of coatings on optical fiber. In this method, the substrate is repeatedly immersed in two different solutions (cationic and anionic), followed by a washing step each time, that sequentially add monolayers to the coating [21]. The charged surface of the substrate attracts the oppositely charged molecules on the first solution. After a washing step, the result is

the adhesion of a single layer and a reversion of the charge on the surface. Now, the process is repeated using a solution of the opposite charge. This process can be cyclically repeated, providing a process for the construction of bilayer-based coatings with a high quality and a precise thickness control. For instance, this method has been used for the fabrication of coatings based on PAH/PAA [22], tin oxide [23], or graphene oxide [24] with the purpose of developing LMR-based sensors.

2.3.2. Chemical Vapor Deposition

The chemical vapor deposition (CVD) methods involve 'the dissociation and/or chemical reactions of gaseous reactants in a activated (heat, light, plasma) environment, followed by the formation of a stable solid product' [25]. Unlike PVC, a vacuum system is not always mandatory (although some CVD techniques do make use of vacuum), but conventional methods require high deposition temperatures. CVD techniques such as atomic layer deposition (ALD) or plasma-enhanced chemical vapor deposition (PECVD) have been used for the deposition of hafnium oxide, zirconium oxide, tantalum oxide or silicon nitride thin films with the purpose of fabricating LMR-based sensors [11].

2.3.2.1. Atomic Layer Deposition

Atomic layer deposition, ALD, (also known as atomic layer epitaxy) is capable of a great control of epitaxial growth, as is capable to generate monoatomic layers [25,26]. This process is based on the chemical absorption of a reactive vapor on a heated surface, which permits the attachment of a single layer. The sequential addition (and removal) of different reactive vapors that chemically react with each other, allows the deposition of consecutive single atomic layers. The nature of this technique provides great precision in the control of the thickness and structure of the thin-film, although its slow deposition rate and the need of heating the substrate can be a limitation for certain purposes.

2.3.2.2. Plasma-Enhanced CVD

In plasma-enhanced CVD a RF signal in a couple of electrodes generates plasma from the reactive vapors in order to induce the chemical reactions that result in the deposition of the film on the substrate [25]. This mechanism allows to maintain the substrate at a lower temperature, making possible the deposition of a wider range of materials than other conventional CVD methods. Another characteristic difference of PECVD is that it typically provides a faster deposition rate which, in turn, may reduce the accuracy in the film thickness.

2.3.3. Physical Vapor Deposition

The term physical vapor deposition (PVD) refers to a group of techniques that involve the vaporization of a material in order to build a thin film from it [27,28]. These methods usually require a high vacuum to avoid contamination from residual gases in the resulting coating and to facilitate the vaporization. PVD includes techniques such as thermal evaporation or cathodic sputtering deposition, which will be explained in more detail in the next subsections since they have been reportedly used in the fabrication of LMR-based sensors.

2.3.3.1. Thermal Evaporation

Thermal evaporation deposition takes place inside a vacuum chamber. The material that is desired to use for the fabrication of the thin film is located in the chamber and heated until it evaporates (if liquid) or sublimes (if solid), and then vapor is deposited on the substrate [27]. There are many variants on this method, depending on the heating mechanism (resistance-heated or electron beam evaporator), or the disposition of the elements in the chamber (evaporation can take place from bottom to top or from top to bottom), for instance. The nature of the deposition material or the substrate will determine the best thermal evaporation technique for each case. This method has been used for the fabrication of LMR-based sensors with ITO [8] and zinc oxide [9,12,29,30] thin films.

2.3.3.2. Cathodic Sputtering

In cathodic sputtering deposition, a solid source material (target) for the fabrication of the film is placed in a cathode inside a vacuum chamber with a small flow of an inert gas (typically argon) (fig. 2.6). In these conditions the electric field ionizes the gas generating a glow discharge plasma [28,31]. The highly energetic ions bombard the target, sputtering (detaching) particles of the material which later deposit on the substrate generating the film. Nowadays, this technique commonly makes use of a magnetic field parallel to the cathode (magnetron sputtering) in order to trap electrons and create a denser plasma, which increases the deposition rate and allows to work at lower pressure and voltage.

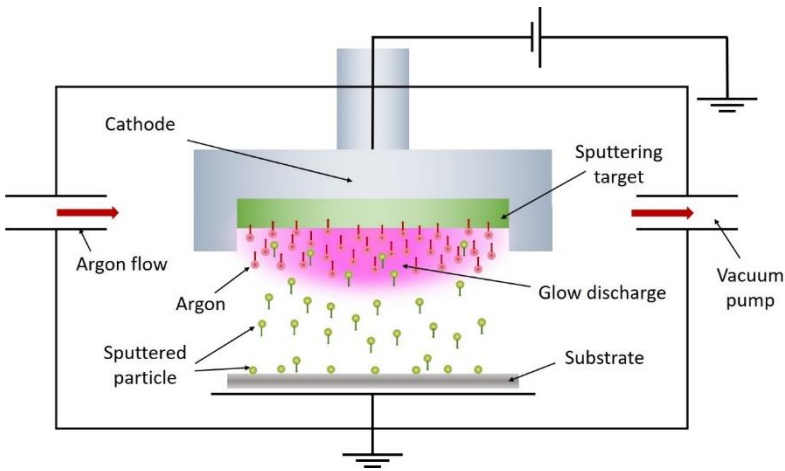

Figure 2.6: *Diagram of the key elements in a sputtering deposition process. The argon atoms are ionized by the electric fields and attracted towards the target, sputtering it and creating a vapor that produces the deposited thin-film on the substrate.*

The use of a DC source can be problematic when fabricating thin-films of insulating materials, such as oxides, due to low deposition rates and arc discharges. To overcome this, usually a pulsed source (pulsed magnetron sputtering, PMS) or a RF source (RF-sputtering) is chosen. Another variant in the cathodic sputtering process is the reactive sputtering. In this option, a reactive gas is also injected in

the vacuum chamber, so that it chemically reacts with the sputtered material from the target. For instance, the use of oxygen gas in a reactive sputtering process in combination with a metallic target, allows to fabricate coatings of the oxidized metal.

Cathodic sputtering has been widely used for the fabrication of thin films on the development of LMR based sensors, mainly for the deposition of alloys and metal oxides (ITO [14], tin oxide [14], titanium dioxide [32], etc.).

2.4. Coating Materials

The above-mentioned methods have been recurrently used in the fabrication of LMR-based sensors that made use of very different coating materials. The following sections will describe the principal characteristics of each coating and their main achievements, as well as their differences. Some of the proposed applications and their performance as sensors will also be explained.

2.4.1. Indium Tin Oxide (ITO)

Indium tin oxide is a well-known transparent conductive oxide (TCO) widely used in optics and electronics. One very interesting particularity of ITO is the fact that in can generate both LMR and SPR as it fulfills the requisites for the generation of both resonances: LMR at lower wavelength and SPR at a range above 2000 nm [33], see Fig. 2.7. In the last decade, several sensors have been studied using ITO as a coating material for the generation of LMR. It has been used on multimode fiber of different diameters [8,18,34], as well as D-shaped fiber [14,35] or glass slide in Kretschmann configuration [36]. Most authors have studied ITO as a coating material fabricating a thin film by means of sputtering [14,37,38] or thermal evaporation technique [8], but also other techniques such as dip-coating have been used [18]. While most studies have been focused on homogeneous ITO thin films, some works have been reported using nanoparticle-based ITO coatings [8].

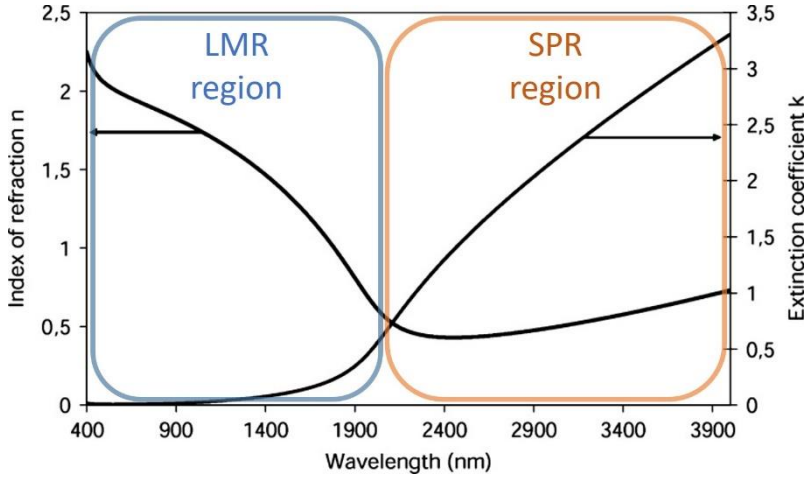

Figure 2.7: *ITO refractive index curve. It presents optical properties suitable for the generation of LMR and SPR at shorter and longer wavelength range respectively. Reprinted from* [33] *© 2010 IEEE.*

The deposition of ITO on flat surfaces has been reported as a successful mechanism for LMR generation. Using a Kretschmann configuration [15] ITO thin-film proved to be able to generate resonances in both TE and TM polarizations, obtaining sensitivities of 700 and 1,200 nm/RIU respectively, while a SPR is simultaneously observed with a sensitivity of 8,300 nm/RIU, for SRI around 1.47. Recently, microscope glass slides and coverslips coated with an ITO layer located in a Poly(methyl methacrylate) (PMMA) block have been used as planar waveguides in a fiber setup to induce LMR for the fabrication of a relative humidity (RH) sensor based on LMR [39].

Precisely, one of the multiple applications of ITO coatings for the fabrication of LMR based sensors is the measuring of relative humidity. In [18], a segment of cladding-removed 200/225 μm core/cladding MMF coated with ITO was used for the fabrication of a RH sensor with a sensitivity of 0.283 nm/%RH. This research also showed how the deposition of an overlay of a material highly sensitive to humidity as PAH/PAA over the ITO coating improved the sensitivity to 0.833 nm/%RH. The same fiber configuration was also used for the fabrication of a turbine oil degradation sensor in [40].

Here, the reported device was capable to measure the degradation of oil by measuring the LMR shift induced by the variation on the RI as a function of the oil degradation obtaining a sensitivity of $0.15 \cdot 10^{-3}$ nm/h (each hour of degradation would induce a $0.15 \cdot 10^{-3}$ nm shift in average).

ITO coated MMF has also been used for other interesting applications, such as the detection of hydrogen (H_2) [8]. This work compares the performance of three H_2 sensors using a LMR supporting coating that consisted of an ITO thin film, ITO nanoparticles (NPs) and a layer of ITO NPs over a ITO thin film. These devices obtained a sensitivity of 0.32, 0.58 and 0.71 nm/ppm respectively, probing that the use of ITO NPs enhances the sensitivity of the layer in the presence of H_2.

Some novel setups have been designed for the improvement of the sensitivity of LMR based sensors. In particular, in [41] has been proposed the fabrication of an ITO coating on a tapered MMF end, to observe a LMR in a reflection setup. This configuration theoretically achieves a sensitivity of 12,005 nm/RIU, which is 1.4 higher than the value simulated on a straight fiber.

As it was mentioned before, one of the most relevant differences in practice in LMR compared to SPR is the fact that LMR can be observed in both TE and TM modes, making it easier to observe them without the use of polarized light. However, as the LMR can be generated at different wavelengths for each mode (TE and TM), the isolation of modes facilitates the possibility to obtain narrower resonances with higher sensitivity. This allows to obtain a better figure of merit (FOM), defined as the sensitivity/FWHM ratio, since such parameter increases for more sensitive and narrower resonances. With that purpose, D-shaped fibers have been used for the fabrication of LMR based sensors. Fig. 2.8 shows an example of a typical D-shaped fiber setup, including a depolarizer and a polarization controller to select the desired polarization state. It also shows SEM section images of a D-shaped fiber and a detail of the film fabricated on its surface. A refractometer based on a D-shaped

fiber achieved a very narrow LMR (5.3 nm of FWHM) and reported a sensitivity of 8,742 nm/RIU in the range of 1.36-1.38 RI [42]. Such performance doubles the sensitivity experimentally obtained previously in a CRMOF setup in similar RI and spectral ranges (3125 nm/RIU) [43]. A more recent work on D-shaped fibers [14] reported a sensitivity of 136,276 nm/RIU in the range of 1.447-1.449 RI, with a peak of 304,361 nm/RIU. Here, it is important to consider the measuring SRI range because a characteristic behavior of LMRs is that the sensitivity increases at high RI range, which is confirmed by these results.

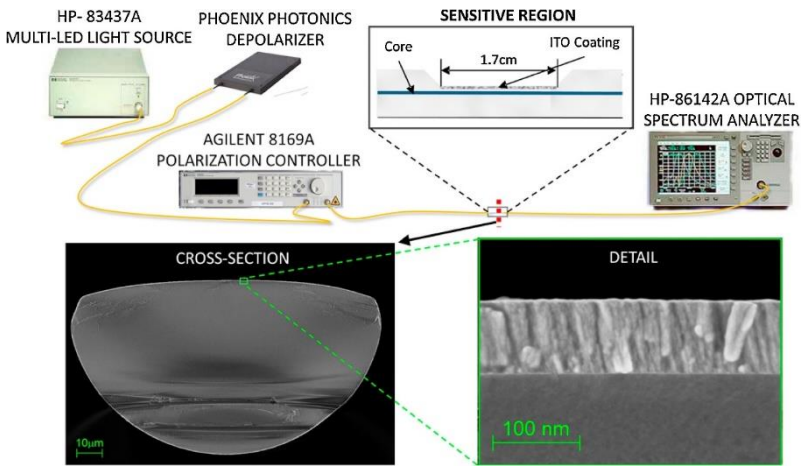

Figure 2.8: *Example of LMR based refractometer using a D-shaped fiber. A 17 mm long segment of side-polished SMF was coated with an ITO thin film. The geometry of this structure can be appreciated in the Cross-Section image obtained by SEM* [14].

Several biosensors based on ITO thin-films have also been reported in literature. For example, a C-Reactive protein (CRP) sensor was designed using a combination of ITO and PAH/PSS (poly(allylamine hydrochloride) and poly(sodium 4-styrenesulfonate)) coatings, followed by a receptor layer of CRP-aptamer on a D-shaped fiber [35]. This device showed a sensitivity of up to 169.93 nm/mg·l^{-1} and achieved a limit of detection (LOD) of 0.0625 mg/l. Another example is an Immunoglobulin G sensor fabricated onto an ITO coated MMF,

functionalized by adding a poly(methyl methacrylate) layer and immobilized antibodies, which achieved a LOD of 3.5 μg/l [44].

From another perspective, some authors have taken advantage of the electrical conductivity of ITO for the development of LMR based electrochemical sensors using ITO coated MMF [34,38,45,46]. For instance, an optical ketoprofen sensor was reported by Smietana et al. in [34]. This device monitored the electropolymerization of ketoprofen on the ITO coating showing a LOD of 0.536 mM.

As a summary, the most relevant studies reported using ITO coatings for the fabrication of LMR based refractometers are shown in Table 2.1.

Material	Config.	Deposition Technique	Sensitivity (nm/RIU)	RI range	Ref.
ITO	200 μm MMF	Dip Coating	3,125	1.32-1.44	[43]
ITO*	Tapered 600 μm MMF	Theoretical	12,005	N/A	[41]
ITO	D-shaped	Sputtering	304,361	1.447-1.449	[14]
ITO	D-shaped	Sputtering	8,742	1.365-1.38	[42]
ITO	Glass slide/ Krestch.	N/A	1,200	1.33-1.47	[15]

*Theoretical results

Table 2.1: *Summary of the different refractometers presented that use ITO thin films.*

2.4.2. Tin Oxide

Another widely used material for the fabrication of LMR refractometers is tin oxide. It presents a number of similarities in comparison with ITO, since tin oxide is one of the components of ITO. Optically, SnO_2 presents a slightly higher refractive index (fig. 2.9), which according to theory, permits to obtain higher sensitivities to SRI [7]. This idea has been experimentally proved in several works using D-shaped fibers coated with a SnO_2 thin-film. In particular, a sensor working in the 1.321-1.326 RI range obtained a

sensitivity of 14,501 nm/RIU [14], which is 1.6 times higher than the sensitivity obtained with ITO in the same RI range [42].

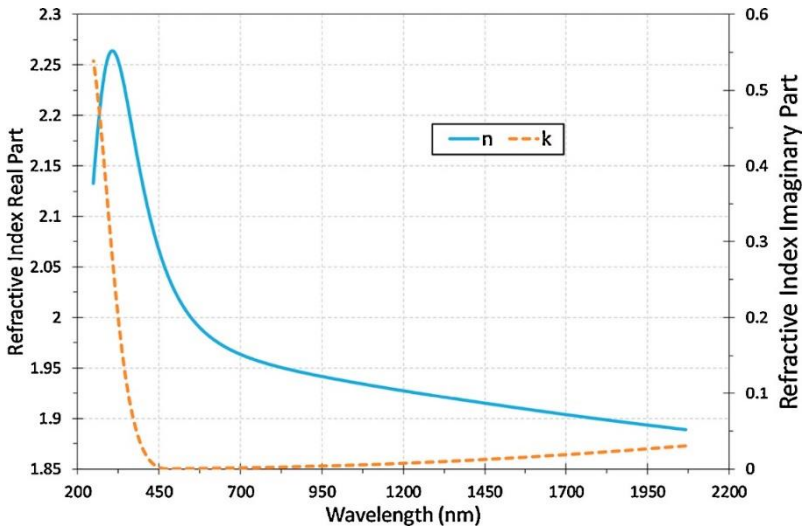

Figure 2.9: *Complex refractive index of tin oxide. Compared with ITO, it presents a higher real part (n) and a lower imaginary part (k) in the region of interest. Reprinted from* [14] *with permission from Elsevier.*

A tin oxide thin-film based LMR refractometer was also used for monitoring turbine oil degradation [40]. In this case, the sensitivity was improved up to $0.27 \cdot 10^{-3}$ nm/h. This material has also been reported for the fabrication of relative humidity sensors. In this sense, an etched SMF coated with SnO_2 thin-film of 140 nm demonstrated a sensitivity of 1.9 nm/%RH [47].

In the field of biosensing, SnO_2 has also been frequently studied. An Immunoglobulin G (IgG) sensor using tin oxide over two different fiber structures was reported in [44]. Here, the configuration based on a 200 μm core MMF was capable to achieve a LOD of 0.9 μg/l, while the setup based on a D-shaped fiber reached a LOD of 0.15 μg/l, which are comparatively better than the results obtained using an ITO coating. This improvement is a direct consequence of the higher sensitivity of the tin oxide coating based refractometers. Also a D-dimer sensor has been studied in [48] using a tin oxide coated

D-shaped fiber. This work presents a LOD of 10 ng/ml and 100 nm/ml when tested in buffer and human serum respectively.

Most of the analyzed studies report SnO_2 coatings fabricated by means of sputtering. However, there are other methods available for this purpose. Layer by Layer has also been proved as a valid option for the fabrication of SnO_2 coatings. In [23], a 600 μm core MMF coated with SnO_2/PSS bilayers was used in the design of a fiber refractometer in the range of 1.33-1.38 RI. This device reached a sensitivity of 4,080 nm/RIU, but this value could be raised up to 4,704 nm/RIU when a SnO_2 NPs layer was added to the previous film.

Tin oxide thin-films were also fabricated by means of dip-coating. A 200 μm CRMOF coated with SnO_2 generated a LMR in the spectral range between 850 and 1,450 nm that achieved an average sensitivity of 7,198 nm/RIU in the 1.321-1.423 RI range [49]. It is interesting that this device presented two differentiated sensitivity regions, due to the increase in sensitivity caused by the increment in SRI range. The first region, for the SRI values between 1.321 and 1.380 presented an average sensitivity of 4,127 nm/RIU, while this parameter increased for higher SRI values, up to 16,167 nm/RIU.

Dip-coating techniques have also been described for the fabrication of LMR based sensors using SnO_2 nanoparticles. In [50] four possible combinations of a dual coating were tested for the development of an arsenite sensor. The two possibilities for the first layer were a tin oxide thin-film or a SnO_2 NPs coating. Then, there were two different possibilities for the second layer: one was a α-Fe_2O_3 NPs layer, and the second was a core-shell nanostructure comprising α-Fe_2O_3 NPs (core) and SnO_2 (shell), abbreviated as α-Fe@Sn CS. The combination of SnO_2 NPs and α-Fe@Sn CS, which achieved the highest performance, allowed the generation of a LMR at a wavelength of 370 nm. This device presented a sensitivity of 1.31 nm/μg·l^{-1}, with a LOD of 0.99 μg/l.

Those are not the only cases where two different layers are combined to improve the sensing characteristics of the devices. The use of a Graphene oxide (GO) overlayer onto a 220 nm thick SnO_2 thin film proved to improve the sensitivity to ethanol by 210 % as it is described in [51].

Another promising structure consisting on Multi Mode-Coreless-Multi Mode fiber (MCM) has also been recently reported in [52]. In this configuration, a 20 mm segment of SnO_2 coated Coreless fiber is fused to a couple of MMF pigtails. The proposed device reached a sensitivity of 7,346 nm/RIU when characterized as a refractometer. Additionally, the device was also used for the fabrication of a IgG detector, obtaining a LOD of 0.6 mg/l.

We can find a comparison of the refractometric performance of the discussed sensors on Table 2.2.

Material	Config.	Deposition Technique	Sensitivity (nm/RIU)	RI Range	Ref.
SnO_2	200 μm MMF	Dip Coating	7,198	1.321-1.423	[49]
SnO_2/PSS	600 μm MMF	Layer by Layer	4,080	1.33-1.38	[23]
SnO_2/PSS + SnO_2 NPs	600 μm MMF	Layer by Layer + Dip Coating	4,704	1.33-1.38	[23]
SnO_2	D-shaped	Sputtering	14,501	1.321-1.326	[14]

Table 2.2: *Comparison of optical refractometers base don LMRs making use of tin oxide thin films.*

2.4.3. Indium Oxide

The other component of ITO, indium oxide (In_2O_3), has not received as much attention as ITO or tin oxide in the LMR field. Most of the reported devices are associated to humidity or refractive index sensors. An early work demonstrates the fabrication of In_2O_3 coatings on 200 μm core diameter CRMOF using the dip-coating method [53]. In this case three refractometers with increasing In_2O_3 film thickness were manufactured. All three devices presented 2

resonances, corresponding to the TE and TM modes, that could be observed separately in wavelength. As the film thickness increased, the position of these resonances shifted to a longer wavelength. The sensor with the thickest coating (86 nm) presented the resonances in the longest wavelengths (950 and 1,400), which caused these resonances to have the highest sensibility (4,255 and 4,926 nm/RIU). Such behavior is explained [7] as the LMR located at longer wavelength shows a greater sensitivity than when they are observed at shorter wavelength due to a thinner coating. This extensive work also demonstrates the response of this device to several VOCs (isopropyl alcohol, ethanol, methanol and acetone) and the cross-sensitivity to RH and temperature.

A research work where ITO thin-films were fabricated using the dip-coating technique for the development of RH sensors also describes the utilization of In_2O_3 for the same purpose [18]. In this case, an 85 nm layer of In_2O_3 was deposited onto a 200 μm CRMOF, allowing to observe two dips corresponding to the LMR caused by the two propagation modes, as explained above. A second device was designed depositing a 115 nm layer of ITO on a similar procedure. These probes were later coated by PAH/PAA coatings by means of LbL, to observe the effect of such overlays in the response of RH. Prior to the deposition of the polymeric coatings, the sensitivity to SRI variations was tested, showing that the case of In_2O_3 reached higher values (4,000 and 3,333 nm/RIU for TE and TM mode respectively) than ITO (1520 nm/RIU). In contrast, when the response to relative humidity was studied, it was seen that the resonances generated by In_2O_3 showed lower sensitivity (0.133 and 0.042 nm/%RH) than the resonance obtained with the ITO probe (0.283 nm/%RH). This difference in the sensitivity response to SRI and RH is explained by the more porous nature of the ITO coating, which permits a greater penetration and interaction with water molecules, inducing a greater LMR wavelength shift. However, when the RH sensitive PAH/PAA coating was added, the response of the In_2O_3 sensor was better. In particular, the resonance located at a longer wavelength (corresponding to the TE Mode) in the case of

In_2O_3 reached a sensitivity of 0.935 nm/%RH, whereas the device based on the ITO and PAH/PAA layers got a sensitivity of 0.833 nm/%RH.

The sputtering technique has also been reported for the fabrication of indium tin oxide [54]. Three probes with different coating thickness (70, 300 and 690 nm) were fabricated on CRMOF setup. This experiment permitted to analyze the behavior of the LMRs generated with different coating thickness. Fig. 2.10 shows the spectra of the three probes when tested under increasing SRI. It can be seen how the thinnest film allows to observe only the 1st LMR and, as the coating thickness increases, LMRs of higher order are generated. In terms of sensitivity, the first LMR achieves the greatest sensitivity (5,680 nm/RIU). In the rest of the probes, the maximum sensitivity is achieved by the LMR of lower order observed (1,165 and 1,790 nm/RIU in the probes with 300 and 690 nm coating, respectively). The fact that the 3rd order LMR achieves a higher sensitivity in the third probe than the 3rd and 2nd order LMR in the second probe is an example of the increase of sensitivity when the LMR is tuned at a longer wavelength.

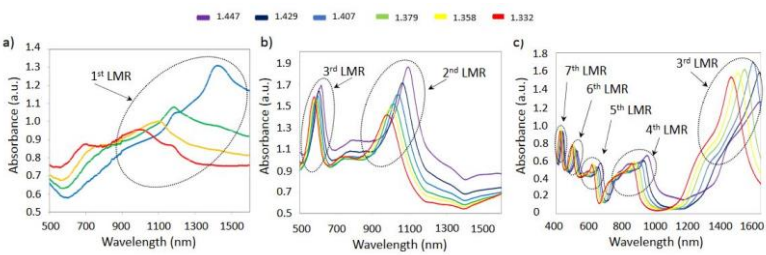

Figure 2.10: *Spectra obtained by the probes with a 70 nm thick coating (a), 300 nm thick coating (b) and 690 thick coating (c). As the thickness of the film grows, the LMR shift to longer wavelengths and LMR of higher order are observed. Reprinted from* [54] *with permission from SPIE.*

Recently, a new approach has been made regarding indium oxide coatings for LMR generation. In this case, the In_2O_3 films were fabricated by a sputtering system onto microscope glass slide and coverslips [55]. These devices acted as planar waveguides when

light was launched laterally from an optical fiber in one side and collected back on the opposite side. The In_2O_3 film on the slides allowed the generation of LMRs and the introduction of a light polarizer before the slide permitted the easy separation of propagation modes. A first probe was fabricated with a 276 nm thick In_2O_3 coating, which allowed the observation of a second order LMR. This device got a sensitivity of 162 nm/RIU in the RI range of 1.33-1.357, that raised to 1,375 nm/RIU when the RI range increased to 1.492-1.508. A second device was fabricated with a thinner coating (74 nm), in order to observe the first order resonance, which should be more sensitive. In this case, the sensitivity in the range between 1.33 and 1.357 reached a value of 929 nm/RIU, which is almost 6 times higher than the sensitivity obtained for the same RI range with the second order LMR.

The discussed results obtained with In_2O_3 based coatings are summarized on Table 2.3.

Material	Config.	Deposition Technique	Sensitivity (nm/RIU)	RI range	Ref.
In_2O_3	200 μm MMF	Dip Coating	4,444	1.32-1.37	[53]
In_2O_3	200 μm MMF	Sputtering	5,680	1.332-1.407	[54]
In_2O_3	Coverslip	Sputtering	929	1.333-1.357	[55]
In_2O_3	Coverslip	Sputtering	1,375	1.492-1.508	[55]

Table 2.3: *Summary of the refractometric performance of the devices fabricated with indium oxide coatings.*

2.4.4. Zinc Oxide

The next relevant group of metal oxides used for the generation of LMR consists of those based on zinc oxide. This material also fulfills the optical requirements for the generation of LMR and can be fabricated by common methods such as sputtering or thermal evaporation. However, the first experimental demonstrations of LMR based optical fiber refractometers using zinc oxide were

reported only a few years ago [12,30]. These works rely on the capability of zinc oxide to react with hydrogen sulfide (H_2S) gas for the design and fabrication of LMR-based hydrogen sulfide sensors. Different structures involving ZnO nanoparticles (NP) and ZnO nanorods (NR) are analyzed in these works in order to maximize the sensitivity of the LMR-based devices to H_2S gas. A sensitivity of 1.06 nm/ppm was obtained when a ZnO NPs layer was deposited directly on the fiber, which could be raised up to 1.49 nm/ppm when a 12 nm thin film of ZnO is fabricated onto the fiber before the deposition of the NPs [30]. These figures are well above the results obtained when the same fiber structure is coated with silver thin film and an overlayer of zinc oxide to fabricate a SPR based sensor, which could only achieve a sensitivity of 0.24 nm/ppm. Later, this mechanism was further enhanced by integrating ZnO nanorods, with a sensitivity enhancement up to 4.14 nm/ppm [12].

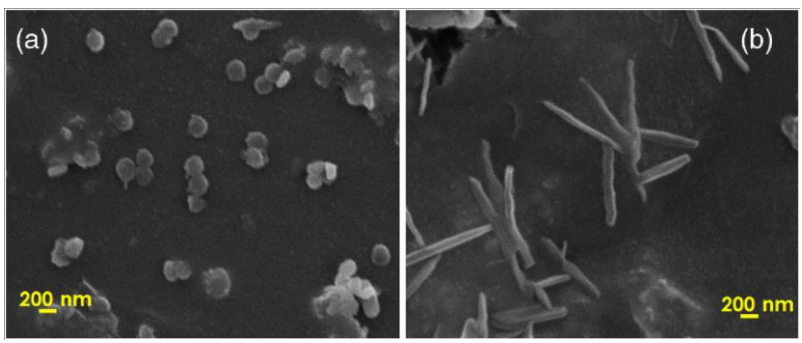

Figure 2.11: *SEM images of the zinc oxide nanoparticles (a) and nanorods (b) used in the fabrication of LMR based refractometers. Reprinted with permission from [9] © The Optical Society.*

A posterior work analyzed and compared the performance of this kind of LMR generating coatings as refractometers [9]. This way, 400 um core CRMOFs were coated with a ZnO thin film, a ZnO thin film followed by a ZnO NPs coating (fig. 2.11a), and a ZnO thin film followed by a ZnO NRs layer (fig. 2.11b). All three structures were fabricated in a way that they presented LMR in a close wavelength (between 350 and 390 nm), so that their performance could be compared more directly. This study showed that a single zinc oxide

thin film could provide a sensitivity of 760 nm/RIU, which could be raised to 950 nm/RIU adding a layer of ZnO NPs and it could be further improved using a layer of ZnO nanorods (1,160 nm/RIU).

Aiming to improve the performance of LMR based refractometers, ZnO thin-film has also been used in a other structures [56]. This structure consisted of a CRMOF of 400 μm core diameter, which has been bent in order to achieve a U-shaped fiber, and proposes a dual sensing approach to enhance the accuracy of the refractometer, measuring the LMR shift and the absorbance variation simultaneously. Besides, this paper also introduces a novel approach to the use of LMR based sensor, determining the SRI in function of the variation on FWHM of the LMR, instead of the wavelength shift. It claims that the use of FWHM reports a 4 times higher sensitivity than the measure of wavelength shift (895 nm/RIU compared to 220 nm/RIU respectively).

Although zinc oxide coatings have not been as extensively reported for the fabrication of LMR based sensors as the previous cases, they have already been considered for the development of LMR-based biosensors. A cortisol sensor using ZnO thin film and a molecularly imprinted polymer layer (MIP) was developed on a MMF [29]. In this work it was demonstrated that a variation of the concentration of cortisol could induce a shift above 51 nm in a LMR, providing a sensitivity of up to 12.86 nm/log(g/ml) and a LOD of 25.9 fg/ml. Similarly, a urinary p-cresol sensor, also relaying on the MIP mechanism was developed [57]. In this case, a zinc oxide and molybdenum sulphide (MoS_2) nanocomposite was used for the fabrication of LMR supporting coating. MoS_2 was included in the nanocomposite with the purpose of altering the refractive index of the coating, improving the sensitivity of the device. This way, the proposed sensor achieved a sensitivity of 11.86 nm/μM with a LOD of 28 nM.

Zinc oxide thin film has also been considered for the development of LMR-based pressure sensors [58]. This theoretical work proposes the fabrication of a hafnium dioxide (HfO_2) overlay on top of the zinc

oxide thin film in order to maximize the sensitivity. With such structure, a sensitivity of 837 nm/MPa (and a maximum of 2,000 nm/MPa) is calculated when a LMR based refractometer is inserted in a rubber block whose refractive index is dependent on the applied pressure. A summary of the LMR-based refractometers using ZnO thin-films can be found in Table 2.4.

It is interesting to note that some coatings based on doped zinc oxide have also been studied for the development of LMR based sensors. In particular, an Aluminum-doped zinc oxide (AZO) thin film was theoretically proposed for the fabrication of LMR based refractometers on a MMF tip. Here, simulations reported a sensitivity of 3,500 nm/RIU that would rise to 8,500 nm/RIU with the utilization of a dual coating (AZO/TiO_2) [59].

Material	Config.	Deposition Technique	Sensitivity (nm/RIU)	RI range	Ref.
ZnO	400 μm U-shaped MMF	Sputtering	220/895 (wavelength shift/FWHM)	1.33-1.42	[56]
ZnO	400 μm MMF	Thermal Evaporation	760	1.33-1.44	[9]
ZnO + ZnO NPs	400 μm MMF	Thermal Evaporation + Dip Coating	950	1.33-1.44	[9]
ZnO + ZnO NRs	400 μm MMF	Thermal Evaporation + Dip Coating	1,160	1.33-1.44	[9]
AZO*	400 μm Tapered tip	Theoretical	3,500	1.33-1.45	[59]
AZO + TiO_2*	400 μm Tapered tip	Theoretical	8,500	1.33-1.45	[59]
**Theoretical results*					

Table 2.4: *Comparison of different refractometers fabricated using zinc oxide based thin films.*

2.4.5. Titanium Dioxide

It was mentioned in the previous section that a structure consisting of a TiO_2 film over an AZO layer was considered for the design of LMR based refractometers. Titanium dioxide itself is also considered a very promising material for the development of optical LMR sensors since it possesses a high refractive index and TiO_2 based coatings can be fabricated in a number of ways such as sputtering or Layer-by-Layer. An early work presented a TiO_2/PSS thin film fabricated by LbL technique onto a 200 μm core diameter CRMOF. This device enables the generation of a LMR at a wavelength of 1,100 nm, achieving a sensitivity of 2,872 nm/RIU [60]. A recent work using a similar coating on a 600 μm core CRMOF obtained a sensitivity of 6,754 nm/RIU at a wavelength of 650 nm [61]. In this case, a reflection setup was used for the characterization of the device, which also presented thinner coatings than the previous case (126 μm instead of 460 μm). These conditions permitted the observation of LMRs of lower order, which show a greater sensitivity. Another work presented the use of reactive sputtering technique for the fabrication of a TiO_2 thin-film on a D-shaped fiber [32]. This 84 nm film generated a resonance at a wavelength of 1,300 nm, but showed a sensitivity lower than the previous case, of 4,122 nm/RIU. Following the experiences described with the previous materials, the use of a D-shaped fiber should not decrease the sensitivity of the sensor. The fact that a different deposition technique and different reagents are used in this research implies that the optical properties of the fabricated film may be quite different, which could lead to this unexpected result.

Another experimental use of TiO_2 for the fabrication of optical LMR sensors was reported, seeking to design an ammonia sensor [62]. This work reports a TiO_2 based coating deposited onto a tapered SMF by a process of Liquid Phase Deposition (LPD). This coating contains porphyrin, which is capable to interact with ammonia as a functional material. Such coating induces a LMR at 850 nm, which shifts in the presence of ammonia obtaining a LOD of 0.116 ppm.

It should be noted that TiO_2 thin films have also been used for the theoretical study of new fiber structures to fabricate LMR based refractometers. The use of TiO_2 coatings on grapefruit PCF with exposed core has been recently reported [63]. This study suggest that the appropriate waveguide selection could improve the sensitivity of this LMR based refractometers to 68,000 nm/RIU using a 100 nm thick TiO_2 film. It also suggests the fabrication of a HfO_2 layer on top of the TiO_2 film since the appropriate combination of thickness (80/20 nm) could enhance the sensitivity to 84,000 nm/RIU, with a maximum peak of 140,000 nm/RIU. A similar work proposed the addition of a rubber layer on top of the TiO_2/HfO_2 coating with a varying RI in function of the applied pressure (fig. 2.12) [64]. This would allow the fabrication of a pressure sensor, which according to the simulations could achieve a sensitivity of 5 μm/MPa.

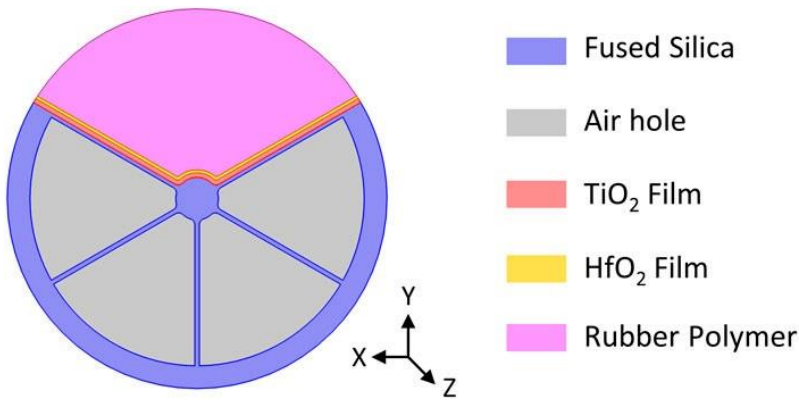

Figure 2.12: *Cross section of the grapefruit PCF structure proposed for the fabrication of a LMR based pressure sensor* [64].

Table 2.5 presents a brief summary of the devices presented in this section.

Material	Config.	Deposition Technique	Sensitivity (nm/RIU)	RI range	Ref.
TiO2/PSS	200 μm MMF	Layer by Layer	2,872.73	1.32-1.43	[60]
TiO2/PSS	600 μm MMF	Layer by Layer	6,754	1.33-1.38	[61]
TiO2	D-shaped	Sputtering	4,122	1.333 - 1.398	[32]
TiO2*	Microstruct. D-shaped PCF	Theoretical	68,000	1.33-1.40	[63]
TiO2 + HfO2*	Microstruct. D-shaped PCF	Theoretical	84,000	1.33-1.40	[63]

* Theoretical results

Table 2.5: *Summary of optical fiber LMR based sensors using titanium dioxide coatings.*

2.4.6. Polymers

Previous sections have dealt with coatings based on metal oxides for the generation of lossy mode resonances. It should be noted that some of the discussed coatings also included polymeric layers in their composition, mainly associated but not limited to the sensing application. In fact, LMR generation is not restricted to the use of metal oxides. Polymeric films are also capable to support LMR generation on their own, as long as their optical properties match the required conditions. For instance, a LMR based sensor using polymeric coatings was reported for the sensing of pH [22]. A coating consisted on PAH/PAA bilayers deposited by LbL was chosen due to the swelling/deswelling behavior it presents with a variation in pH. Such change in the thickness of the coatings induces a wavelength shift in the LMR and thus acts like a pH monitor. Fig. 2.13 shows the transmission spectra on the fiber as PAH/PAA bilayers are added. It can be seen how several LMRs are generated as the coating thickens, each resonance with a different slope. It is worth noting that the first LMR presents the greatest slope, and the following ones present lower values. This slope indicates the sensitivity of the LMR to the thickness variation and is related to the sensitivity to SRI, and agrees with the premise that the lower order

LMRs are more sensitive. Following this procedure, two different probes were fabricated with 100 and 25 polymeric bilayers respectively, in order to generate a LMR of second and first order in the 500-700 nm range. These devices showed a sensitivity to pH in the 3-6 range of 25 and 36.67 nm/pH respectively.

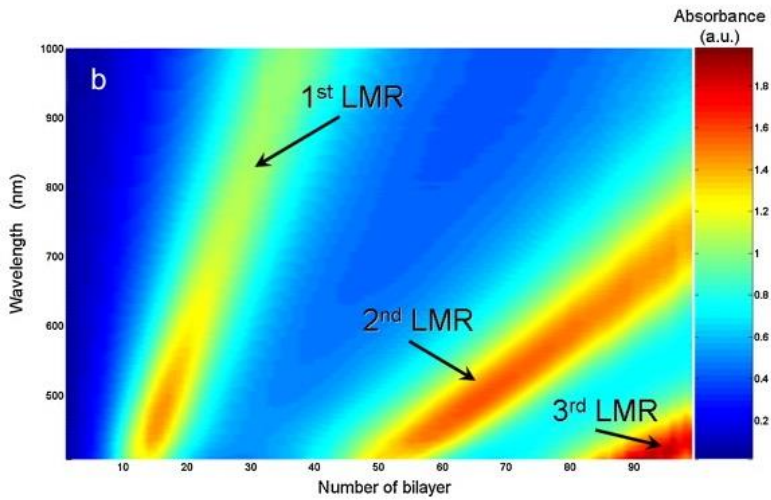

Figure 2.13: *Transmittance spectra of a 200 μm CRMOF as PAH/PAA bilayers are being deposited on it. Several absorption bands can be observed, corresponding to LMRs* [22].

A different kind of polymeric coating was also studied for the development of pH optical sensors, including gold nanoparticles in the polymeric matrix [65]. A PAH/PAA-Au NPs coating deposited by Layer-by-Layer method on a CRMOF induced a LMR at 750 and a LSPR (localized surface plasmon resonance) at 530 nm. This probe was submerged in buffer solutions of different pH between 4.0 and 6.0 showing a resonance shift of both resonances as a function of the pH of the solutions. In particular, the LSPR and LMR showed a sensitivity of 0.75 nm/pH and 67.35 nm/pH respectively.

With the same purpose, D-shaped fibers were also coated with PAH/PAA bilayers. In this case, the pH of the solutions involved in the LbL fabrication process were adjusted in order to obtain two

probes working in two different pH ranges [13]. The first probe was designed to operate in a pH range of 7-8 while the second probe was conceived for operation in the pH range between 4 and 5. In the first probe, the LMR corresponding to the TM and TE reached sensitivities of 30 and 34 nm/pH respectively. In the second probe, the two resonances obtained sensitivities of 61 and 69 nm/pH respectively.

Polymeric coatings were also used for the measurement of other parameters, such as relative humidity [10]. As mentioned previously, PAH/PAA layers present a high sensitivity to relative humidity. The indicated work studied several probes coated with PAH/PAA bilayers characterizing LMRs of first and second orders at different wavelengths. The device with the best performance obtained a sensitivity of 0.51 nm/%RH. This value falls behind the previously reported sensitivity of 0.935 nm/%RH when the probe presents a In_2O_3 thin-film beneath the PAH/PAA coating [18]. These results demonstrate the importance of using a LMR supporting coating that presents a high sensitivity, in combination in this case with the polymeric coating that reacts with the parameter to measure.

Nanoparticles were also included in the polymeric coating matrices for the fabrication of relative humidity sensors. A PAH/PAA-Ag NPs coating, for instance, was fabricated on a 200 μm core CRMOF in order to induce simultaneously a LMR and a LSPR, thanks to the addition of silver NPs[66]. In this device, the LMR achieved a sensitivity to RH of 0.943 nm/%RH, while the LSPR remained almost invariant (0.06 nm/%RH). A similar behavior was reported in another work where the dual LSPR and LMR phenomena were observed thanks to the presence of gold nanorods (GNR) [67]. A LbL coating of PAH/GNR@PSS (Gold nanorods embedded in PSS) was capable to generate LSPR in two bands (LSPR-T at 530 nm and LSPR-L at 720 nm, related to the transverse and longitudinal plasmons respectively) and a LMR at 850 nm. As in the previous case, the

LSPRs were not very sensitive to RH variations (below 0.13 nm/%RH). In contrast, LMR achieved a sensitivity of 11.2 nm/%RH.

Table 2.6 presents a brief summary of all these sensors.

Material	Config.	Deposition Technique	App.	Sensitivity	Ref.
PAH/PAA	200 μm MMF	Layer by Layer	Relative Humidity	0.51 nm/%RH	[10]
PAH/GNR @PSS	200 μm MMF	Layer by Layer	Relative Humidity	11.2 nm/%RH	[67]
PAH/PAA-AG NPs	200 μm MMF	Layer by Layer	Relative Humidity	0.943 nm/%RH	[66]
PAH/PAA-Au NPs	200 μm MMF	Layer by Layer	pH (4-6)	67.35 nm/pH	[65]
PAH/PAA	D-shaped	Layer by Layer	pH (7-8)	34 nm/pH	[13]
PAH/PAA	D-shaped	Layer by Layer	pH (4-5)	69 nm/pH	[13]

Table 2.6: *Summary of the RH and pH described optical sensors based on polymeric coatings.*

Polymers have proven to be a very interesting medium for the generation of LMRs and the development of sensors. However, it should be noted that they are not so convenient for achieving a high sensitivity as this requires a coating with a high refractive index and most polymers do not satisfy such conditions.

2.4.7. Other materials

Previous sections have summarized the most widely used materials for the fabrication of LMR based sensors. Several metal oxides and some polymers present the ideal properties, in terms of electrical dispersion and thin film fabrication possibilities, that make them good choices for this purpose. However, there are other materials, not cited in the previous sections, that are getting more attention for the support of LMR in recent works. For instance, graphene oxide (GO), which has already been described above because of its use as an overlay to enhance the sensitivity of a SnO_2 thin film based sensor, has also been experimentally tested in [24]. Two different

sensors were fabricated in this work using 8 and 20 bilayers of GO and polyethyleneimine (PEI) by means of the LbL technique on 200 μm core CRMOF. The number of bilayers was chosen to obtain LMRs of different order but at the same wavelength (550 nm) in both probes. The probes were later tested on solutions of increasing refractive index in the ranges of 1.33-1.42 and 1.39-1.42, obtaining a sensitivity of 2,631 nm/RIU and 12,460 nm/RIU for the devices with 20 and 8 bilayers respectively.

A recent work [11] presented a number of coating materials that can be deposited by atomic layer deposition (ALD) and demonstrated their capability to fabricate LMR based sensors. This deposition technique is chosen because of its capacity to control the growth rate with great precision, which is a key aspect for the fabrication of LMR based sensors. ALD was used to fabricate hafnium oxide (HfO_2) and zirconium oxide (ZrO_2) thin films on 400 μm core CRMOF. Fig. 2.14 shows the transmission spectra for such devices when immersed on solutions of increasing SRI. Thin films of silicon nitride (Si_xN_y) were also fabricated by PECVP (plasma-enhanced chemical vapor deposition). This technique is not as precise as ALD, but in contrast, it allows the fabrication of thicker coatings in a reasonable time. A fourth kind of probe consisted of the fabrication by ALD of a tantalum oxide (Ta_2O_5) film on top of the silicon nitride layer. This structure is designed so that a thick coating can be fabricated in a reasonable time (Si_xN_y by PECVD), but at the same time allowing a fine tuning with the addition of the Ta_2O_5 overlay with ALD. The ZrO_2 probe obtained a sensitivity of 195 and 880 nm/RIU for the RI ranges of 1.33-1.45 and 1.41-1.43 respectively. In the case of the silicon nitride based sensor it obtained sensitivities of 289.5 and 593.5 nm/RIU for the same RI ranges. When the tantalum oxide film was deposited on the silicon nitride layer, the sensitivity of the device for the lower RI range increased to 1,077 nm/RIU but the opposite behavior was obtained for the 1.43-1.45 range as the sensitivity slightly decreased to 483 nm/RIU. Table 2.7 summarizes these results.

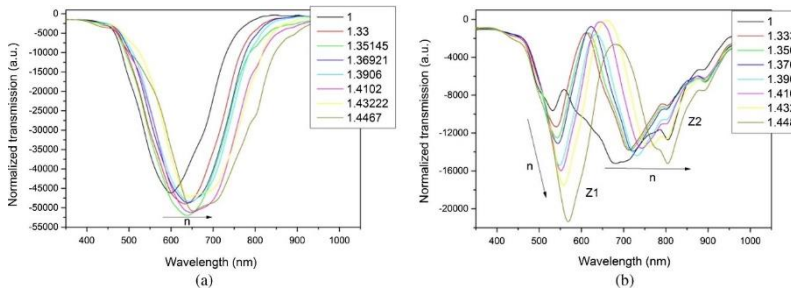

Figure 2.14: *Transmission spectra of a HfO2 (a) and a ZrO2 (b) coated CRMOF for different SRI* [11].

Material	Config.	Deposition Technique	Sensitivity (nm/RIU)	RI Range	Ref.
Graphene Oxide (GO)	200 μm MMF	Layer by Layer	12,460	1.39-1.42	[24]
ZrO_2	400 μm MMF	Atomic Layer Deposition	880 and 195	1.41-1.43 and 1.33-1.35	[11]
Si_xN_y	400 μm MMF	RF PECVD	289.5 and 593.5	1.33-1.35 and 1.43-1.45	[11]
Si_xN_y + Ta_2O_5	400 μm MMF	RF PECVD + Atomic Layer Deposition	1,077 and 483	1.33-1.35 and 1.43-1.45	[11]

Table 2.7: *Performance of the LMR based refractometers on multimode fiber using a variety of coating materials.*

2.5. Conclusions

A number of materials have already been studied for the generation of LMR based sensors. Each coating material has led to the development of LMR based sensors for different purposes with diverse results. The increasing number of studies in this field during the last decade highlights the versatility of LMR-based for the development of sensors. Table 2.8 provides a quick overview to compare the best results obtained with the different LMR generating materials presented above. In this sense, materials such as ITO, tin oxide, indium oxide, PAH, PAA and even silver

nanoparticles or gold nanorods have been used for the fabrication of relative humidity sensors [10,18,47,66,67], for instance.

Nanoparticles (NPs) have been widely used in layers for the fabrication of gas sensors, as this structure increases the surface of interaction. For example, in the development of sensors for the detection of arsenite (tin oxide NPs) [50], hydrogen (ITO NPs) [8] or hydrogen sulphide (zinc oxide NPs and NRs) [12,30].

Zinc oxide thin films have also been used in the fabrication of LMR based sensors using molecularly imprinted polymers (MIPs) [29,57].

The sensitivity of the lossy mode resonances to external refractive index variations has been extensively studied especially in the range close to water (1.33), since most biological applications work here. For instance, a graphene oxide coating [24] could provide a sensitivity of 2,631 nm/RIU (at a wavelength of 550 nm), while a TiO_2/PSS film [61] produced a LMR with a sensitivity of 6,754 nm/RIU (at 650 nm). Also a In_2O_3 based refractometer [53] reported a value of 3,003 nm/RIU at 600 nm, which raised to 4,926 nm/RIU when a thicker coating shifted the LMR to 1400 nm, all of them using CRMOF. Using a D-shaped fiber setup, a refractometer based on an ITO thin film [42] obtained a sensitivity of 8,742 nm/RIU. That figure was almost doubled (14,501 nm/RIU) when a coating of tin oxide was used instead [14].

In terms of sensitivity, the highest figure was achieved with ITO coatings in the refractive index range of fused silica [42]. However, in the RI range of water SnO_2 provided a better performance [14] (while tin oxide was not previously tested in the fused silica RI range). These results are due to the optical properties of the thin-film, and are in agreement with the established theory that predicts that a LMR supporting coating with a high refractive index will lead to devices with high sensitivity to SRI variations [7]. Accordingly, several biosensors have been designed using tin oxide coatings as LMR supporting coatings, aiming to get the lowest possible limit of

detection (LOD), as it is the case of a Dimer-D [48] or a Immunoglobulin G [44] sensor.

However, tin oxide optical properties are not so exceptional. In fact, there are other materials whose refractive indices do not differ much from that of SnO_2 that are potentially capable of generating LMR with as good or even higher sensitivity. Materials such a copper oxide, that possesses a higher refractive index and a low extinction coefficient, could surpass the performance of tin oxide in the fabrication of lossy mode resonance based sensors. Although very important, a potentially high sensitivity must not be the only parameter to consider when it comes to finding the best material for the fabrication of sensors. Other considerations such as the porosity of the films, stability, fabrication process or affinity with the functionalizing layer must be taken into consideration for the selection of the LMR supporting material. The possibility of designing a structure of two (or more) layers [11,51] offers also a promising perspective for the optimization of these sensors. The phenomenon of LMR for the fabrication of optical sensors has already proved to have a great potential and the vast number of possible materials to design them represents a limitless field of research.

This situation leads to the research presented in the current PhD thesis, which in the following chapters will describe the development and fabrication of a number of LMR-based sensors using different novel thin-film materials.

Material	Config.	Deposit. Tech.	RI Range	Wav. (nm)	Sens. (nm/RIU)	Ref.
ITO	200 µm MMF	Dip Coating	1.32-1.44	950	3,125	[43]
ITO	D-shaped	Sputtering	1.365-1.38	1,250	8,742	[42]
ITO	D-shaped	Sputtering	1.447-1.449	1,280	304,361	[14]
SnO_2	200 µm MMF	Dip Coating	1.321-1.423	900	7,198	[49]
SnO_2	D-shaped	Sputtering	1.321-1.326	1,380	14,501	[14]
In_2O_3	200 µm MMF	Sputtering	1.332-1.407	999	5,680	[54]
In_2O_3	Coverslip	Sputtering	1.333-1.357	730	929	[55]
ZnO + ZnO NRs	400 µm MMF	Thermal Evaporation + Dip Coating	1.33-1.44	390	1,160	[9]
TiO_2/PSS	600 µm MMF	Layer by Layer	1.33-1.38	650	6,754	[61]
TiO_2	D-shaped	Sputtering	1.333-1.398	1,300	4,122	[32]
Graphene Oxide (GO)	200 µm MMF	Layer by Layer	1.39-1.42	550	12,460	[24]
ZrO_2	400 µm MMF	ALD	1.41-1.43	700	880	[11]
Si_xN_y + Ta_2O_5	400 µm MMF	RF PECVD + ALD	1.33-1.35	770	1,077	[11]

Table 2.8: *Performance of the different sensors based on LMR detailed in this paper. The sensitivity achieved is highly dependent on the coating material, the wavelength and the RI range.*

Bibliography

1. Lazcka, O.; Campo, F. J. Del; Muñoz, F. X. Pathogen detection: A perspective of traditional methods and biosensors. *Biosens. Bioelectron.* 2007, *22*, 1205–1217.

2. Fine, G. F.; Cavanagh, L. M.; Afonja, A.; Binions, R. Metal Oxide Semi-Conductor Gas Sensors in Environmental Monitoring. *Sensors* **2010**, *10*, 5469–5502, doi:10.3390/s100605469.

3. Luppa, P. B.; Sokoll, L. J.; Chan, D. W. Immunosensors - Principles and applications to clinical chemistry. *Clin. Chim. Acta* 2001, *314*, 1–26.

4. Mukhopadhyay, S. C. Wearable sensors for human activity monitoring: A review. *IEEE Sens. J.* 2015, *15*, 1321–1330.

5. Del Villar, I.; Arregui, F. J.; Zamarreño, C. R.; Corres, J. M.; Bariain, C.; Goicoechea, J.; Elosua, C.; Hernaez, M.; Rivero, P. J.; Socorro, A. B.; Urrutia, A.; Sanchez, P.; Zubiate, P.; Lopez, D.; De Acha, N.; Ascorbe, J.; Matias, I. R. *Optical sensors based on lossy-mode resonances*; Elsevier B.V., 2017; Vol. 240, pp. 174–185;.

6. *Surface Plasmon Resonance Based Sensors*; Homola, J., Ed.; Springer Berlin Heidelberg: Berlin, Heidelberg, 2006; Vol. 4; ISBN 978-3-540-33918-2.

7. Del Villar, I.; Hernaez, M.; Zamarreño, C. R.; Sánchez, P.; Fernández-Valdivielso, C.; Arregui, F. J.; Matias, I. R. Design rules for lossy mode resonance based sensors. *Appl. Opt.* **2012**, *51*, 4298, doi:10.1364/AO.51.004298.

8. Mishra, S. K.; Usha, S. P.; Gupta, B. D. A lossy mode resonance-based fiber optic hydrogen gas sensor for room temperature using coatings of ITO thin film and nanoparticles. *Meas. Sci. Technol.* **2016**, *27*, 045103, doi:10.1088/0957-0233/27/4/045103.

9. Usha, S. P.; Gupta, B. D. Performance analysis of zinc oxide-implemented lossy mode resonance-based optical fiber

refractive index sensor utilizing thin film/nanostructure. *Appl. Opt.* **2017**, *56*, 5716, doi:10.1364/AO.56.005716.

10. Sanchez, P.; Zamarreno, C. R.; Hernaez, M.; Del Villar, I.; Matias, I. R.; Arregui, F. J. Considerations for Lossy-Mode Resonance-Based Optical Fiber Sensor. *IEEE Sens. J.* **2013**, *13*, 1167–1171, doi:10.1109/JSEN.2012.2227717.

11. Kosiel, K.; Koba, M.; Masiewicz, M.; Śmietana, M. Tailoring properties of lossy-mode resonance optical fiber sensors with atomic layer deposition technique. *Opt. Laser Technol.* **2018**, *102*, 213–221, doi:10.1016/j.optlastec.2018.01.002.

12. Usha, S. P.; Mishra, S. K.; Gupta, B. D. Zinc oxide thin film/nanorods based lossy mode resonance hydrogen sulphide gas sensor. *Mater. Res. Express* **2015**, *2*, 095003, doi:10.1088/2053-1591.

13. Zubiate, P.; Zamarreño, C. R.; Del Villar, I.; Matias, I. R.; Arregui, F. . Tunable optical fiber pH sensors based on TE and TM Lossy Mode Resonances (LMRs). *Sensors Actuators B Chem.* **2016**, *231*, 484–490, doi:10.1016/j.snb.2016.03.024.

14. Arregui, F. J.; Del Villar, I.; Zamarreño, C. R.; Zubiate, P.; Matias, I. R. Giant sensitivity of optical fiber sensors by means of lossy mode resonance. *Sensors Actuators B Chem.* **2016**, *232*, 660–665, doi:10.1016/j.snb.2016.04.015.

15. Torres, V.; Beruete, M.; Sánchez, P.; Del Villar, I. Indium tin oxide refractometer in the visible and near infrared via lossy mode and surface plasmon resonances with Kretschmann configuration. *Appl. Phys. Lett.* **2016**, *108*, 043507, doi:10.1063/1.4941077.

16. Zamarreno, C. R.; Matias, I. R.; Arregui, F. J. Nanofabrication techniques applied to the development of novel optical fiber sensors based on nanostructured coatings. *IEEE Sens. J.* **2012**, *12*, 2699–2710, doi:10.1109/JSEN.2012.2199750.

17. Elosua, C.; Arregui, F. J.; Del Villar, I.; Ruiz-Zamarreño, C.; Corres, J. M.; Bariain, C.; Goicoechea, J.; Hernaez, M.; Rivero, P. J.; Socorro, A. B.; Urrutia, A.; Sanchez, P.; Zubiate, P.;

Lopez-Torres, D.; De Acha, N.; Ascorbe, J.; Ozcariz, A.; Matias, I. R. Micro and Nanostructured Materials for the Development of Optical Fibre Sensors. *Sensors* **2017**, *17*, 2312, doi:10.3390/s17102312.

18. Sanchez, P.; Zamarreño, C. R.; Hernaez, M.; Del Villar, I.; Fernandez-Valdivielso, C.; Matias, I. R.; Arregui, F. J. Lossy mode resonances toward the fabrication of optical fiber humidity sensors. *Meas. Sci. Technol.* **2012**, *23*, 014002, doi:10.1088/0957-0233/23/1/014002.

19. Hench, L. L.; West, J. K. The Sol-Gel Process. *Chem. Rev.* **1990**, *90*, 33–72, doi:10.1021/cr00099a003.

20. Brinker, C. J.; Frye, G. C.; Hurd, A. J.; Ashley, C. S. Fundamentals of sol-gel dip coating. *Thin Solid Films* **1991**, *201*, 97–108, doi:10.1016/0040-6090(91)90158-T.

21. Decher, G. Fuzzy Nanoassemblies: Toward Layered Polymeric Multicomposites. *Science (80-.).* **1997**, *277*, 1232–1237, doi:10.1126/science.277.5330.1232.

22. Zamarreño, C. R.; Hernáez, M.; Del Villar, I.; Matías, I. R.; Arregui, F. J. Optical fiber pH sensor based on lossy-mode resonances by means of thin polymeric coatings. *Sensors Actuators B Chem.* **2011**, *155*, 290–297, doi:10.1016/j.snb.2010.12.037.

23. Wang, Q.; Li, X.; Zhao, W.-M.; Jin, S. Lossy mode resonance-based fiber optic sensor using layer-by-layer SnO2 thin film and SnO2 nanoparticles. *Appl. Surf. Sci.* **2019**, *492*, 374–381, doi:10.1016/j.apsusc.2019.06.168.

24. Hernaez, M.; Mayes, A. G.; Melendi-Espina, S. Lossy Mode Resonance Generation by Graphene Oxide Coatings Onto Cladding-Removed Multimode Optical Fiber. *IEEE Sens. J.* **2019**, *19*, 6187–6192, doi:10.1109/JSEN.2019.2906010.

25. Choy, K. Chemical vapour deposition of coatings. *Prog. Mater. Sci.* **2003**, *48*, 57–170, doi:10.1016/S0079-6425(01)00009-3.

26. Goodman, C. H. L.; Pessa, M. V. Atomic layer epitaxy. *J. Appl. Phys.* **1986**, *60*, R65–R82, doi:10.1063/1.337344.

27. Frey, H. Vacuum Evaporation. In *Handbook of Thin-Film Technology*; Springer Berlin Heidelberg: Berlin, Heidelberg, 2015; pp. 13–71 ISBN 9783642054303.

28. Mattox, D. M. Deposition Processes. In *The Foundations of Vacuum Coating Technology*; Elsevier, 2003; pp. 11–33.

29. Usha, S. P.; Shrivastav, A. M.; Gupta, B. D. A contemporary approach for design and characterization of fiber-optic-cortisol sensor tailoring LMR and ZnO/PPY molecularly imprinted film. *Biosens. Bioelectron.* **2017**, *87*, 178–186.

30. Usha, S. P.; Mishra, S. K.; Gupta, B. D. Fiber optic hydrogen sulfide gas sensors utilizing ZnO thin film/ZnO nanoparticles: A comparison of surface plasmon resonance and lossy mode resonance. *Sensors Actuators B Chem.* **2015**, *218*, 196–204.

31. Kelly, P. .; Arnell, R. . Magnetron sputtering: a review of recent developments and applications. *Vacuum* **2000**, *56*, 159–172, doi:10.1016/S0042-207X(99)00189-X.

32. Tien, C.-L.; Lin, H.-Y.; Su, S.-H. High Sensitivity Refractive Index Sensor by D-shaped Fibers and Titanium Dioxide Nanofilm. *Adv. Condens. Matter Phys.* **2018**, *2018*, 1–6, doi:10.1155/2018/2303740.

33. Del Villar, I.; Zamarreño, C. R.; Hernaez, M.; Arregui, F. J.; Matias, I. R. Generation of Lossy Mode Resonances With Absorbing Thin-Films. *J. Light. Technol.* **2010**, *28*, 3351–3357, doi:10.1109/JLT.2010.2082492.

34. Bogdanowicz, R.; Niedziałkowski, P.; Sobaszek, M.; Burnat, D.; Białobrzeska, W.; Cebula, Z.; Sezemsky, P.; Koba, M.; Stranak, V.; Ossowski, T.; Śmietana, M. Optical Detection of Ketoprofen by Its Electropolymerization on an Indium Tin Oxide-Coated Optical Fiber Probe. *Sensors* **2018**, *18*, 1361, doi:10.3390/s18051361.

35. Zubiate, P.; Zamarreño, C. R.; Sánchez, P.; Matias, I. R.;

Arregui, F. J. High sensitive and selective C-reactive protein detection by means of lossy mode resonance based optical fiber devices. *Biosens. Bioelectron.* **2017**, *93*, 176–181, doi:10.1016/j.bios.2016.09.020.

36. Villar, I. Del; Torres, V.; Beruete, M. Experimental demonstration of lossy mode and surface plasmon resonance generation with Kretschmann configuration. *Opt. Lett.* **2015**, *40*, 4739, doi:10.1364/OL.40.004739.

37. Del Villar, I.; Zubiate, P.; Zamarreño, C. R.; Arregui, F. J.; Matias, I. R. Optimization in nanocoated D-shaped optical fiber sensors. *Opt. Express* **2017**, *25*, 10743, doi:10.1364/OE.25.010743.

38. Smietana, M.; Sobaszek, M.; Michalak, B.; Niedzialkowski, P.; Bialobrzeska, W.; Koba, M.; Sezemsky, P.; Stranak, V.; Karczewski, J.; Ossowski, T.; Bogdanowicz, R. Optical Monitoring of Electrochemical Processes With ITO-Based Lossy-Mode Resonance Optical Fiber Sensor Applied as an Electrode. *J. Light. Technol.* **2018**, *36*, 954–960, doi:10.1109/JLT.2018.2797083.

39. Fuentes, O.; Corres, J. M.; Matias, I. R.; Villar, I. Del Generation of Lossy Mode Resonances in Planar Waveguides Toward Development of Humidity Sensors. *J. Light. Technol.* **2019**, *37*, 2300–2306, doi:10.1109/JLT.2019.2902045.

40. Sanchez, P.; Zamarreno, C. R.; Arregui, F. J.; Matias, I. R. LMR-Based Optical Fiber Refractometers for Oil Degradation Sensing Applications in Synthetic Lubricant Oils. *J. Light. Technol.* **2016**, *34*, 4537–4542, doi:10.1109/JLT.2016.2562701.

41. Vikas; Verma, R. K. Sensitivity enhancement of a lossy mode resonance based tapered fiber optic sensor with an optimum taper profile. *J. Phys. D. Appl. Phys.* **2018**, *51*, 415302, doi:10.1088/1361-6463/aadb0f.

42. Zubiate, P.; Zamarreño, C. R.; Villar, I. Del; Matias, I. R.; Arregui, F. J. J.; Del Villar, I.; Matias, I. R.; Arregui, F. J. J. High

sensitive refractometers based on lossy mode resonances (LMRs) supported by ITO coated D-shaped optical fibers. *Opt. Express* **2015**, *23*.

43. Zamarreo, C. R.; Hernaez, M.; Del Villar, I.; Matias, I. R.; Arregui, F. J. ITO Coated Optical Fiber Refractometers Based on Resonances in the Infrared Region. *IEEE Sens. J.* **2010**, *10*, 365–366, doi:10.1109/JSEN.2009.2034628.

44. Chiavaioli, F.; Zubiate, P.; Del Villar, I.; Zamarreño, C. R.; Giannetti, A.; Tombelli, S.; Trono, C.; Arregui, F. J.; Matias, I. R.; Baldini, F. Femtomolar Detection by Nanocoated Fiber Label-Free Biosensors. *ACS Sensors* **2018**, *3*, 936–943, doi:10.1021/acssensors.7b00918.

45. Niedziałkowski, P.; Białobrzeska, W.; Burnat, D.; Sezemsky, P.; Stranak, V.; Wulff, H.; Ossowski, T.; Bogdanowicz, R.; Koba, M.; Śmietana, M. Electrochemical performance of indium-tin-oxide-coated lossy-mode resonance optical fiber sensor. *Sensors Actuators B Chem.* **2019**, *301*, 127043, doi:10.1016/j.snb.2019.127043.

46. Sobaszek, M.; Burnat, D.; Sezemsky, P.; Stranak, V.; Bogdanowicz, R.; Koba, M.; Siuzdak, K.; Śmietana, M. Enhancing electrochemical properties of an ITO-coated lossy-mode resonance optical fiber sensor by electrodeposition of PEDOT:PSS. *Opt. Mater. Express* **2019**, *9*, 3069, doi:10.1364/ome.9.003069.

47. Ascorbe, J.; Corres, J. M.; Matias, I. R.; Arregui, F. . High sensitivity humidity sensor based on cladding-etched optical fiber and lossy mode resonances. *Sensors Actuators B Chem.* **2016**, *233*, 7–16, doi:10.1016/j.snb.2016.04.045.

48. Zubiate, P.; Urrutia, A.; Zamarreño, C. R.; Egea-Urra, J.; Fernández-Irigoyen, J.; Giannetti, A.; Baldini, F.; Díaz, S.; Matias, I. R.; Arregui, F. J.; Santamaría, E.; Chiavaioli, F.; Del Villar, I. Fiber-based early diagnosis of venous thromboembolic disease by label-free D-dimer detection. *Biosens. Bioelectron. X* **2019**, *2*, 100026, doi:10.1016/j.biosx.2019.100026.

49. Sánchez, P.; Zamarreño, C. R.; Hernaez, M.; Del Villar, I.; Matias, I. R.; Arregui, F. J. SnO2 based optical fiber refractometers. In *OFS2012 22nd International Conference on Optical Fiber Sensors*; Liao, Y., Jin, W., Sampson, D. D., Yamauchi, R., Chung, Y., Nakamura, K., Rao, Y., Eds.; SPIE, 2012; Vol. 8421, pp. 84216B-84216B–4.

50. Sharma, S.; Gupta, B. D. Lossy Mode Resonance-Based Fiber Optic Sensor for the Detection of As (III) Using α -Fe 2 O 3 /SnO 2 Core–Shell Nanostructures. *IEEE Sens. J.* **2018**, *18*, 7077–7084, doi:10.1109/JSEN.2018.2851610.

51. Hernaez, M.; Mayes, A.; Melendi-Espina, S. Graphene Oxide in Lossy Mode Resonance-Based Optical Fiber Sensors for Ethanol Detection. *Sensors* **2017**, *18*, 58, doi:10.3390/s18010058.

52. Vicente, A.; Santano, D.; Zubiate, P.; Urrutia, A.; Del Villar, I.; Zamarreño, C. R. Lossy mode resonance sensors based on nanocoated multimode-coreless-multimode fibre. *Sensors Actuators B Chem.* **2020**, *304*, 126955, doi:10.1016/j.snb.2019.126955.

53. Zamarreno, C. R.; Sanchez, P.; Hernaez, M.; Del Villar, I.; Fernandez-Valdivielso, C.; Matias, I. R.; Arregui, F. J. Sensing Properties of Indium Oxide Coated Optical Fiber Devices Based on Lossy Mode Resonances. *IEEE Sens. J.* **2012**, *12*, 151–155, doi:10.1109/JSEN.2011.2142181.

54. Sanchez, P.; Gonzalez, K.; Zamarreño, C. R.; Hernaez, M.; Matias, I. R.; Arregui, F. J. High-sensitive lossy mode resonance-based optical fiber refractometers by means of sputtered indium oxide thin-films. In *Smart Sensors, Actuators, and MEMS VII; and Cyber Physical Systems*; Sánchez-Rojas, J. L., Brama, R., Eds.; SPIE, 2015; Vol. 9517, p. 95171V.

55. Fuentes, O.; Del Villar, I.; Corres, J. M.; Matias, I. R. Lossy mode resonance sensors based on lateral light incidence in nanocoated planar waveguides. *Sci. Rep.* **2019**, *9*, 8882, doi:10.1038/s41598-019-45285-x.

56. Paliwal, N.; Punjabi, N.; John, J.; Mukherji, S. Design and Fabrication of Lossy Mode Resonance Based U-Shaped Fiber Optic Refractometer Utilizing Dual Sensing Phenomenon. *J. Light. Technol.* **2016**, *34*, 4187–4194, doi:10.1109/JLT.2016.2585922.

57. Usha, S. P.; Gupta, B. D. Urinary p-cresol diagnosis using nanocomposite of ZnO/MoS2 and molecular imprinted polymer on optical fiber based lossy mode resonance sensor. *Biosens. Bioelectron.* **2018**, *101*, 135–145, doi:10.1016/j.bios.2017.10.029.

58. Paliwal, N.; John, J. Design and Modeling of Highly Sensitive Lossy Mode Resonance-Based Fiber-Optic Pressure Sensor. *IEEE Sens. J.* **2018**, *18*, 209–215, doi:10.1109/JSEN.2017.2771313.

59. Paliwal, N.; John, J. Theoretical modeling and investigations of AZO coated LMR based fiber optic tapered tip sensor utilizing an additional TiO2 layer for sensitivity enhancement. *Sensors Actuators B Chem.* **2017**, *238*, 1–8, doi:10.1016/j.snb.2016.07.032.

60. Hernáez, M.; Del Villar, I.; Zamarreño, C. R.; Arregui, F. J.; Matias, I. R. Optical fiber refractometers based on lossy mode resonances supported by TiO_2 coatings. *Appl. Opt.* **2010**, *49*, 3980, doi:10.1364/AO.49.003980.

61. Zhao, W.-M.; Wang, Q.; Wang, X.-Z.; Li, X.; Jing, J.-Y.; Sun, H.-Z. Theoretical and experimental research of lossy mode resonance-based high-sensitivity optical fiber refractive index sensors. *J. Opt. Soc. Am. B* **2019**, *36*, 2069, doi:10.1364/JOSAB.36.002069.

62. Tiwari, D.; Mullaney, K.; Korposh, S.; James, S. W.; Lee, S.-W.; Tatam, R. P. An ammonia sensor based on Lossy Mode Resonances on a tapered optical fibre coated with porphyrin-incorporated titanium dioxide. *Sensors Actuators B Chem.* **2017**, *242*, 645–652, doi:10.1016/j.snb.2016.11.092.

63. Wang, X.-Z.; Wang, Q. Theoretical Analysis of a Novel Microstructure Fiber Sensor Based on Lossy Mode Resonance. *Electronics* **2019**, *8*, 484, doi:10.3390/electronics8050484.

64. Wang, X.; Wang, Q.; Song, Z.; Qi, K. Simulation of a microstructure fiber pressure sensor based on lossy mode resonance. *AIP Adv.* **2019**, *9*, 095005, doi:10.1063/1.5112090.

65. Rivero, P. J.; Goicoechea, J.; Hernaez, M.; Socorro, A. B.; Matias, I. R.; Arregui, F. J. Optical fiber resonance-based pH sensors using gold nanoparticles into polymeric layer-by-layer coatings. *Microsyst. Technol.* **2016**, *22*, 1821–1829, doi:10.1007/s00542-016-2857-8.

66. Rivero, P. J.; Urrutia, A.; Goicoechea, J.; Arregui, F. J. Optical fiber humidity sensors based on Localized Surface Plasmon Resonance (LSPR) and Lossy-mode resonance (LMR) in overlays loaded with silver nanoparticles. *Sensors Actuators B Chem.* **2012**, *173*, 244–249, doi:10.1016/j.snb.2012.07.010.

67. Urrutia, A.; Goicoechea, J.; Rivero, P. J.; Pildain, A.; Arregui, F. J. Optical fiber sensors based on gold nanorods embedded in polymeric thin films. *Sensors Actuators B Chem.* **2018**, *255*, 2105–2112, doi:10.1016/j.snb.2017.09.006.

Chapter 3

Tin oxide thin-films for LMR-based refractometers development

Tin dioxide thin-films have been studied in order to optimize the sensitivity of lossy mode resonances (LMR) based sensors in the refractive index working range of fused silica. The effects of the thin film thickness and the polarization of light in a SnO_2 coated D-shaped single mode optical fiber have been evaluated and optimized. This work led to an unprecedented sensitivity of over one million nanometers per refractive index unit (RIU), which means that a variation below 10^{-9} RIU with a 1 pm resolution detector could be achieved. This research is a milestone for the development of new high sensitivity devices and proves once again the great potential of LMR-based sensors opening the door to new applications, such as gear oil degradation, or biomedical devices where previous devices could not provide enough sensitivity.

The contents of this chapter have been partially published under the title "*Is there a frontier in sensitivity with Lossy mode resonance (LMR) based refractometers?*" in Scientific Reports 7, 10280 (2017).

3.1. Introduction

The wide number of materials that fulfill the requirements for the generations of lossy mode resonances provide a great flexibility in the development of sensors based on such phenomenon. This way, LMR-based sensors have been fabricated using indium tin oxide (ITO) [1,2], titanium dioxide [3], zinc oxide [4] or polymeric [5] coatings by means of layer-by-layer [5], sputtering deposition [1,2], thermal evaporation [4] or dip-coating [4,6] techniques, to name a few. It is clear that the coating material causes a direct impact on the performance of the LMR-based sensors and a fil with the adequate optical properties (such as a high refractive index) can maximize their sensitivity [7].

It has been explained previously how the maximum sensitivity for a LMR-based refractometer was achieved in the fused silica RI working range (n = 1.449) using an ITO coating (304,361 nm/RIU) [1]. In the RI range of water, a comparison of refractometers designed with ITO and tin oxide films proved that tin oxide was capable to provide a higher sensitivity (14,501 nm/RIU vs. 8,742 nm/RIU) [1,2]. This behavior is explained by the higher refractive index of tin oxide coating which, according to the theoretical work by Del Villar et al. [7], produced LMRs with higher sensitivity. Therefore, it was expected that a LMR based refractometer working in a higher RI range would surpass the performance obtained with ITO thin-films.

The aim of the research explained in this chapter is to corroborate the expected behavior of tin oxide coating as a material capable to support highly sensitive LMRs in a high refractive index (RI) range, close to the RI of fused silica. Tin oxide presents a high refractive index (n) and a low extinction coefficient (k), as it was shown on fig. 2.9. These characteristics make it a great choice for LMR based sensors. Besides the expected good performance of tin dioxide, it is a good candidate to be widely used for LMR fabrication because of its relatively low cost, high availability, and the multiple methods that can be applied to fabricate tin oxide thin-films. These methods

include spray [8], sol-gel [9] and DC-Sputtering [1], which will be the method used in this research. Tin oxide has also been widely studied as a material for the development of sensing applications [10].

3.2. Experimental considerations

For the purpose of this research, a D-shaped fiber (Phoenix Photonics LTD.) was chosen as the base to develop the refractometer. It is constructed form a standard single mode fiber (Corning SMF-28) where a segment of 1.7 cm has been side-polished. It presents an attenuation of 3 dB at 1550 nm and SRI of 1.5 due to the polishing. It was chosen due to its capability to allow separation of propagation modes using polarized light, which permits to observe narrower LMR and, in consequence, optimize the figure of merit. The optimal wavelength working range in this case is the NIR (1150-1650 nm), considering the working range of the elements involved in this setup.

3.2.1. Fabrication setup

Tin oxide thin-films were fabricated both on D-shaped fibers and silicon wafers. A DC-Sputter coater (Emitech K675X, Quorum Technologies) was used for this purpose. The sputtering target was a SnO_2 99.99% purity target from Zhongnuo Advanced Materials. It is worth noting that the dark color of the target used in these experiments indicate that it was a not fully oxidized tin oxide (SnO_x), which raised the electrical conductivity of the material facilitating the deposition by DC sputtering. The conditions for the sputtering depositions were a pressure of $9 \cdot 10^{-2}$ mbar of argon and a current of 90 mA. The fiber was placed directly below the target at a fixed distance of 8 cm. The thickness of the coating is determined by the deposition time, as a deposition rate of 0.793 nm/s was estimated under those conditions. During the fabrication, the setup involved the use of two laser sources at wavelengths of 1310 and 1550 nm (BCP 400 A), a set of two wavelength division multiplexers (WDM) and a couple of power meters (RIFOCS 575 L) to observe the evolution of the transmission at said wavelengths during the

deposition process. The power meters were connected to a data logger (HP 34970 A) to save the information. A schematic representation of this setup can be observed in fig. 3.1.

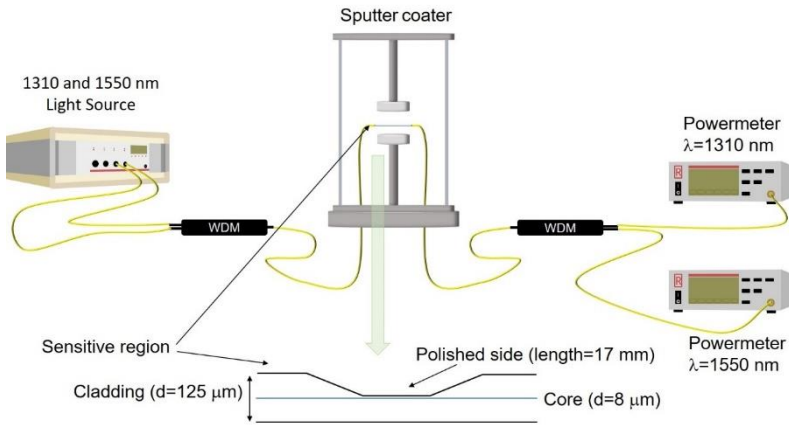

Figure 3.1: *Fabrication setup which allows to monitor the output at two different wavelengths during the deposition of the SnO_2 thin-film. The sensitive region of the sensor is a 17 mm side polished (D-shaped) segment of SMF, which is placed horizontally under the target in the sputter coater.*

3.2.2. Characterization setup

In order to characterize the device as a refractometer, a different setup is needed (fig. 3.2). For this purpose, a superluminescent emitting diodes light source (SLED, HP 83437 A) is used as a broadband light source, and an optical spectrum analyzer (OSA, HP 86142 A) receives the signal. This setup also makes use of an in-fiber linear light polarizer (Phoenix Photonics) and a manual polarization controller (Thorlabs FPC 032). These elements play a key role in this configuration. Noting that this setup makes no use of polarization-maintaining fibers, the combination of the polarizer and the polarization controller is necessary to isolate and select the desired polarization state in the sensitive region.

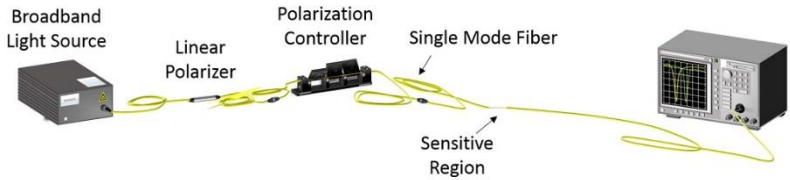

Figure 3.2: *Characterization setup used to test the sensor as a refractometer. The polarization controller allows to control the polarization state of the light propagated through the sensitive region and the output is monitored in the OSA.*

This setup was used to analyze the optical spectrum when the sensitive region of the fiber was tested under different SRI values. In order to do so, water-glycerol (Panreac Technical Grade) solutions of different concentrations were prepared. Obtained solutions refractive indices ranged between 1.44 and 1.45. The refractive index of such solutions was measured with a commercial refractometer (Mettler Toledo Refracto 30GS). The refractive index of each solution was measured 10 times and then averaged, in order to minimize the error. The D-shaped fiber was submerged in such solutions and the spectra received in each case was later processed using a Matlab® algorithm.

3.3. Results

The experimental procedures involved the deposition of several tin oxide coatings in order to study the fabrication process. Prior to the fabrication of a practical refractometer, the fabrication setup described in the previous section was employed for a long-time deposition process, in order to observe how the LMRs behave during the thin-film growth. This experiment was not designed to fabricate highly sensitive refractometers, but to study and analyze the thin-film fabrication process on the D-shaped optical fiber. Silicon wafers were also placed next to the D-shaped fibers during the depositions to use them as probes to measure the film thickness.

Once this process was completed, the obtained information was used for the fabrication of the practical sensors, which were later characterized as refractometers.

3.3.1. Probe development and fabrication

Before analyzing the optical phenomena involved in the sensor development, it is important to study the physical performance of the deposition. During the fabrication of the different fiber probes, a piece of silicon wafer was placed in the sputtering chamber. This allows to obtain a thin-film on the wafer with the same characteristics as the one on the fiber, that can be later used to measure the film thickness. We can see on fig. 3.3 an example of a SEM image of one of the samples coated for a total time of 3 minutes, used to measure the thickness of the tin oxide coating.

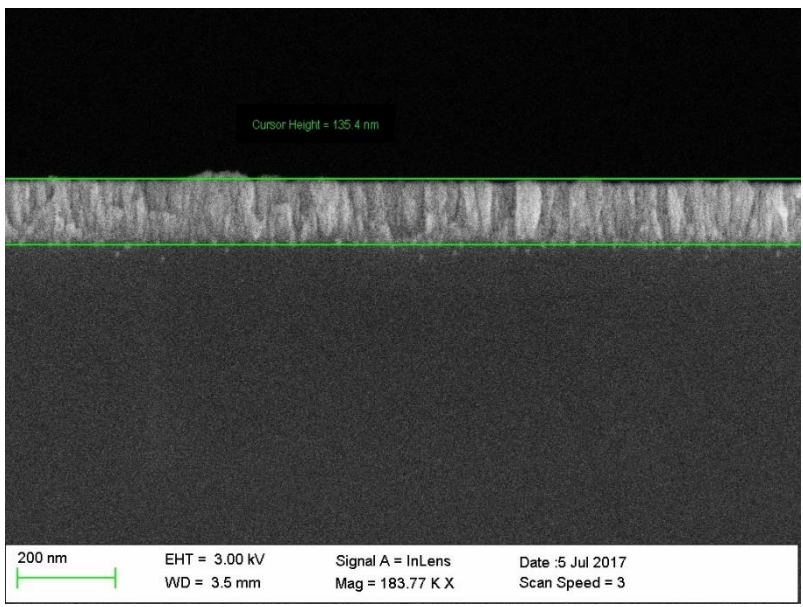

Figure 3.3: *SEM image of a transversal cut of a tin oxide coated silicon wafer. The film was fabricated on the same conditions as the D-shaped optical fibers for a deposition time of 3 minutes, which allows to measure the thickness of the coatings.*

The thickness of the film of several samples coated with a deposition time of 2, 3 and 4 minutes were measured. Table 3.1

shows the obtained values, which were used for the estimation of the deposition rate at the established deposition parameters. This data determined that the process had a constant deposition rate of 0.793 nm/s in average.

Time (minutes)	Thickness (nm)
2	93.81
	89.11
	92.29
	93.90
	90.82
	91.52
3	128.0
	137.5
	131.2
	135.4
4	182.8
	200.1
	207.3
	200.1
	200.4

Table 3.1: *Measured thickness of several tin oxide coated samples. It allows to determine the estimated deposition rate of the sputtering process.*

It is important to analyze the behavior of the LMRs with coatings of different thicknesses. The above-mentioned fabrication setup (fig. 3.1) was designed to study the evolution of the LMRs as the thickness of the tin oxide thin-film increases. It allows to observe the transmission of the device at the selected wavelengths (λ_1=1310 and λ_2=1550 nm) during the deposition process. It is known that LMRs shift to longer wavelengths when the thickness of the coating increases. Therefore, in this setup it is expected to observe the appearance of LMRs firstly at the shorter wavelength λ_1 and next at the longer wavelength λ_2.

Accordingly, we can observe such phenomenon in fig. 3.4. This graph shows the temporal evolution of the transmitted power at the established wavelengths while the film is being deposited for a total of 50 minutes. Considering the study of the deposition rate explained above, we can estimate the thickness of the coating at any given point in time in this process. It can be seen a number of 'dips' or absorbance peaks in the measured power, which correspond to the appearance of LMRs at the wavelength in question for the corresponding coating thickness. In all cases we can see how the absorbance peaks (LMRs) take place first at λ_1 and later at λ_2. The first order LMR is actually observed as two very narrow absorbance peaks, which correspond to the LMRs at the TE (transverse electric) and TM (transverse magnetic) modes of propagation. Note that in this setup no polarizer is used so both contributions are observed simultaneously. It is worth noting that in the second order LMR this phenomenon can be also appreciated at λ_1 as two close peaks are seen, but at λ_2 it is only seen a single, wider peak. For the rest of the LMRs monitored during this experiment both contributions are observed together as a single LMR at both λ_1 and λ_2. This is due to the fact that in the first order LMR both components are separated in wavelength, which makes it possible to distinguish them in this setup without polarized light. In contrast, for LMRs of higher order these components overlap and, as a result, in this setup they are observed as single wider resonances.

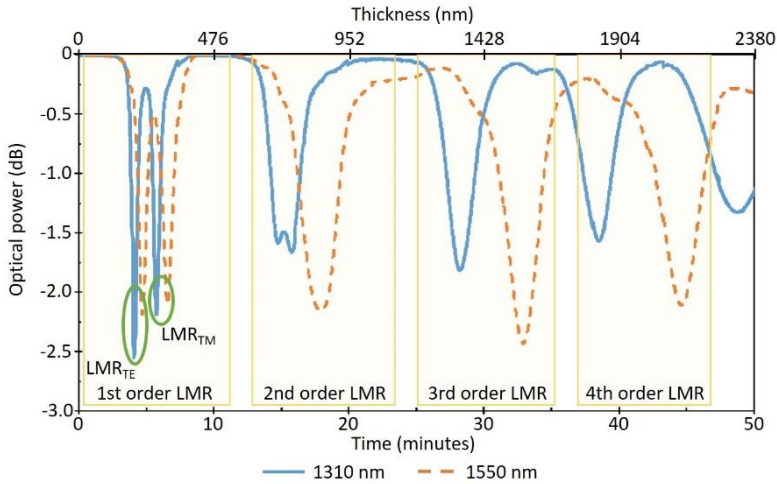

Figure 3.4: *Output optical power at the monitored wavelengths (λ_1=1310 and λ_2=1550 nm) during the deposition process. The bottom axis shows the deposition time and the top axis represents the projected coating thickness at that moment. LMRs of several orders can be observed. In the first order LMR, two components can be distinguished, corresponding to the LMRs of the TE and TM modes.*

There is another characteristic behavior of the LMRs that can be appreciated in this graph. It is clearly noticeable that the temporal distance between the same order LMR at λ_1 and at λ_2 gradually increases from the first to the fourth order LMR. It is known that the lower the order of the resonance, the more sensitive to both SRI and coating thickness the LMR is. In this graph, this phenomenon is observed precisely in the increment of the thickness needed for the LMR to shift from λ_1 to λ_2. The first order LMR (both TE and TM) require a very little increment in thickness (28 nm) to shift $\Delta\lambda$ ($\Delta\lambda = \lambda_2 - \lambda_1$ = 240 nm), whereas the fourth order resonance requires an increment of 289 nm in thickness to induce a shift of $\Delta\lambda$. This means that the first order LMR presents a sensitivity approximately 10 times higher than the fourth order LMR, pointing that the LMR of the lowest possible order must be chosen in order to achieve the maximum sensitivity.

These experiments provide information of the tin oxide thin-film thickness necessary to observe LMRs of different orders at λ_1 and λ_2

in air (with SRI = 1). Once the fiber is submerged in the glycerol/water solutions, the LMR shifts to longer wavelength. The extreme sensitivity expected for this resonance implies an added difficulty to effectively tune the resonance. It must be considered that the LMR is intended to be in our working wavelength range (1150-1650 nm) in the glycerol/water solutions (SRI in the 1.44-1.45 range). This means that, during the construction when the surrounding media is air (SRI=1), the LMR would be observed at a shorter wavelength, out of such spectral window. This situation complicates the monitorization and tuning of the LMR during the deposition in real time.

3.3.2. Refractometer characterization

Taking into consideration all the information obtained in the previously described experimentation process, new D-shaped fibers were coated with tin oxide so that the first order LMR is located in the working spectral window for SRI above 1.44. This was achieved with a tin oxide coating of 14 nm. Fig. 3.5 shows a SEM image of the SnO_2 thin-film deposited on a silicon wafer under the same conditions and the measured thickness. Such measurement is in agreement with the deposition rate estimated above (0.793 nm/s), given the deposition time of this sample (18 seconds).

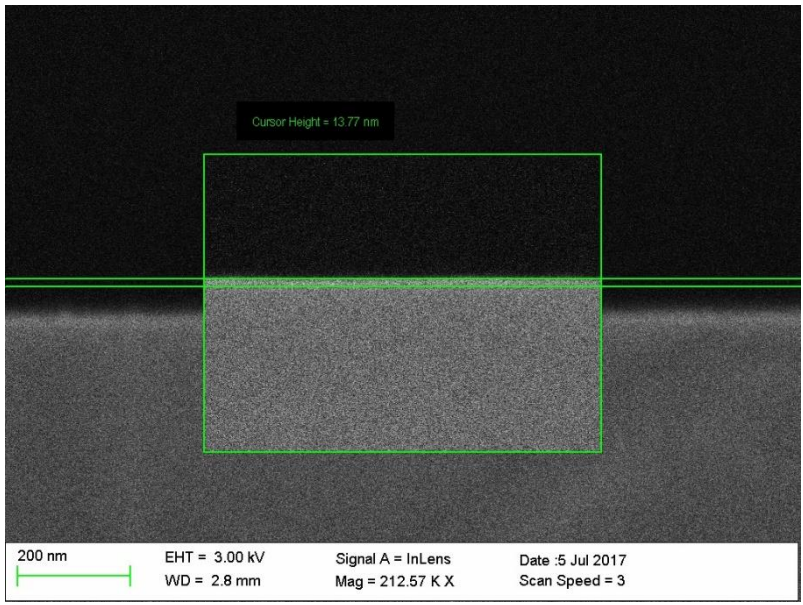

Figure 3.5: *SEM image of a tin oxide coated silicon wafer deposited at the same time as the D-shaped fiber characterized as a refractometer for a total deposition time of 18 seconds. The measured thickness is in agreement with the calculated value obtained from the estimated deposition rate.*

It should be considered the impact that a thick or a thin coating would have on the tuning of these resonances. Thicker SnO_2 films would shift the LMRs to longer wavelengths. Therefore, they could be used for the monitorization of lower SRI values. Contrarily, thin SnO_2 coatings cause the LMRs to be observed at shorter wavelengths, which enables the monitorization of higher SRI values in our spectral working range, which is the purpose of this study. However, there are some limitations that must be considered. First of all, as the SRI approaches the refractive index of the optical fiber, the absorbance of the D-shaped fiber increases and masks the LMRs. There is also a practical issue, which is the fact that the fabrication of thin coatings may lead to inhomogeneous films that could distort the resonances.

The characterization setup described in the previous section (fig. 3.2) was used while the D-shaped fiber was immersed in solutions

of different refractive index to analyze the response of the LMR to variations of SRI. The use of the polarizer and polarization controller allowed to isolate the modes and observe each mode (TE and TM) and the corresponding resonances (LMR_{TE} and LMR_{TM}) separately. It permitted to obtain much narrower resonances, which led to a better figure of merit (FOM), defined as the ratio sensitivity/FWHM (where FWHM is the full width at half maximum). Previous studies showed that the LMR that appears first (with lower SRI values) corresponds to the TE mode, and the following one corresponds to the TM mode [11,12]. This device showed two different resonances: one for a SRI between 1.4415 and 1.4446 corresponding to LMR_{TE}, and a second one for the SRI in the range of 1.4481-1.4486 corresponding to LMR_{TM}. Fig. 3.6 shows the transmittance spectra obtained during such tests. It should be noted that in this case both, TE and TM, resonances are spectrally separated enough in a way they are not seen simultaneously for any SRI value in our spectral window. It should be also remarked that they belong to different propagation modes because it is necessary to alter the polarization state (using the manual polarization controller) in order to observe the corresponding LMR when the SRI changes from the range of LMR_{TE} to the range of LMR_{TM}.

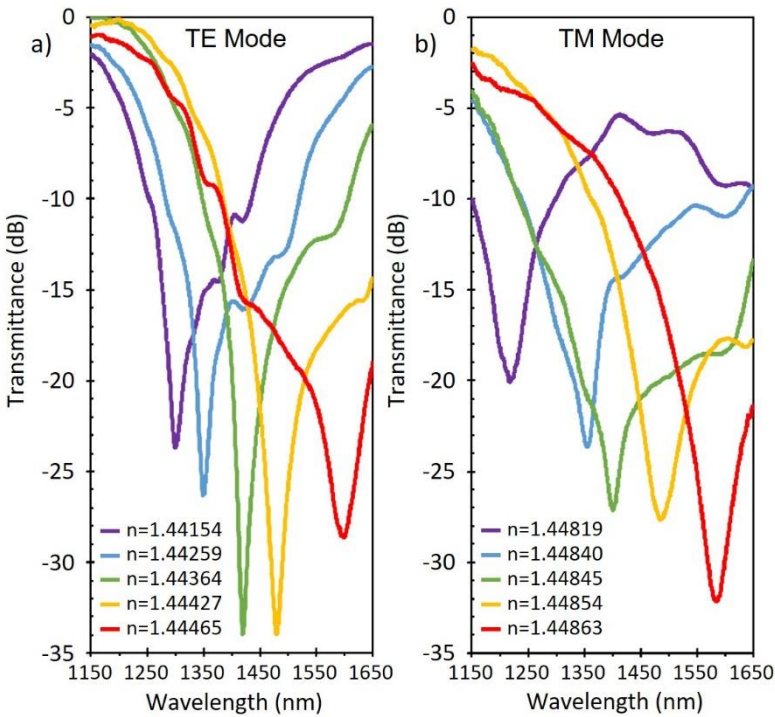

Figure 3.6: *Transmittance spectra measured when the sensitive region was immersed in solutions of different refractive index. The absorbance peaks showed here correspond to the LMRs and it can be observed how the LMRs shift to longer wavelengths as the SRI increases. (a) Spectra obtained for SRI values between 1.4415 and 1.4447 corresponding to the TE mode (LMR_{TE}) and (b) Spectra corresponding to the TM mode (LMR_{TM}) for SRI values between 1.4481 and 1.4487.*

Fig. 3.6a shows the spectra obtained with the TE mode for 5 different values of SRI, while fig. 3.6b shows the spectra corresponding to the TM mode, with 5 values of SRI higher than those used for the TE mode. In both cases the LMRs show high attenuation (almost 35 dB) and are relatively narrow. Here, it is also important to observe that the LMR_{TE} is narrower, with a minimum FWHM of 9 nm, while the LMR_{TM} presents a minimum FWHM of 36.9 nm. In contrast LMR_{TM} shows greater wavelength shift than LMR_{TE} for a lower SRI variation. This difference is explained by the greater sensitivity shown by the LMRs for higher SRI ranges [7].

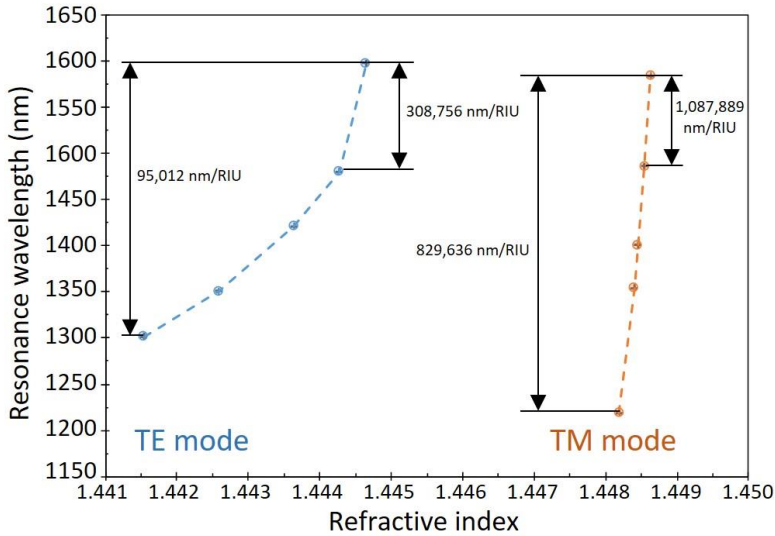

Figure 3.7: *Calibration curve of the developed refractometer. Represents the central wavelengths of the LMRs as a function of the surrounding media refractive index (SRI). The slope, related to the sensitivity, increases for greater SRI values.*

A key element to understand the behavior of these devices is the refractometric calibration curve (fig. 3.7). It represents the central spectral location of the LMR for each SRI value. These figures are obtained by an algorithm in Matlab® that calculates the central position of the LMR by approximating a region around its lowest point to a parabolic curve. This calibration curve that can be seen on fig. 3.7 permits to determine a SRI value in function of the central wavelength of the LMR measured by our device. The slope of the curve is related to the sensitivity of the device, in a way that a greater slope implies a greater sensitivity, allowing to determine SRI variations with greater precision. It is important to note that the relationship between the LMR position and SRI is not linear, meaning that the sensitivity increases at high wavelengths and SRI values. This phenomenon can be clearly observed in fig. 3.7 where two distinct calibration curves are represented: one for the LMR_{TE} and LMR_{TM}. In the case of LMR_{TE} calibration curve, working in the lower SRI range, it presents an average sensitivity of 95,012 nm/RIU,

with a maximum value of 308,756 nm/RIU for the highest SRI figures. Considering its FWHM parameter, LMR_{TE} reaches a FOM of 10,556.89 RIU^{-1}. The LMR_{TM} in the graph is represented as an almost vertical line, due to its extremely high sensitivity of 829,636 nm/RIU in average. In this case, it also presents a higher sensitivity for the greater SRI values, with a maximum of 1,087,889 nm/RIU. Such figure implies that if a OSA with a standard resolution of 1 picometer were used, a variation of $9.19 \cdot 10^{-10}$ units of refractive index could be measured. This resonance, despite being wider than the LMR_{TE} presents a higher FOM due to its higher sensitivity. The FOM of the LMR_{TM} is 29,805.18 RIU^{-1}, which is almost three times higher than the previous case.

3.4. Conclusions

The research presented here achieved the successful fabrication of a lossy mode resonance based refractometer using tin oxide thin-film in the fused silica refractive index working range. The use of a D-shaped fiber setup and the precise control of the coating fabrication process allowed to obtain films thin enough to tune the LMRs in the desired working range of wavelength and SRI. The use of tin oxide allowed to fabricate a refractometer 3.5 times more sensitive than the most sensitive one reported previously [1], which made use of ITO thin-films. This improvement is directly related to the higher refractive index shown by tin oxide, in comparison with ITO [7].

The working SRI range reported here seems appropriate for the use in industrial applications such as gear lubricant oil degradation [13]. This research has been oriented to the development of refractometers working on the mentioned SRI range, but the capacity to tune the LMR to work in a different operational range by modifying the thickness of the coating can be easily applied to develop sensors for multiple applications. For instance, they could be adapted to purposes such as gas sensing, biomedical applications or measurement of °Brix.

The extremely high sensitivity demonstrated by LMR-based refractometers in this study opens the possibility to achieve limits of detection that could not be obtained before. It also proves the capacity of the LMR phenomenon to be the basis for the development of a successful label-free sensing platform.

The achievements presented in this chapter are a direct consequence of the optical properties of tin oxide. It should be noted, however, that there are other materials which possesses exceptional optical properties that theoretically predict that their use for LMR-based sensors fabrication could improve the performance of tin oxide. It is also worth noting that this study focuses on the bulk modifications of refractive index, but these sensors could also be functionalized to work as surface detectors of a number of elements such as proteins [14] or different gases [4,15–17]. Finally, it is important to remark again that the optimization of the device sensitivity is as important as the chemical stability, ageing, or the affinity of the response to the parameter to measure when it comes to find the right coating material for a target application. Having all that into consideration, the next steps involve the study of new coating materials for the development of LMR-based sensors. The next chapter will detail the experimental study of aluminum-doped zinc oxide (AZO) for such purpose.

Bibliography

1. Arregui, F. J.; Del Villar, I.; Zamarreño, C. R.; Zubiate, P.; Matias, I. R. Giant sensitivity of optical fiber sensors by means of lossy mode resonance. *Sensors Actuators B Chem.* **2016**, *232*, 660–665, doi:10.1016/j.snb.2016.04.015.

2. Zubiate, P.; Zamarreño, C. R.; Villar, I. Del; Matias, I. R.; Arregui, F. J. J.; Del Villar, I.; Matias, I. R.; Arregui, F. J. J. High sensitive refractometers based on lossy mode resonances (LMRs) supported by ITO coated D-shaped optical fibers. *Opt. Express* **2015**, *23*.

3. Tiwari, D.; Mullaney, K.; Korposh, S.; James, S. W.; Lee, S.-W.; Tatam, R. P. An ammonia sensor based on Lossy Mode Resonances on a tapered optical fibre coated with porphyrin-incorporated titanium dioxide. *Sensors Actuators B Chem.* **2017**, *242*, 645–652, doi:10.1016/j.snb.2016.11.092.

4. Usha, S. P.; Mishra, S. K.; Gupta, B. D. Fiber optic hydrogen sulfide gas sensors utilizing ZnO thin film/ZnO nanoparticles: A comparison of surface plasmon resonance and lossy mode resonance. *Sensors Actuators B Chem.* **2015**, *218*, 196–204, doi:10.1016/j.snb.2015.04.108.

5. Zamarreño, C. R.; Hernáez, M.; Del Villar, I.; Matías, I. R.; Arregui, F. J. Optical fiber pH sensor based on lossy-mode resonances by means of thin polymeric coatings. *Sensors Actuators B Chem.* **2011**, *155*, 290–297, doi:10.1016/j.snb.2010.12.037.

6. Sanchez, P.; Zamarreño, C. R.; Hernaez, M.; Del Villar, I.; Fernandez-Valdivielso, C.; Matias, I. R.; Arregui, F. J. Lossy mode resonances toward the fabrication of optical fiber humidity sensors. *Meas. Sci. Technol.* **2012**, *23*, 014002, doi:10.1088/0957-0233/23/1/014002.

7. Del Villar, I.; Hernaez, M.; Zamarreño, C. R.; Sánchez, P.; Fernández-Valdivielso, C.; Arregui, F. J.; Matias, I. R. Design rules for lossy mode resonance based sensors. *Appl. Opt.*

2012, *51*, 4298, doi:10.1364/AO.51.004298.

8. Serin, T.; Serin, N.; Karadeniz, S.; Sarı, H.; Tuğluoğlu, N.; Pakma, O. Electrical, structural and optical properties of SnO2 thin films prepared by spray pyrolysis. *J. Non. Cryst. Solids* **2006**, *352*, 209–215, doi:10.1016/j.jnoncrysol.2005.11.031.

9. Racheva, T. M.; Critchlow, G. W. SnO2 thin films prepared by the sol-gel process. *Thin Solid Films* **1997**, *292*, 299–302, doi:10.1016/S0040-6090(96)08956-0.

10. Preiß, E. M.; Rogge, T.; Krauß, A.; Seidel, H. Gas Sensing by SnO2 Thin Films Prepared by Large-area Pulsed Laser Deposition. *Procedia Eng.* **2015**, *120*, 88–91, doi:10.1016/j.proeng.2015.08.572.

11. Villar, I. Del; Zamarreño, C. R.; Sanchez, P.; Hernaez, M.; Valdivielso, C. F.; Arregui, F. J.; Matias, I. R. Generation of lossy mode resonances by deposition of high-refractive-index coatings on uncladded multimode optical fibers. *J. Opt.* **2010**, *12*, 095503.

12. Del Villar, I.; Zamarreño, C. R.; Hernaez, M.; Arregui, F. J.; Matias, I. R. Lossy mode resonance generation with indium-tin-oxide-coated optical fibers for sensing applications. *J. Light. Technol.* **2010**, *28*, 111–117, doi:10.1109/JLT.2009.2036580.

13. Sanchez, P.; Zamarreno, C. R.; Arregui, F. J.; Matias, I. R. LMR-Based Optical Fiber Refractometers for Oil Degradation Sensing Applications in Synthetic Lubricant Oils. *J. Light. Technol.* **2016**, *34*, 4537–4542, doi:10.1109/JLT.2016.2562701.

14. Zubiate, P.; Zamarreño, C. R.; Sánchez, P.; Matias, I. R.; Arregui, F. J. High sensitive and selective C-reactive protein detection by means of lossy mode resonance based optical fiber devices. *Biosens. Bioelectron.* **2017**, *93*, 176–181, doi:10.1016/j.bios.2016.09.020.

15. Mishra, S. K.; Usha, S. P.; Gupta, B. D. A lossy mode

resonance-based fiber optic hydrogen gas sensor for room temperature using coatings of ITO thin film and nanoparticles. *Meas. Sci. Technol.* **2016**, *27*, 045103, doi:10.1088/0957-0233/27/4/045103.

16. Usha, S. P.; Mishra, S. K.; Gupta, B. D. Zinc oxide thin film/nanorods based lossy mode resonance hydrogen sulphide gas sensor. *Mater. Res. Express* **2015**, *2*, 095003, doi:10.1088/2053-1591.

17. Sharma, S.; Gupta, B. D. Lossy Mode Resonance-Based Fiber Optic Sensor for the Detection of As (III) Using α -Fe 2 O 3 /SnO 2 Core–Shell Nanostructures. *IEEE Sens. J.* **2018**, *18*, 7077–7084, doi:10.1109/JSEN.2018.2851610.

Chapter 4

Aluminum-doped zinc oxide (AZO) for LMR-based refractometers development

The introduction of new coating materials is of high importance to impulse the development of the LMR-based refractometers. This chapter presents the first experimental use of aluminum-doped zinc oxide (AZO) thin-films for the design and fabrication of LMR-based sensors. The AZO thin-films fabricated have demonstrated their capability to support LMRs, opening the possibility to the proposal of new sensing applications.

The contents of this chapter have been partially published in the paper *Aluminum doped zinc oxide (AZO) coated optical fiber LMR refractometers—An experimental demonstration* in Sensors and Actuators B: Chemical vol. 281, 698-704 (2019).

4.1. Introduction

The previous chapter discussed the optimization of tin oxide thin films with the purpose of maximizing the sensitivity achieved by LMR-based refractometers. In this chapter (and the following ones) the fabrication and characterization of new materials for LMR-based sensors development will be presented.

The introduction of new materials is possible because the optical properties required for a thin-film to generate a LMR permit a number of different materials to be used for this purpose [1]. Given the versatility of LMR-based refractometers to develop sensing applications, it is interesting to open the possibility to work with different materials that could widen the range of applications. It is known that several transparent conductive oxides (TCO) possess the optimal properties for LMR generation (amongst other materials). Earlier, it was discussed that zinc oxide had successfully been employed for the fabrication of LMR-based sensors [2–7]. However, there are some doped zinc oxides that are also potential candidates to be used in this field. The doping of zinc oxide with other metals has been previously studied and introduces interesting changes in the properties of the film [8,9].

Aluminum-doped zinc oxide (AZO), for instance, has been suggested in previous works as a good material for LMR-based refractometers fabrication. Paliwal et al. [10,11] presented theoretical studies with AZO coatings in the design of such sensors. Besides, AZO has been successfully used in the development of SPR-based sensors, particularly for gas sensing applications, such as formaldehyde [12], carbon monoxide [13] or sodium acetate [14]. It is also important to consider that AZO is non-toxic, it is widely available at a relatively low cost [15] and the economic and environmental benefits of using TCOs like AZO instead of ITO has been reported [16]. All those factors indicate that AZO should be experimentally studied as a LMR supporting film, to characterize its performance and widen the possibilities of this technique.

4.2. Experimental considerations

Although some theoretical work had been presented using AZO thin-films for LMR generation, no experimental work had been previously reported. Accordingly, the initial experimental procedures must be oriented to the demonstration of the capability of this material to support LMR. For this purpose, a setup based on multimode fiber was chosen due to its wider wavelength range, cost and usability. Once the performance of AZO coatings for LMR-based sensors development is studied on this setup, it could be further optimized by using D-shaped fiber.

For the analysis of the AZO films, additional silicon wafer pieces were used as a substrate. This allows to perform measurements on the films easily. These samples were analyzed in a scanning electron microscope (SEM) and an ellipsometer (HORIBA UVISEL 2).

4.2.1. Experimental setups

The setup used in this case is based on cladding-removed multimode fiber (CRMOF) that will be coated with aluminum zinc oxide in order to induce LMRs. Particularly, a segment of plastic-clad 200/225 μm core/cladding (FT200EMT Thorlabs Inc.) had the cladding chemically removed and was later cleaned ultrasonically in detergent, deionized water, piranha solution and deionized water consecutively. Then, 4 cm segments of these cladding-removed fibers, that will constitute the sensitive region of the device, were cleaved and spliced to MMF pigtails.

The CRMOF setup allows to use a broadband halogen source (Spectral Products Inc.) and a set of spectrometers (USB2000+XR1 and NIR 512, Ocean Optics Inc.) to monitor the spectrum in a wavelength range between 450 and 1600 nm. A bifurcated fiber is used to couple the signal to two separate pigtails, so it can be simultaneously analyzed by the two spectrometers (see fig. 4.1).

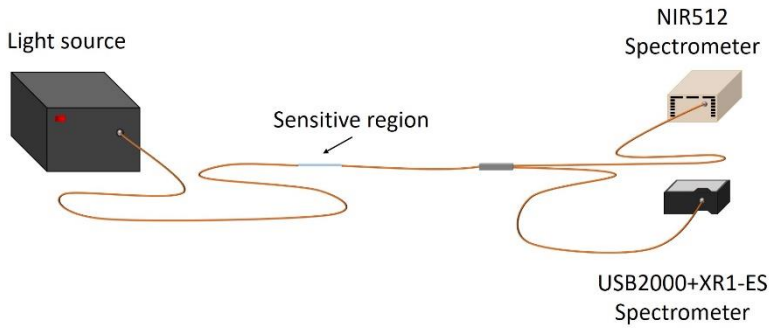

Figure 4.1: *Diagram of the basic setup used to work with CRMOF. The use of two spectrometers allows to work in a broader spectral range.*

In order to fabricate the AZO coatings, the fiber described above was placed inside a sputtering chamber. In this case, an AZO target was used for the fabrication of the film. The light source and spectrometers described above can be used both during the fabrication of the coating and in the characterization process. For the calibration of the refractometer, water glycerol solutions of different refractive index were prepared. Solutions of equal RI and different pH were also prepared (Panreac Inc. PBS Buffer solutions) to study the effect of pH in the response of the device.

4.3. Results

Preliminary studies of the deposition method using silicon wafers as substrate (as well as the optical fibers) determined an average deposition rate of 0.215 nm/s under the fabrication parameters used in these experiments. Fig. 4.2 presents two examples of the SEM images of the AZO films used for thickness measurements.

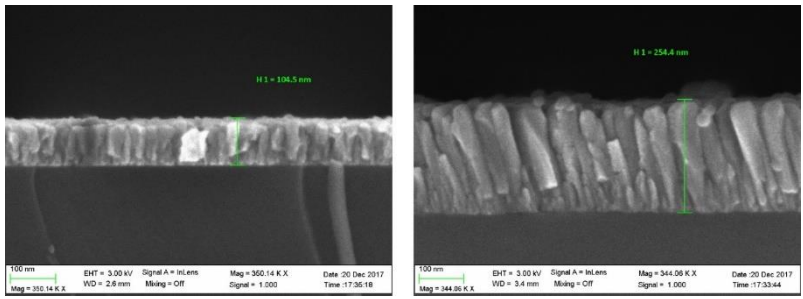

Figure 4.2: *SEM images of two different AZO coatings. The structure of the AZO layer can be clearly distinguished from the silicon substrate.*

An ellipsometry measurement was also performed in order to confirm the optical properties of the AZO coatings and their capacity to support LMR generation. Such analysis (fig. 4.3) demonstrated a relatively high real part of the refractive index (n) and a very low imaginary part, or extinction coefficient (k). In fact, the ellipsometry analysis showed a zero value of k for wavelengths above 400 nm but further experiments showed that this was due to limitations of the mathematical models when working with extremely low k values, as the film showed enough absorption to generate LMRs.

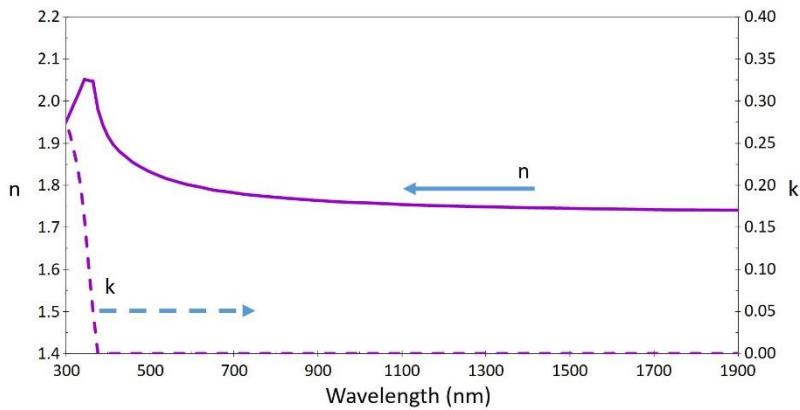

Figure 4.3: *Refractive index of the fabricated AZO thin-films measured by ellipsometry. The real part (n) and the imaginary part (k), also known as extinction coefficient is shown in separated axes to facilitate the analysis of the curves.*

The setup used for the fabrication of the AZO coatings on the CRMOF allowed to monitor the wavelength spectrum in real time, which provided very interesting information. It permitted to observe the generation and evolution of several resonances at the same time that the coating was fabricated. As it was explained in the previous chapter, a LMR observed at a given wavelength shifts to longer wavelengths if the thickness of the coating increases. That behavior can be really well appreciated in fig. 4.4. This graph shows in a colormap the absorbance spectra measured in the specified range (450-1600 nm) for any moment during the deposition process. Soon after the coating fabrication begins, the absorbance starts to increase at the shorter wavelengths. As the process continues, this absorbance, which actually corresponds to a LMR, starts to move to longer wavelengths, until it reaches the upper limit of our spectral window (working range). As the film grows, the same phenomenon is observed also with a second, third, and even a fourth order resonance. In the case of the first LMR, two peaks can be distinguished, corresponding to the LMR of the TE and TM modes of propagation. The same effect can be appreciated in the second order LMR, although in this case the components are spectrally closer. The rest of the LMR are observed as single absorbance peaks since the LMRs corresponding to each mode are closer than in the previous cases.

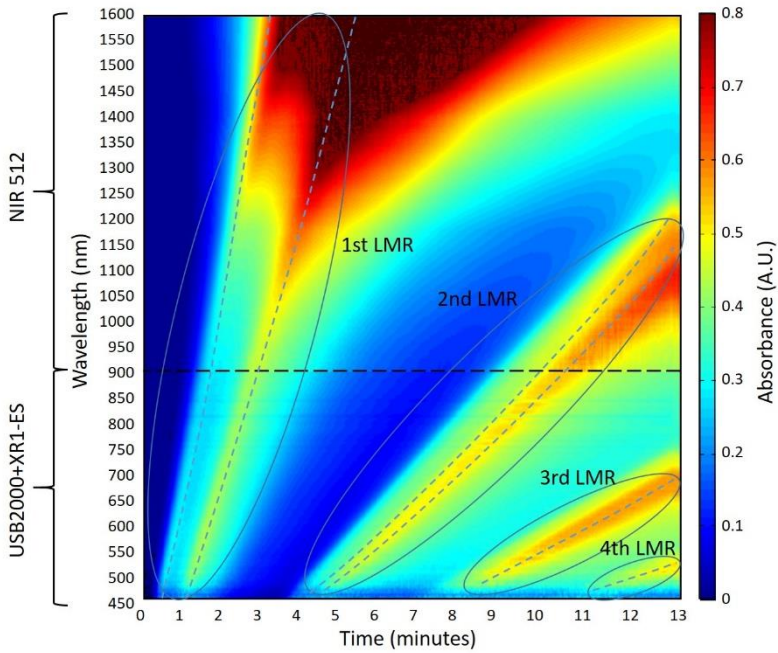

Figure 4.4: *Colormap representing the transmission spectra during the AZO coating fabrication process. The vertical axis shows the wavelength range and the horizontal axis the deposition time. The absorbance at a given wavelength value at any time is indicated by the color.*

This test also corroborates the premise that lower order resonances are more sensitive. Assuming a constant deposition rate, a linear thickness increase is expected in this experiment. Therefore, the LMR sensitivity to film thickness is related to the slope of the LMRs in the figure. A greater slope (like in the first LMR) implies a higher sensitivity, as it requires a lower thickness variation to induce a LMR wavelength shift. It can be clearly observed how the resonances of lower order present a greater slope (sensitivity) than those of greater order. It can also be seen that this slope is not constant for a given LMR, but it is slightly curved. This means that a given LMR possesses a higher sensitivity when it is observed at a longer wavelength than when it is tuned at shorter wavelengths.

At the end of this deposition process the AZO coating reached a thickness of 167 nm and three LMRs could be observed in the wavelength range of study. These resonances correspond to the second, third and fourth order LMRs, and it is possible to study their response to SRI variations and characterize them as refractometers. It should be noted that the first order resonance would have a greater sensitivity. However, the separation of the two components of the first LMR (corresponding to the TE and TM modes) makes it difficult to study this resonance with the MMF setup. To illustrate this, fig. 4.5 shows an example of the first resonance during the above described fabrication process. The contribution of both modes gives as a result a wide distorted resonance that covers almost the whole spectral range where it is difficult to determine a precise location of the peak. In the following LMRs, the components are closer and a single peak can be unequivocally determined. Therefore, this setup using AZO coatings is limited to the use of LMRs of second or higher order.

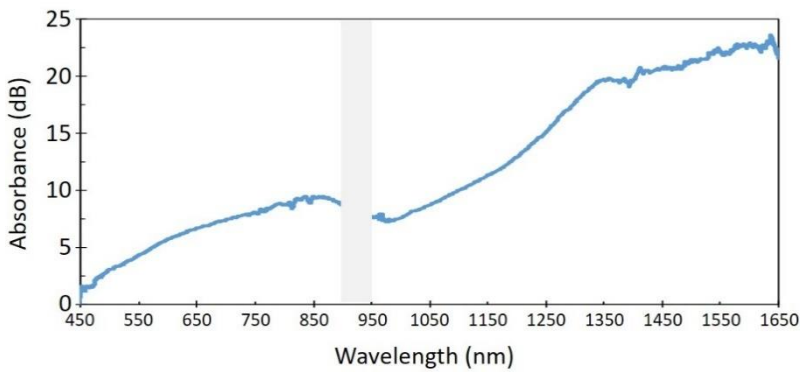

Figure 4.5: *Example of the spectrum obtained during the deposition process (after 2.5 minutes) showing the 1st order LMR. Two components can be appreciated that give as a result a wide and distorted resonance that makes it difficult to determine unequivocally the location of a central peak in the working wavelength range.*

Before performing any further experiment, the sensor is kept at room temperature for 8 hours in order to allow the coating to stabilize. It should be noted that the sputtering deposition is done in an oxygen-free atmosphere and, when the film contacts with a

regular atmosphere a further oxidation may occur. This effect was studied and it was observed that the mentioned oxidation process caused a 5 nm red-shift in the LMRs. After a few hours of oxidation the coating was fully stable and the red-shift was stopped.

Therefore, once stabilized the above-mentioned probe was sequentially tested in solutions of different refractive index. Fig. 4.6 shows the spectrum obtained during such procedure and the shift induced in the LMRs. The second LMR is located in the near infra-red range (NIR), while the third and fourth LMRs are observed in the visible light (VIS) range. The same behavior is observed in the three resonances, as all of them shift to longer wavelength when the SRI increases, but it is expected that they present different sensitivity.

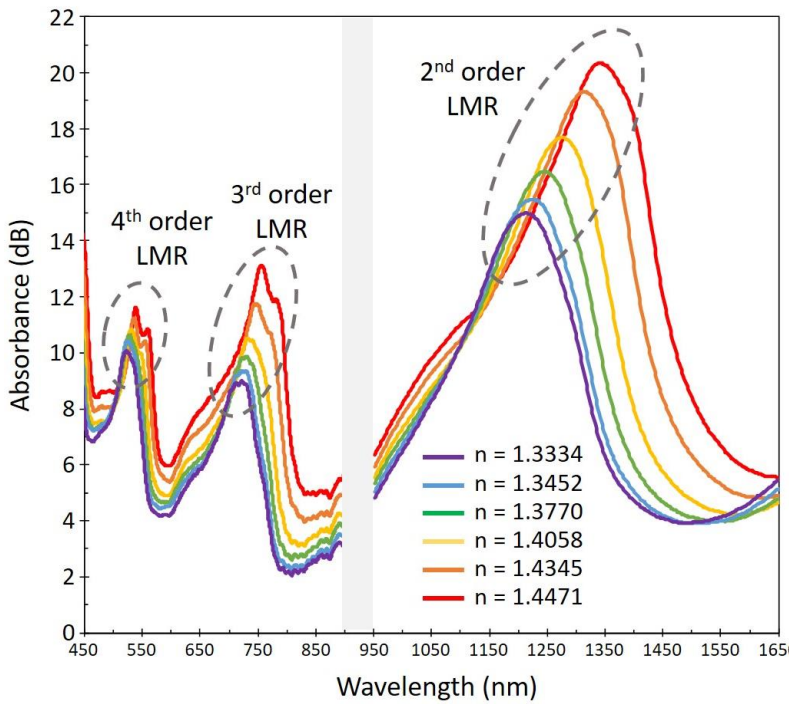

Figure 4.6: *Spectra obtained by the device for several SRI values between 1.3334 and 1.4471. Two LMRs can be observed in the USB2000+XR1-ES spectrometer and another one in the NIR512. In all the cases the LMR experiment a red-shift when the SRI increases.*

To measure the sensitivity of each LMR, the central wavelength of each resonance was calculated and plotted as a function of the SRI (fig. 4.7). This plot shows the curves corresponding to each of the LMR. It can be seen that for the same SRI variation (1.3334-1.4471), the fourth order resonance presents the lowest wavelength shift with an average sensitivity of 134.3 nm/RIU, and the second order LMR shows the greatest shift, with a sensitivity of 1,153.6 nm/RIU. The third order LMR shows an intermediate sensitivity of 326.6 nm/RIU. As it was expected, the sensitivity is not a constant parameter for each LMR. It not only depends on the spectral location of the LMR, but it actually increases for higher SRI values. This way, the 4^{th}, 3^{rd} and 2^{nd} order LMRs achieve a maximum sensitivity of 251, 718 and 2,280 nm/RIU respectively for the 1.4345-1.4471 RI range.

It was considered important to study the impact of pH on the refractometric measurement. For that purpose, the sensor was tested on solutions of different pH values and constant refractive index. It was determined that the sensor showed a sensitivity to pH variations of 0.77 nm/pH unit, which represents a minimal impact considering an average sensitivity of 1,153.6 nm/RIU.

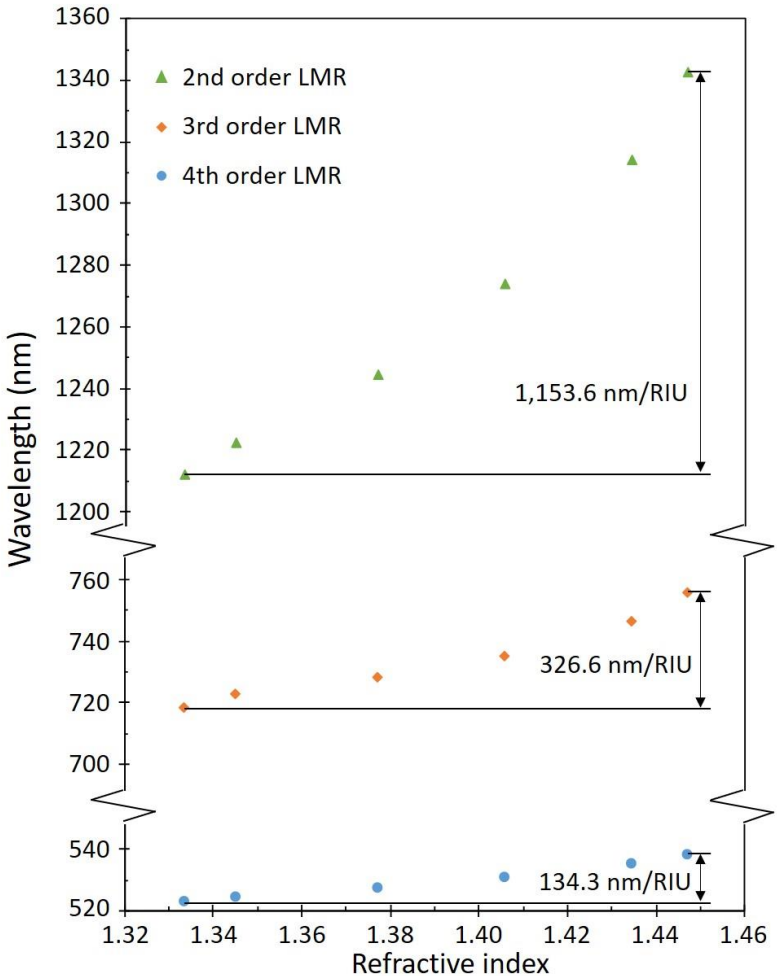

Figure 4.7: *Calibration curves of the LMRs observed in the device. Each curve corresponds to a LMR and present different sensitivity values.*

Given the fact that MMF supports the propagation of visible light and the LMRs have been observed in such range, it was proposed the fabrication of a LMR-based refractometer relying in the variation of the color of the transmitted light. For this purpose, a new probe was fabricated with a thinner AZO film (90 nm) so that a second order LMR is located in the visible light range (450 nm). A variation on the SRI will induce a shift in the LMR which, in the case

of visible light is related to a variation on the transmitted color. The objective of such device is to be able to estimate the SRI by observing the color of the light at the end of the fiber without the need of a spectrometer or OSA. Such configuration would reduce greatly the cost of the setup, although it can only provide a rough SRI estimation.

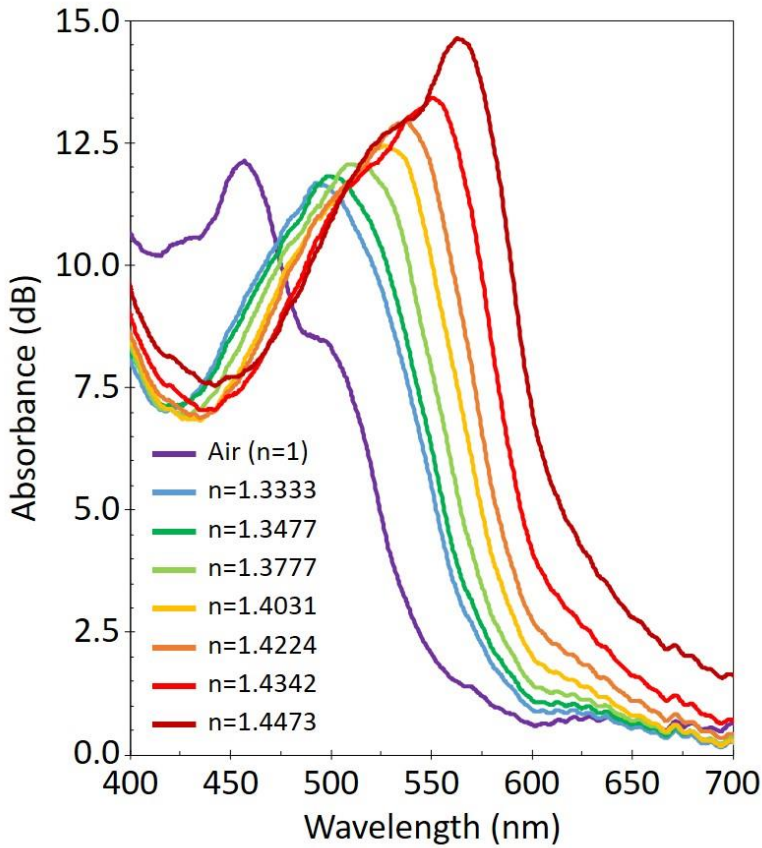

Figure 4.8: *Transmission spectra produced by the second device. It shows a LMR in the visible light range that suffers a red-shift as the SRI rises.*

Such device showed the spectra presented in fig. 4.8. The central position of the LMR varied between 495 and 560 nm for a SRI range between 1.333 and 1.447 (fig. 4.9). This device presents an average

sensitivity of 592 nm/RIU, with a maximum value of 1142 nm/RIU for the highest RI range. It should be noted that this sensitivity value is approximately a half of the figure obtained in the 2nd LMR in the previous probe. It is, nonetheless, in agreement with the theoretical studies that predict that a LMR will present a higher sensitivity if it is located at a longer wavelength [1]. And in this case the LMR is tuned at a wavelength which is a half of the wavelength where the LMR could be observed in the first probe.

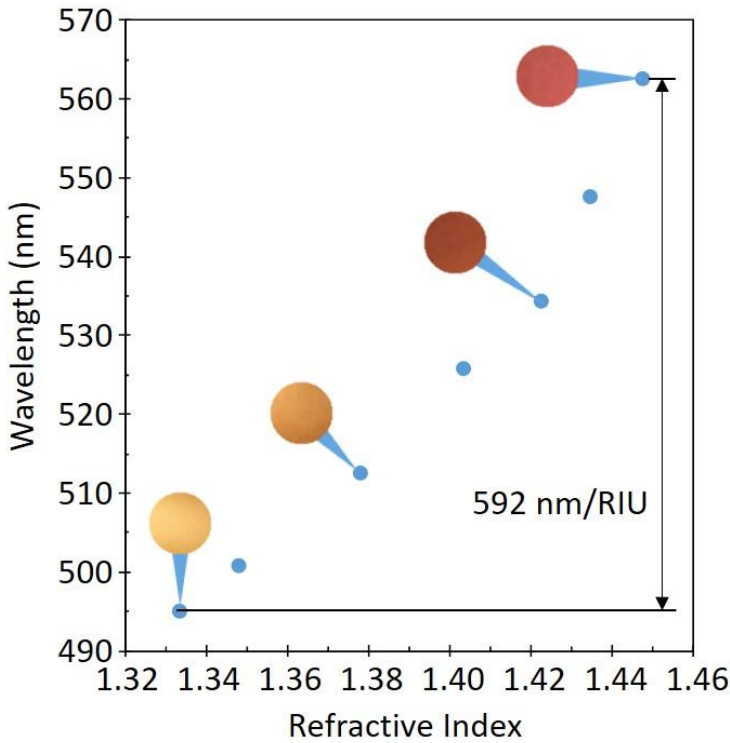

Figure 4.9: *Calibration curve of the second device, based in color variation. The graph also shows photographs of the light projected at the end of the fiber showing that a variation in its color is induced due to the LMR shift.*

Despite the lower sensitivity, a color change can be appreciated for the SRI range studied. The transmitted light when the SRI is close to the water is of yellow color. As the SRI increases, it changes to light

and dark brown, and it ends in a red color for the highest SRI values analyzed. Therefore, this device can be effectively used to estimate the RI value within that range, without the need of an expensive spectrometer.

4.4. Conclusions

Aluminum-doped zinc oxide (AZO) has been successfully proven to be a good coating material for LMR generation. LMRs have been observed in the VIS-NIR range and their sensitivity to SRI variation has been confirmed. The tuning of a LMR induced by AZO thin film in the visible light range also allowed to design a refractometer based on the observation of light color variation. The separation of modes on the first order LMR generated on a AZO coating prevented the study of such LMR in a MMF-based setup. A D-shaped fiber based setup would overcome such limitation and achieve a better sensitivity value. However, the data obtained using the CRMOF setup does not suggest that the AZO thin-film would obtain a better performance in terms of refractometric sensitivity than tin oxide coatings. Nevertheless, AZO could still be an optimal choice for the development of gas sensors due to the intrinsic properties of the material. The performance of LMR refractometers based on AZO coatings could also be enhanced with the design of complex coating structures with additional layers.

Considering the results presented here, it could be of interest the study of other materials based on zinc oxide. The next chapter will introduce the use of IGZO (indium-gallium-zinc oxide) thin films for the generation of LMRs. Its higher refractive index (compared with AZO) suggests a potential to develop more sensitive devices.

Bibliography

1. Del Villar, I.; Hernaez, M.; Zamarreño, C. R.; Sánchez, P.; Fernández-Valdivielso, C.; Arregui, F. J.; Matias, I. R. Design rules for lossy mode resonance based sensors. *Appl. Opt.* **2012**, *51*, 4298, doi:10.1364/AO.51.004298.

2. Paliwal, N.; Punjabi, N.; John, J.; Mukherji, S. Design and Fabrication of Lossy Mode Resonance Based U-Shaped Fiber Optic Refractometer Utilizing Dual Sensing Phenomenon. *J. Light. Technol.* **2016**, *34*, 4187–4194, doi:10.1109/JLT.2016.2585922.

3. Usha, S. P.; Gupta, B. D. Performance analysis of zinc oxide-implemented lossy mode resonance-based optical fiber refractive index sensor utilizing thin film/nanostructure. *Appl. Opt.* **2017**, *56*, 5716, doi:10.1364/AO.56.005716.

4. Usha, S. P.; Gupta, B. D. Urinary p-cresol diagnosis using nanocomposite of ZnO/MoS2 and molecular imprinted polymer on optical fiber based lossy mode resonance sensor. *Biosens. Bioelectron.* **2018**, *101*, 135–145, doi:10.1016/j.bios.2017.10.029.

5. Usha, S. P.; Shrivastav, A. M.; Gupta, B. D. A contemporary approach for design and characterization of fiber-optic-cortisol sensor tailoring LMR and ZnO/PPY molecularly imprinted film. *Biosens. Bioelectron.* **2017**, *87*, 178–186.

6. Usha, S. P.; Mishra, S. K.; Gupta, B. D. Zinc oxide thin film/nanorods based lossy mode resonance hydrogen sulphide gas sensor. *Mater. Res. Express* **2015**, *2*, 095003, doi:10.1088/2053-1591.

7. Usha, S. P.; Mishra, S. K.; Gupta, B. D. Fiber optic hydrogen sulfide gas sensors utilizing ZnO thin film/ZnO nanoparticles: A comparison of surface plasmon resonance and lossy mode resonance. *Sensors Actuators B Chem.* **2015**, *218*, 196–204.

8. Henley, S. J.; Ashfold, M. N. R.; Cherns, D. The growth of transparent conducting ZnO films by pulsed laser ablation.

Surf. Coatings Technol. **2004**, *177–178*, 271–276, doi:10.1016/j.surfcoat.2003.09.005.

9. Hong, C.-S.; Park, H.-H.; Moon, J.; Park, H.-H. Effect of metal (Al, Ga, and In)-dopants and/or Ag-nanoparticles on the optical and electrical properties of ZnO thin films. *Thin Solid Films* **2006**, *515*, 957–960, doi:10.1016/j.tsf.2006.07.055.

10. Paliwal, N.; John, J. Sensitivity Enhancement of Aluminium Doped Zinc Oxide (AZO) Coated Lossy Mode Resonance (LMR) Fiber Optic Sensors Using Additional Layer of Oxides. In *Frontiers in Optics 2014 (2014), paper JTu3A.40*; Optical Society of America, 2014; p. JTu3A.40.

11. Paliwal, N.; John, J. Theoretical modeling and investigations of AZO coated LMR based fiber optic tapered tip sensor utilizing an additional TiO2 layer for sensitivity enhancement. *Sensors Actuators B Chem.* **2017**, *238*, 1–8, doi:10.1016/j.snb.2016.07.032.

12. Chi, C. Y.; Chen, H. I.; Chen, W. C.; Chang, C. H.; Liu, W. C. Formaldehyde sensing characteristics of an aluminum-doped zinc oxide (AZO) thin-film-based sensor. *Sensors Actuators, B Chem.* **2018**, *255*, 3017–3024, doi:10.1016/j.snb.2017.09.125.

13. Chang, J. F.; Kuo, H. H.; Leu, I. C.; Hon, M. H. The effects of thickness and operation temperature on ZnO:Al thin film CO gas sensor. *Sensors Actuators, B Chem.* **2002**, *84*, 258–264, doi:10.1016/S0925-4005(02)00034-5.

14. Lin, K.-C.; Ho, P.-J.; Yang, S.-M.; Tsai, W.-H.; Tsao, Y.-C.; Lin, K.-C.; Yang, S.-M.; Tsao, Y.-C.; Ho, P.-J. Fiber-optic surface plasmon resonance-based sensor with AZO/Au bilayered sensing layer. **2014**, *12*, 042801.

15. Shen, H.; Zhang, H.; Lu, L.; Jiang, F.; Yang, C. Preparation and properties of AZO thin films on different substrates. *Prog. Nat. Sci. Mater. Int.* **2010**, *20*, 44–48, doi:10.1016/S1002-0071(12)60005-7.

16. Minami, T. Present status of transparent conducting oxide

thin-film development for Indium-Tin-Oxide (ITO) substitutes. *Thin Solid Films* **2008**, *516*, 5822–5828, doi:10.1016/J.TSF.2007.10.063.

Chapter 5

Indium-gallium-zinc oxide for LMR-based refractometers development

The following chapter describes the analysis of a new material for the fabrication of LMR-based refractometers: indium-gallium-zinc oxide (IGZO). This material, which is optically similar to AZO with a higher refractive index, is a good candidate for that purpose. Here, it is proved the utilization of IGZO for the generation of LMRs both using cladding-removed multimode optical fibers (CRMOF) and a D-shaped fiber configuration setups. This chapter also studies the impact of the polishing depth on a D-shaped fiber on the performance of a LMR-based refractometer using IGZO coatings.

The contents of this chapter have been partially published in the paper *Lossy mode resonance optical sensors based on indium-gallium-zinc oxide thin film* in Sensors and Actuators A: Physical vol. 290, 20-27 (2019).

5.1. Introduction

Thin-films of aluminum-doped zinc oxide (AZO) proved in the previous chapter to be valid for the development of LMR-based sensors. Zinc oxide thin-films were also successfully tested [1,2], as it was explained in chapter 2. There are still other materials based on zinc oxide that could potentially achieve a better performance. In particular, indium gallium zinc oxide (IGZO) is one of such materials.

IGZO possesses advantageous optical properties to support LMR generation, and also presents some extra benefits, such as stability [3–5], compared to other materials like ITO. In addition, IGZO shows a high electron mobility, which also makes it a good candidate for gas sensing [6,7]. It has been widely used as a semiconductor material in microelectronics, playing an important role in the fabrication of thin-film transistors (TFTs) for displays [3], as well as being used for the development of ozone [8], temperature [9], or glucose [10] sensors.

In this chapter it is explored the utilization of IGZO thin-films for the generation of LMR-based optical fiber refractometers. This study shows the first experimental characterization of IGZO thin-films for LMR-based sensors development. The LMR phenomenon will be first analyzed on a multimode fiber setup. Due to the optimal optical properties of IGZO thin-film, it will also be applied on a D-shaped fiber setup to achieve the best possible performance of such films. In this research it will also be studied the impact of the polished-surface/core distance on the performance of D-shaped fiber LMR-based refractometers.

5.2. Experimental considerations

The experimental procedure to study IGZO as new coating material for LMR generation will follow a strategy analogous to the one described in the previous chapter. Initially, it is necessary to determine the optimal parameters for the fabrication of the IGZO

thin films. Such films are fabricated in a DC sputtering chamber (K675XD, Quorum Technologies) using an IGZO target from Beijing Loyaltarget Technology Co. The sputtering process is performed at a partial Ar pressure of $8 \cdot 10^{-2}$ mbar and a current of 100 mA. Then, the properties of such films must be analyzed using various techniques. In particular, the thickness of the coatings is measured using a field emission scanning electron microscope (SEM) UltraPlus from Carl Zeiss Inc. with an in-lens detector at 3 kV and an aperture diameter of 30 μm. Additionally, an energy-dispersive X-ray spectroscopy (EDX) measurement, obtained with an INCA X-ray microanalysis system (Oxford Instruments) will also permit to analyze the main components of the coating, and a spectroscopic ellipsometer (UVISEL 2, Horiba) will provide its complex refractive index.

Next, the IGZO thin-film can be deposited on the optical fibers for the manufacture of the sensors. The setup used for the fabrication monitoring is similar to the one described in the previous chapter. A 4 cm CRMOF segment is spliced to multimode fiber (MMF) pigtails and placed in the sputtering chamber. A halogen light source and a set of two spectrometers permits to study the evolution of the transmission spectra in the 450-1650 nm wavelength range. A similar setup can be used for the characterization of the device as a refractometer, using water/glycerol solutions of different concentrations (fig. 5.1).

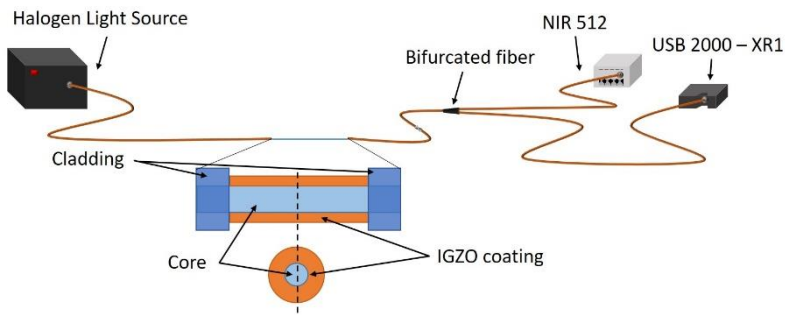

Figure 5.1: *Experimental setup used for the fabrication and characterization of the CRMOF device.*

The IGZO thin-films will be then fabricated on D-shaped fibers in order to analyze the components of each propagating mode (TE and TM) separately. During the fabrication process a setup including a LED (light emitting diode) source and a power meter was used to monitor the optical power at a wavelength of 850 nm. This allowed to tune the resonances in the desired window. In this configuration, D-shaped fibers of different polishing degree (distance between the core and the outer medium) will be used. The characterization setup in this case (fig. 5.2) includes broadband light based on superluminescent emitting diodes (HP83437A) and an optical spectrum analyzer (HP86142A) to receive the signal. This setup also makes use of a linear polarizer (Phoenix Photonics) and a manual polarization controller (Thorlabs).

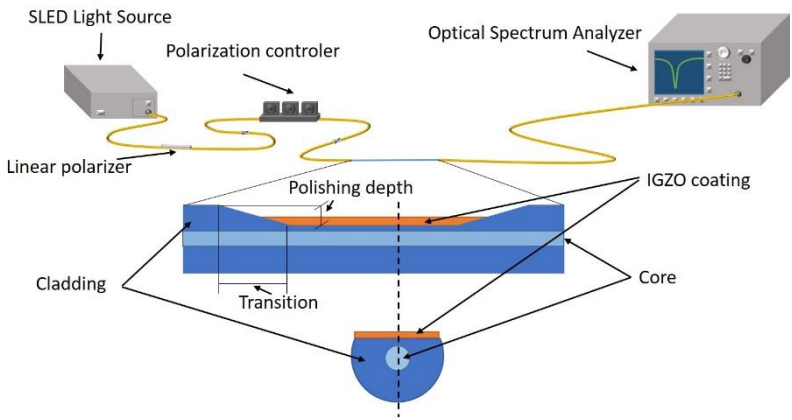

***Figure 5.2**: Diagram of the experimental setup employed for the characterization of the D-shaped fiber-based refractometer. It includes a detail of the D-shaped zone (17 mm long), where the polishing depth is defined as the distance to core difference between the external cladding and the polished region.*

5.3. Results

5.3.1. IGZO film fabrication and characterization

Silicon wafers were used as a substrate to analyze the properties of the film. It was calculated that the deposition rate for this process

was 0.355 nm/s in average. Therefore, the deposition time will determine the final thickness of the coating. The calculation of such parameter is based on the SEM measurements shown on fig. 5.3a. These samples were also measured by EDX, which confirmed the presence of indium, gallium and zinc, as well as oxygen, and silicon from the substrate (fig. 5.3b).

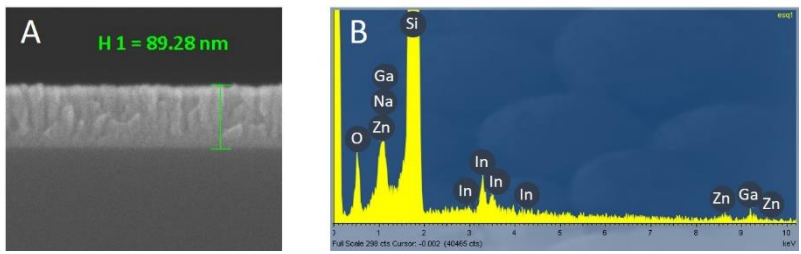

Figure 5.3: *(A) SEM image and (B) EDX measurement of a IGZO thin-film on a silicon wafer. It allowed to measure the thickness of the coatings and corroborate the composition of the films.*

Finally, the analysis of the spectroscopic ellipsometry measurement permitted to obtain the complex refractive index of the film. The curves of both n and k can be seen on fig. 5.4. These curves are quite similar to those obtained for AZO coatings and, again, fulfill the criteria for LMR generation. The main difference with the optical properties of AZO is that in this case IGZO presents higher values for n, indicating that it could potentially generate LMRs with higher sensitivities than previously studied materials [11].

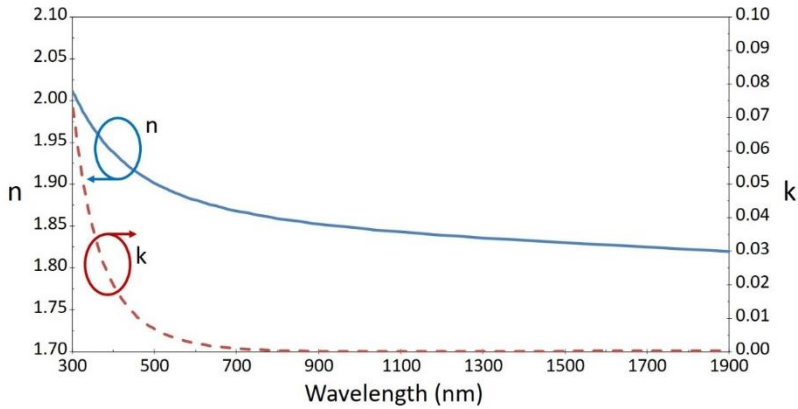

Figure 5.4: *Complex refractive index of the IGZO thin-film measured by spectroscopic ellipsometry.*

5.3.2. CRMOF configuration

Once the IGZO thin-film fabrication process is fully characterized, it is necessary to study the LMR generation phenomenon on optical fibers. Initially, the spectrum was monitored during a long deposition (setup on fig. 5.1) to analyze the response of the LMR to the coating growth. Fig. 5.5 shows a colormap of the absorbance spectra in the 450-1650 nm wavelength range during a fabrication process of 20 minutes. A scale with the projected coating thickness at each moment is included in the upper axis, assuming a linear growth at the above mentioned rate. Several absorption peaks can be observed, corresponding to 7 LMRs. Taking into account a normalized flat spectrum at the beginning of the process, the LMRs start from the shortest wavelength and progressively shift to longer wavelengths, disappearing (in the case of the 2 first LMRs) completely from the spectral window. The first resonance appears in the first minute of the process and presents the fastest shift due to its greatest sensitivity to the thickness increment. It also widens as the thickness increases, revealing the two components corresponding to TE and TM modes, which present slightly different sensitivity. For the rest of the LMRs the two components cannot be dissociated directly in the CRMOF setup. These resonances, which start being observed with a calculated thickness of 64, 128, 192,

245, 298 and 362 nm respectively, show a consecutively reduction of sensitivity as the order of the LMR increases. For instance, the TE component of the first LMR requires an increment in thickness of 50 nm approximately to undergo a shift of the whole spectral window (which is a shift of 1200 nm). The second order LMR, in contrast, requires an increment in thickness over 200 nm, meaning that its sensitivity to thickness variations is more than 4 times lower. At the end of the 20 minutes deposition process, a 426 nm coating has been fabricated and 5 resonances can be seen simultaneously in the spectral window of study.

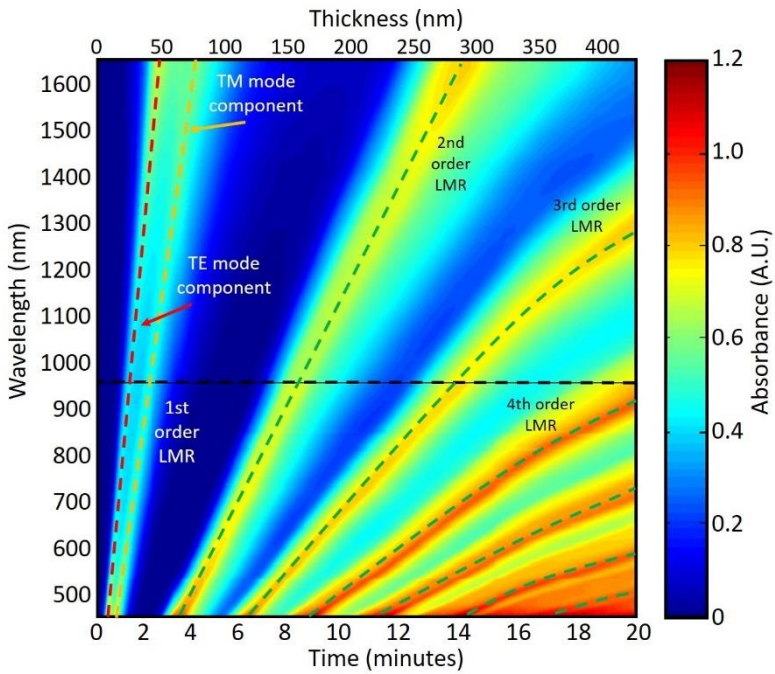

Figure 5.5: *Colormap representing the transmittance spectrum evolution during the fabrication of the IGZO thin-film. The bottom axis shows the time since the deposition started and the upper axis shows the projected coating thickness at the moment. Up to seven LMRs can be observed during this process.*

To test the response of the LMRs to SRI variations, a new probe with a 106 nm IGZO film is fabricated. This probe presents a second order LMR in the VIS range. This LMR was chosen because of its sensitivity,

considering that the two components of the 1st order LMR make it difficult to determine precisely the central peak of the resonance. The coincidence of these components at two relatively close wavelengths causes them to overlap, resulting in the observation of a distorted and wide resonance. Such situation leads to an increment in the FWHM parameter described in the previous chapters as the full width at half maximum. The high FWHM in combination with the distorted shape causes the determination of the peak in the first order LMR to have a high error margin, making the second order LMR a better choice. This probe was also kept for 24 hours at room temperature before any further experimental procedure, to allow it to stabilize. The characterization consisted on immersing the coated fiber in water/glycerol solutions of different concentrations. This increase in the SRI of the probe caused a red-shift in the resonance. Fig. 5.6a shows the spectra obtained with solutions with a refractive index between 1.3330 and 1.4462. The central position of the LMR varies in function of the SRI value, and Fig. 5.6b displays the corresponding calibration curve: the spectral position of the LMR vs. the SRI value. This LMR presents an average sensitivity of 839.87 nm/RIU, with a maximum value of 1,666 nm/RIU for the highest SRI range. These figures are comparable to those obtained with the second order LMR generated using AZO thin-films, considering that the sensitivity is directly influenced by the spectral location of the LMR (a LMR at a longer wavelength will present a higher sensitivity than if it were observed at a shorter wavelength). The achievement of a better sensitivity using IGZO would require a different approach. The first order LMR, as seen from fig. 5.5, presents a higher sensitivity but, in order to properly observe such resonance, it would be necessary to separate the polarization modes, which is not possible on CRMOF setup. A configuration based on a D-shaped fiber, however, would enable the use of polarized light and the effective separation of modes to observe the first order LMR.

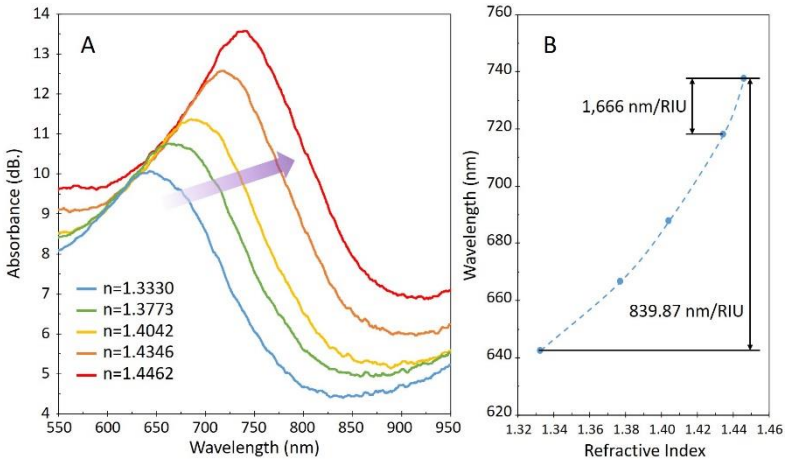

Figure 5.6: *(A) Transmission spectra obtained with the IGZO coated CRMOF device for several SRI values. A second order LMR is observed in the range of study. (B) LMR spectral location for each SRI value.*

5.3.3. D-shaped fiber configuration

Taking into account that IGZO has demonstrated a higher refractive index than AZO, it is potentially capable to accomplish a higher sensitivity. Therefore, IGZO was considered as a good candidate material to optimize the performance of LMR-based sensors in terms of sensitivity. For that purpose, IGZO thin-films were fabricated on D-shaped fibers, intending to observe the first order LMR (the most sensitive ones) and its two components LMR_{TE} and LMR_{TM} corresponding to the TE and TM modes of propagation, respectively.

In this experiment, two kinds of D-shaped fibers were used, with different polishing degree, identified as 1 dB D-shaped and 4 dB D-shaped fibers. These names refer to the optical losses at a wavelength of 1330 nm induced by the polishing process with a SRI of 1.5. The 4 dB D-shaped fiber possesses a greater degree of polishing than the 1 dB D-shaped fiber. These two different fibers were used in this experiment to analyze the impact of this polishing process on the performance of the LMR.

The fibers were coated with an IGZO thin-film of approximately 85 nm. The use of polarized light (and polarization controllers) in the setup allowed to observe separately LMR_{TE} and LMR_{TM} in both kind of fibers. The LMR_{TE} can be observed for SRI values between 1.32 and 1.36 (figs. 5.7a and 5.7c), while LMR_{TM} is observed for the SRI range between 1.36 and 1.42 (figs. 5.7b and 5.7d), being the LMRs on the 4 dB D-shaped fiber tuned at a slightly shorter wavelength. Note that the solutions utilized in the characterization do not present the same refractive index values in the different experiments, as they were specifically prepared for the range of each resonance, and its impact will be discussed later. The graph shows two obvious differences between the 1 dB and the 4 dB D-shaped fibers. The first big difference that will be discussed is the amplitude of the resonances. The LMRs seen on the 4 dB D-shaped fiber show a greater amplitude of up to 35 dB, but also show a more irregular shape, with multiple side-lobes or ripples (figs. 5.7a and 5.7b). In the case of the 1 dB D-shaped fiber, in contrast, a lower amplitude is observed (14 dB maximum), but the LMRs show a smoother shape with no evident side-lobes (figs. 5.7c and 5.7d). It should be noted that both phenomena will also have a significant impact on the FWHM of each resonance. The following analysis will study the causes of these differences on the performance of the sensor, as well as the impact of the polishing degree on the sensitivity of the LMR.

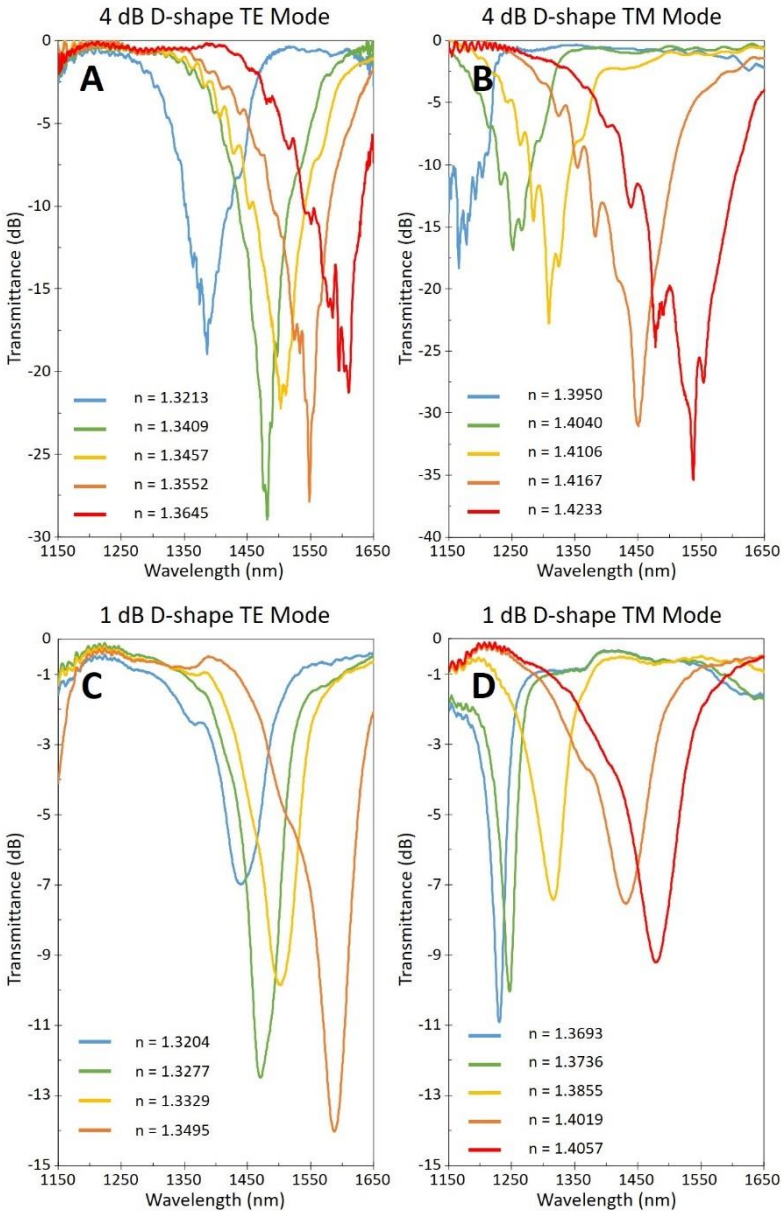

Figure 5.7: *Transmittance measured on the D-shaped fibers for several SRI values. (A) and (B) show the LMR_{TE} and LMR_{TM}, respectively, observed on the 4 dB D-shaped fiber. (C) and (D) show the LMR_{TE} and LMR_{TM} measured on the 1 dB D-shaped fiber.*

The calibration curve of each of the 4 LMRs has been plotted on the same graph to compare and analyze their sensitivity (fig. 5.8). In the LMR_{TE} the sensitivities obtained with the two fibers is very similar. The average sensitivity achieved with the 1 dB D-shaped fiber is 5,062 nm/RIU, while the value for the 4 dB D-shaped fiber is 5,111 nm/RIU. In contrast, a greater divergence is observed for the LMR_{TM}. In the case of the 1 dB D-shaped fiber, the average sensitivity is 6,855 nm/RIU, whereas an average sensitivity of 12,929 nm/RIU is achieved with the 4 dB D-shaped fiber. However, there are some factors that should be taken into consideration for the comparison of both probes in the case of the LMR_{TM}. The tuning of the LMR_{TM} at shorter wavelength in the case of the 4 dB D-shaped fiber causes that the characterization is performed at a higher SRI range, and it is known that the LMR sensitivity depends on the SRI range. This difference in wavelength is due to a coating thickness divergence in the two fibers and the high sensitivity of the LMRs to thickness variations. To make a fair comparison, it is necessary to evaluate the sensitivity values in the same or close SRI range. If only the coincident SRI range between 1.3855 and 1.4106 is considered, the average sensitivities provided by the LMR_{TM} are 8,120 nm/RIU and 8,974 nm/RIU for the 1 dB and 4 dB D-shaped fibers, respectively. It can be concluded that the divergence in sensitivity is primarily caused by the difference in wavelength location of the LMRs (due to a coating thickness difference), and not so influenced by the polishing degree of the D-shaped fibers.

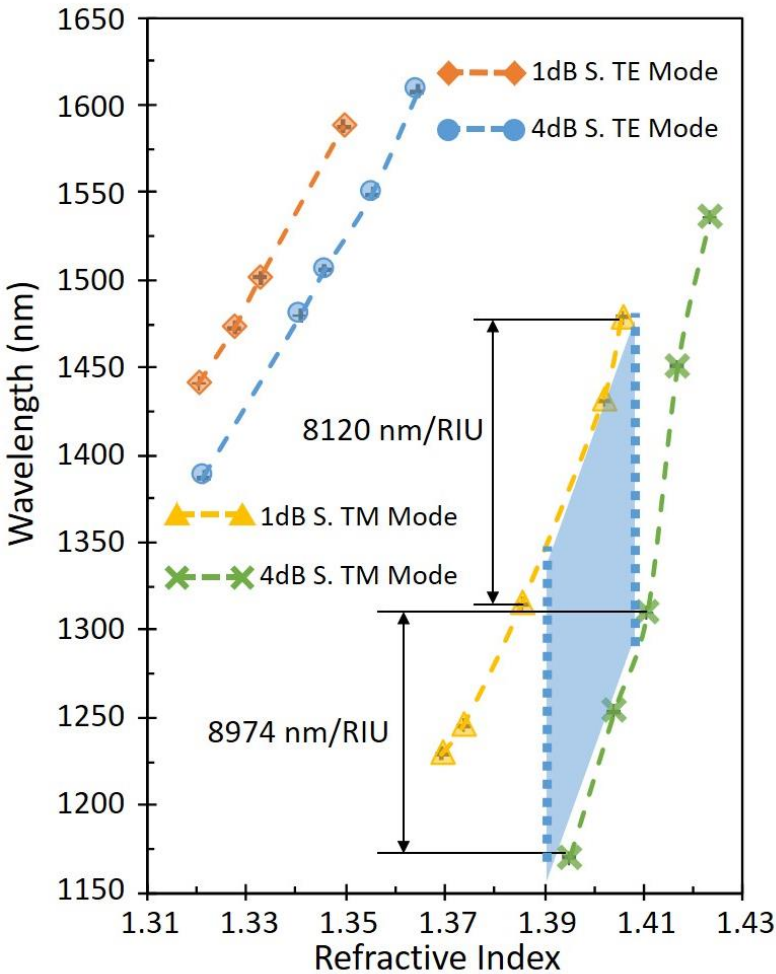

Figure 5.8: *Wavelength position of the LMRs observed on the D-shaped fibers for several SRI values. The LMRs observed in the 1 dB and 4 dB D-shaped fibers show a similar sensitivity.*

Once the impact on the sensitivity has been considered, it is important to analyze the already mentioned effect on LMR shape and amplitude. Such difference will likely affect the FWHM (full width at half maximum, measured 3 dB above the LMR peak), which will also have an impact on the figure of merit (FOM), measured as the ratio Sensitivity/FWHM. This way, the LMR_{TE} and LMR_{TM} for the

1 dB D-shaped fiber obtained a FWHM of 48 and 44.8 nm respectively, with a FOM of 105.46 and 155.09 RIU^{-1}. In the case of the 4 dB D-shaped fibers, although the resonances present a more irregular shape, they are also narrower at the peak. The LMR_{TE} presents a FWHM of 12.9 nm and a FOM of 396.20 RIU^{-1}. The LMR_{TM} achieves a better performance with a FWHM of 11.1 nm and a FOM of 1,164.77 RIU^{-1}. It can be concluded that the greater polishing degree does not cause a significant improvement on the sensitivity, but it does lead to a better FOM due to the narrower resonances. The distortion observed on the LMRs shape when there is a greater polishing degree. However, it could be a drawback, depending on the mechanism used to determine the central peak of the LMRs. Compared with the performance achieved on D-shaped setup using other materials, IGZO provided a better SRI sensitivity than TiO_2 [12], but lower than other materials such as ITO [13] or SnO_2 (chapter 3). However, IGZO could still be a great alternative considering its stability and the sensing capabilities that its interaction with gases present.

After analyzing all the data, it can be concluded that the main impact of the polishing degree on the LMRs is the transmittance (seen on the amplitude of the resonance), and their shape ('side-lobes'). The former can be easily explained by the polishing depth, since a deeper polishing causes an increase in the evanescent field, inducing a greater resonance amplitude. The latter (the 'side-lobes or smoothness on the LMR) is a more complex phenomenon. Previous studies [11] shown that a variation in the extinction coefficient (k) may affect the shape of the LMR. Since in this work the fabrication conditions of the IGZO coatings are identical, it can be assumed that the optical properties of the IGZO thin-films are the same, being the only difference the geometrical shape of the fiber. It should be considered that there is a transition zone between the regular SMF and the D-shaped fiber. Such geometry is difficult to analyze as it depends on the fabrication process and the polishing degree. However, we can assume that the deeper the polishing depth the longer the transition zone, which may excite undesired

transmission modes. Consequently, the impact of these transmission modes on the LMRs will be more relevant for deeper polished fibers (like in the case of the 4 dB D-shaped fibers), and could be the cause of the side lobes in Figs 7a and 7b.

5.4. Conclusions

It has been proven that IGZO is a suitable material for LMR-based sensors fabrication. The observance of LMRs has been demonstrated for different IGZO thin-film thicknesses in a wide spectral range. A second order LMR observed on a CRMOF has been characterized as a refractometer, with an average sensitivity of 839.87 nm/RIU. Considering the wavelength range of the resonance, IGZO seems to achieve a better performance than AZO.

The LMRs corresponding to the TE and TM modes of propagation have also been successfully studied in a D-shaped fiber setup. An average sensitivity of 12,929 nm/RIU was achieved in a LMR_{TM} using a 4 dB D-shaped fiber, with a FOM of 1,164.77 RIU^{-1}. It could be considered a good performance, better than the one achieved using titanium dioxide, but lower than the one demonstrated using tin oxide (chapter 3).

The effect of the polishing depth on the D-shaped fiber was also studied. It was determined that a deeper polishing does not affect significantly the SRI sensitivity of the LMR, but it does have an impact on the shape and transmittance of the LMR.

The performance obtained with the IGZO thin film is relevant in terms of sensitivity as it is close to the one demonstrated by ITO in a similar SRI range, but still is not higher than that provided by tin oxide described in chapter 3. In contrast, the intrinsic properties of IGZO, including its stability and its wide experience of use in the electronic industry make it a good choice for designing gas sensors (for nitrogen dioxide [6] or ozone [7], for instance) based on LMR

Observing the performance demonstrated using IGZO in this chapter and AZO in chapter 4, it is clear that it is necessary a coating

with a much higher refractive index to beat the sensitivity achieved using tin oxide on chapter 3. The next chapter will discuss the use of a material with a refractive index considerably higher than the one of tin oxide, as is the case of copper oxide, in order to achieve a LMR-based sensor with a maximum sensitivity.

Bibliography

1. Usha, S. P.; Mishra, S. K.; Gupta, B. D. Fiber optic hydrogen sulfide gas sensors utilizing ZnO thin film/ZnO nanoparticles: A comparison of surface plasmon resonance and lossy mode resonance. *Sensors Actuators B Chem.* **2015**, *218*, 196–204, doi:10.1016/j.snb.2015.04.108.

2. Usha, S. P.; Mishra, S. K.; Gupta, B. D. Zinc oxide thin film/nanorods based lossy mode resonance hydrogen sulphide gas sensor. *Mater. Res. Express* **2015**, *2*, 095003, doi:10.1088/2053-1591.

3. Kamiya, T.; Nomura, K.; Hosono, H. Present status of amorphous In–Ga–Zn–O thin-film transistors. *Sci. Technol. Adv. Mater.* **2010**, *11*, 044305, doi:10.1088/1468-6996/11/4/044305.

4. Tohsophon, T.; Dabirian, A.; De Wolf, S.; Morales-Masis, M.; Ballif, C. Environmental stability of high-mobility indium-oxide based transparent electrodes. *APL Mater.* **2015**, *3*, 116105, doi:10.1063/1.4935125.

5. Kwon, J. H.; Park, J.; Lee, M. K.; Park, J. W.; Jeon, Y.; Shin, J. Bin; Nam, M.; Kim, C.-K.; Choi, Y.-K.; Choi, K. C. Low-Temperature Fabrication of Robust, Transparent, and Flexible Thin-Film Transistors with a Nanolaminated Insulator. *ACS Appl. Mater. Interfaces* **2018**, *10*, 15829–15840, doi:10.1021/acsami.8b01438.

6. Knobelspies, S.; Bierer, B.; Daus, A.; Takabayashi, A.; Salvatore, G. A.; Cantarella, G.; Ortiz Perez, A.; Wöllenstein, J.; Palzer, S.; Tröster, G. Photo-Induced Room-Temperature Gas Sensing with a-IGZO Based Thin-Film Transistors Fabricated on Flexible Plastic Foil. *Sensors (Basel).* **2018**, *18*, doi:10.3390/s18020358.

7. Chen, K. L.; Jiang, G. J.; Chang, K. W.; Chen, J. H.; Wu, C. H. Gas sensing properties of indium-gallium-zinc-oxide gas sensors in different light intensity. *Anal. Chem. Res.* **2015**, *4*, 8–12, doi:10.1016/j.ancr.2015.03.001.

8. Wu, C.-H.; Jiang, G.-J.; Chang, K.-W.; Deng, Z.-Y.; Li, Y.-N.; Chen, K.-L.; Jeng, C.-C. Analysis of the Sensing Properties of a Highly Stable and Reproducible Ozone Gas Sensor Based on Amorphous In-Ga-Zn-O Thin Film. *Sensors* **2018**, *18*, 163, doi:10.3390/s18010163.

9. Jeong, H.; Kong, C. S.; Chang, S. W.; Park, K. S.; Lee, S. G.; Ha, Y. M.; Jang, J. Temperature Sensor Made of Amorphous Indium-Gallium-Zinc Oxide TFTs. *IEEE Electron Device Lett.* **2013**, *34*, 1569–1571, doi:10.1109/LED.2013.2286824.

10. Du, X.; Li, Y.; Motley, J. R.; Stickle, W. F.; Herman, G. S. Glucose Sensing Using Functionalized Amorphous In-Ga-Zn-O Field-Effect Transistors. *ACS Appl. Mater. Interfaces* **2016**, *8*, 7631.

11. Del Villar, I.; Hernaez, M.; Zamarreño, C. R.; Sánchez, P.; Fernández-Valdivielso, C.; Arregui, F. J.; Matias, I. R. Design rules for lossy mode resonance based sensors. *Appl. Opt.* **2012**, *51*, 4298, doi:10.1364/AO.51.004298.

12. Tien, C.-L.; Lin, H.-Y.; Su, S.-H. High Sensitivity Refractive Index Sensor by D-Shaped Fibers and Titanium Dioxide Nanofilm. *Adv. Condens. Matter Phys.* **2018**, *2018*, 1–6, doi:10.1155/2018/2303740.

13. Zubiate, P.; Zamarreño, C. R.; Villar, I. Del; Matias, I. R.; Arregui, F. J. J.; Del Villar, I.; Matias, I. R.; Arregui, F. J. J. High sensitive refractometers based on lossy mode resonances (LMRs) supported by ITO coated D-shaped optical fibers. *Opt. Express* **2015**, *23*.

Chapter 6

Copper Oxide coatings for LMR-based refractometers development

Copper(II) oxide presents a high refractive index, potentially capable to support very sensitive LMRs. This chapter explains the utilization of copper oxide thin-films for the fabrication of LMR-based sensors on CRMOF and D-shaped fiber configurations. Copper oxide has demonstrated to be a material with a great potential for the manufacturing of LMR-based optical fiber sensors.

6.1. Introduction

Previous chapters have been focused on the optimization of thin-films of materials already studied for LMR-based sensors fabrication (tin oxide), or the introduction of new alloy materials based on oxides that had previously proved to be successful (zinc oxide and indium oxide) which could widen the sensing application possibilities (AZO and IGZO). This chapter will also discuss the research of a new material for LMR-based sensors development, but in this case, its optical properties will be significantly different from the previous cases.

The material chosen for this purpose is copper(II) oxide (CuO), which presents a refractive index (n) considerably higher than the rest of the materials studied previously [1]. This parameter is important because it directly enhances the sensitivity of the LMRs. A higher refractive index causes the LMR to have a higher SRI sensitivity, and this is a key element to optimize the performance of this kind of refractometers [2].

Copper oxide is present in two forms: cupric oxide (CuO) and cuprous oxide (Cu_2O), and both are considered p-type semiconductor materials, being CuO the more stable phase. They have been extensively studied for the use on thin film transistors (TFTs) in microelectronics [1,3]. Copper oxide has also been considered for biomedical applications [4] and in the development of sensors [5].

This chapter will explain the study of copper oxide thin films for the development of LMR-based sensors. This material presents a very high refractive index, above 2.2 in the visible light and near infra-red spectrum (NIR), which indicates that it could generate LMRs with an extremely high sensitivity. This characteristic is one of the greatest motivations for the use of copper oxide, but such an extreme sensitivity also introduces some difficulties, as it will be discussed in this research.

6.2. Experimental considerations

Copper oxide thin-films are fabricated on silicon wafers and optical fibers by means of pulsed sputtering deposition. This process is carried out at a partial Ar pressure of $2 \cdot 10^{-3}$ mbar and a current of 100 mA, using a CuO target from Beijing Loyaltarget Technology Co. The thin-film thickness and complex refractive index was calculated by spectroscopic ellipsometry (Horiba UVISEL 2).

The characterization setup for the CRMOF consisted of a halogen light source, the copper oxide coated optical fiber segment, and a spectrometer that will analyze the spectrum on either the VIS (USB2000-XR1) or NIR (NIR512) range (fig. 6.1).

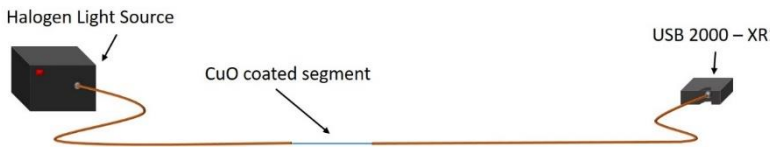

Figure 6.1: *Diagram of the setup used for the fabrication and characterization of the sensor in the CRMOF configuration. It shows a USB2000-XR1 refractometer as an example.*

For the D-shaped setup, a 1 dB D-shaped fiber was chosen (1 dB of absorption induced by the polishing measured at 1330 nm having a SRI of 1.5). The light sources will be either a set of two lasers (BCP 400 A) connected to the D-shaped segment by a WDM for the fabrication probes (fig. 6.2a), or a broadband light source based on superluminescent emitting diodes (SLED, HP 83437 A) connected to a linear polarizer and a manual polarization controller for the characterization setup (fig. 6.2b). The spectrum is received by a couple of optical power meters (RIFOCS 575 L), measuring the corresponding power at the wavelength of each laser after the signals have been separated by another WDM, or an optical spectrum analyzer (OSA, HP 86142 A), respectively. The schematics of the fabrication and characterization setups are shown on fig. 6.2a and fig. 6.2b, respectively.

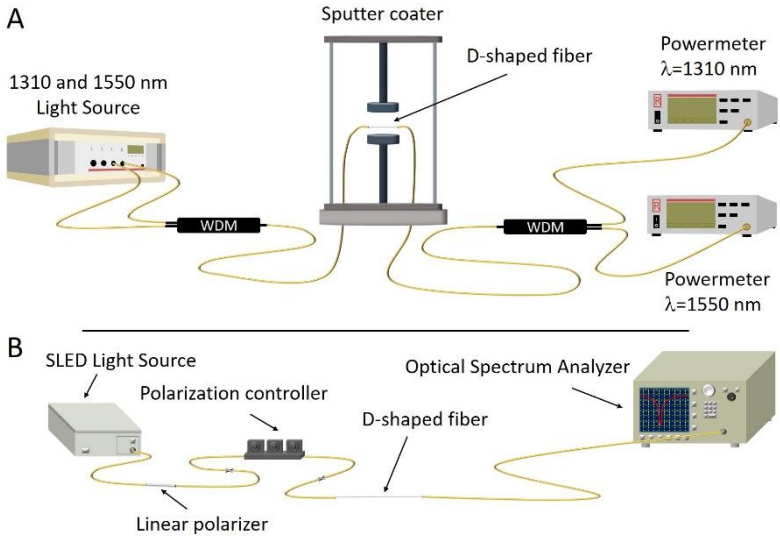

Figure 6.2: *Setups used for the fabrication (A) and characterization (B) of the sensor based on the D-shaped configuration.*

6.3. Results

6.3.1. Copper Oxide thin-film characterization

The spectroscopic ellipsometry measurements performed on CuO coated silicon wafers allowed to calculate an average deposition rate for the fabrication process used in this study, as well as the complex refractive index of the coating. Fig. 6.3 shows the thickness values obtained for several samples with different deposition times. From this data, an average deposition rate of 0.678 nm/s can be estimated.

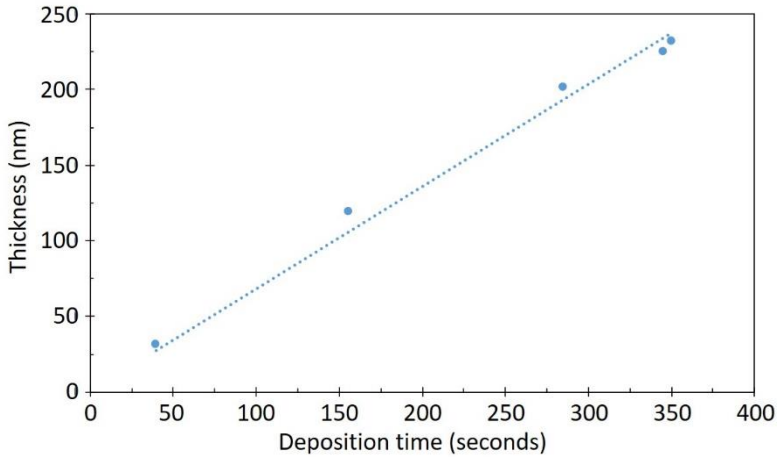

Figure 6.3: *Thickness values measured by spectroscopic ellipsometry for several copper oxide coating samples fabricated with different deposition times. An average deposition rate of 0.678 nm/s is calculated.*

After deposition, the samples were kept in an environmental chamber at 25ºC and 50% of relative humidity for at least 14 hours, in order to stabilize the coatings. The spectroscopic ellipsometry measurements were carried out before and after this step, in order to analyze the refractive index as deposited and after stabilization. Fig. 6.4 shows the complex refractive index measured in both cases. A significant increase in the real part (n) can be observed (from 2.07 to 2.19 at a wavelength of 1550 nm) while the extinction coefficient is lower. Both effects are beneficial for the sensitivity of the LMR [2].

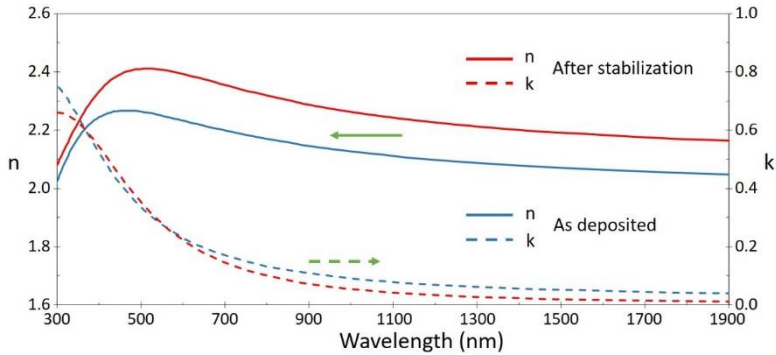

Figure 6.4: *Complex refractive index measured by spectroscopic ellipsometry as deposited and after a 14 hours stabilization process.*

6.3.2. CRMOF setup

The spectrum transmitted through the CRMOF was initially recorded to observe the generation of LMRs for different copper oxide film thicknesses. Such information is represented on fig. 6.5. In this case, due to the high absorption induced by the fiber pigtails in this sputtering chamber, the spectrum could only be monitored on a single spectrometer on the wavelength range between 450 and 950 nm. It can be appreciated how in a 6 minutes long deposition process a first LMR appears in the shortest wavelength and shifts out of the working range, as a second LMR starts to show on the shortest range of the spectrum again. From this figure some common characteristics already seen with other coating materials can be noticed. First of all, the separation between the first and the second LMR progressively increases during the fabrication process, which indicates the higher sensitivity of the first LMR in comparison with the second one. The width of the first LMR (and its progressive widening during the fabrication) also seems to indicate the presence of two components, corresponding to the two propagation modes (TE and TM), although their peaks cannot be distinguished in this setup. The mentioned increase in the spectral width of the resonance is a consequence of the different sensitivities presented by its components. One of the components presents a greater

sensitivity and shows a greater shift, separating from the other component as the film thickens.

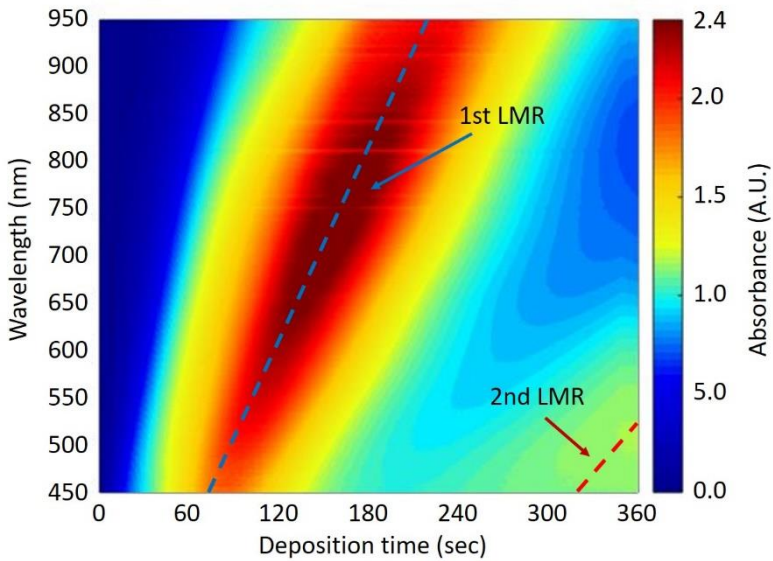

Figure 6.5: *Transmittance spectrum of the CRMOF during the copper oxide fabrication process. The vertical axis represents the wavelength and the horizontal axis shows the time since the beginning of the deposition. The color indicates the transmittance at a given wavelength at any instant.*

Another important information provided by this experiment, is the effect of the stabilization time after deposition on the LMRs. The increase in the film refractive index observed after this process induces a great shift in the LMRs, of approximately 100 nm for a 2nd order LMR in the 500-700 nm wavelength range, which is considerably larger than the one observed with other materials. Fig. 6.6 shows an example of this phenomenon, where it can be seen a LMR shift from 620 to 712 nm after the stabilization.

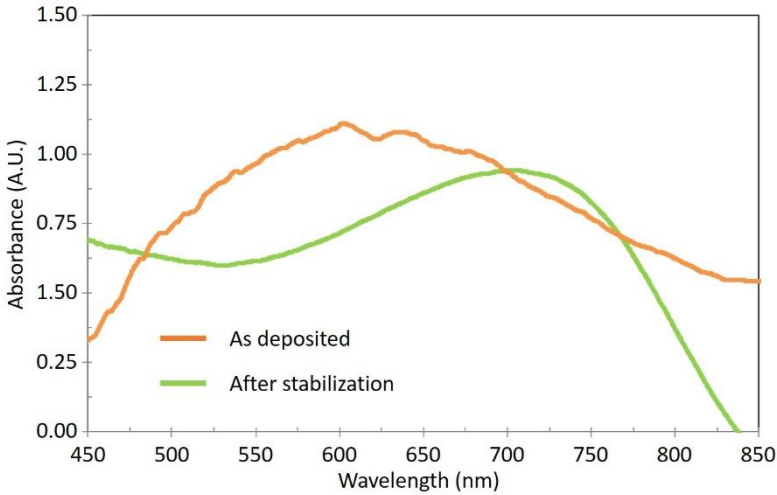

***Figure 6.6**: Example of the variation suffered in the transmission spectra after a 10 hours stabilization process (25ºC, 4 % HR). The LMR peak shifts from 620 to 712 nm.*

The first order LMR in this setup is comparatively broad (with a FWHM above 150 nm) considering the LMRs shown on the previous chapters but, in contrast, the distortion due to the separation of modes seen in the CRMOF setup with the other materials does not occur with copper oxide. This implies that, despite the difficulty in tuning due to the great stabilization shift it undergoes, it was possible to utilize the first order LMR for the development of refractometers. Two different probes were fabricated using copper oxide thin-films. A first probe where the first order LMR is visible at a wavelength around 600 nm, and a second one with a thicker film where the LMR is at a wavelength around 1200 nm (in both cases after the stabilization process). These probes present a copper oxide coating with thicknesses of 27 and 176 nm, respectively. Here, it is expected that the LMR tuned at a higher wavelength achieves a higher sensitivity. Fig. 6.7 shows the spectra obtained in both cases when the probes were tested in solutions of different refractive indices.

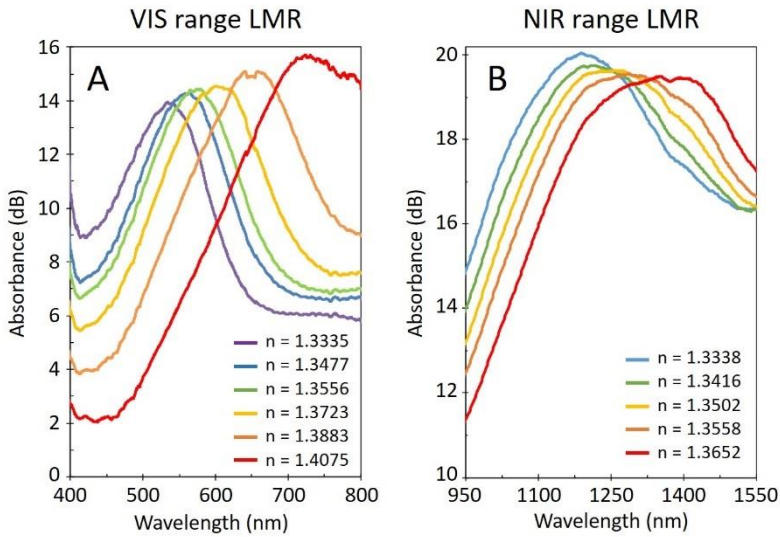

Figure 6.7: *Transmission spectra measured for different SRI values in the probe working on the VIS range (A) and the probe working on the NIR range (B).*

Fig. 6.7a shows the spectra of the probe working in the VIS range, while fig. 6.7b shows the spectra of the probe tuned in the NIR range. The absorption peak shifts to longer wavelengths as the SRI increases in both cases. In the case of the probe working in the VIS range, the LMR is narrower (initial FWHM of 113 nm) than in the probe working in the NIR range (with an initial FWHM of 420 nm). This effect was already observed in the fabrication process (fig. 6.5), and it is probably due to the separation of the polarization components of the LMR. It should also be noted that the probe working in the NIR range is limited to a lower SRI range, as the higher sensitivity of this LMR causes it to shift out of the working spectral range for higher SRI values. The calibration curves of these probes show an average sensitivity of 2,630 nm/RIU (fig. 6.8a) and 5,032 nm/RIU (fig. 6.8b) for the VIS and NIR probes respectively. It is interesting to note that the LMR in the NIR range almost doubles the sensitivity of that in the VIS range, confirming once again the relationship between sensitivity and central wavelength location of the LMR. In terms of maximum sensitivity, it was achieved in both

cases for the highest SRI values, with 3,994 and 7,234 nm/RIU, respectively. It must be noted that, as it is characteristic of the LMRs that their sensitivity increases for higher SRI values, had been possible to study the NIR probe in a SRI range as high as in the VIS probe case, the maximum sensitivity would probably have been greater.

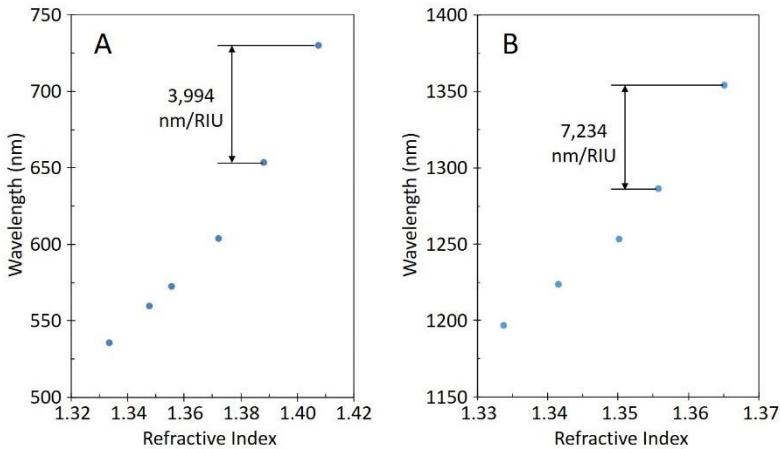

Figure 6.8: *Calibration curves of the probes working on the VIS (A) and NIR (B) range. The LMR on the NIR range presents a higher sensitivity.*

The values of sensitivity reported here in this CRMOF setup are considerably higher than the ones described in chapters 4 and 5 for the probes using AZO and IGZO thin-films. The performance of copper oxide is comparable to tin oxide, which demonstrated an average sensitivity of 4,127 nm/RIU at a wavelength of 890 nm in the 1.33-1.38 SRI range [6].

6.3.3. D-shaped configuration

The high sensitivity obtained in the CRMOF setup indicates the great potential of copper oxide thin-films for the development of LMR-based refractometers. This justifies the need to experiment with a D-shaped setup, in order to maximize the sensitivity that this material could provide. For that purpose, D-shaped fibers were coated with copper oxide thin-films. During the fabrication process,

light at 1310 and 1550 nm from two laser sources was transmitted through the D-shaped fiber and the optical power measured at given wavelengths was monitored.

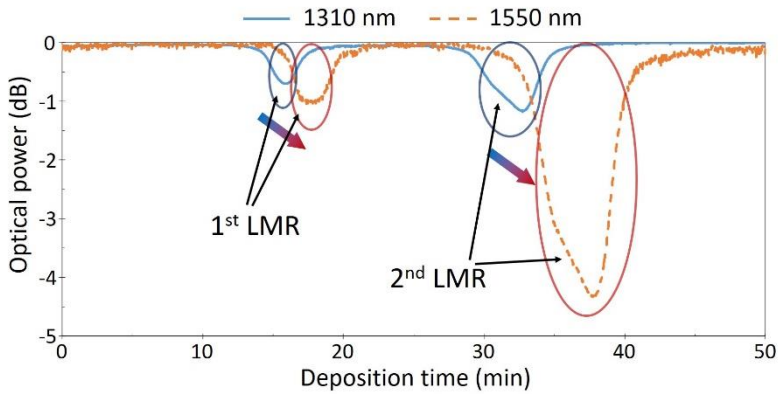

Figure 6.9: *Optical power transmitted through the D-shaped fiber at the wavelengths of 1310 and 1550 nm during the copper oxide thin-film fabrication process.*

Fig. 6.9 represents the optical power measured at 1310 and 1550 nm during a 50 minutes copper oxide deposition process. Note that this deposition was performed under the same conditions as the rest of the experiments described in this chapter but after performing a modification on the sputtering chamber, that might have reduced the deposition rate on this experiment. Two LMRs can be separately observed. A first LMR is observed first at 1310 nm after 15 minutes of deposition approximately and next it is observed at 1550 nm. After 30 minutes, a second LMR is observed in the same way, in this case with a greater amplitude particularly at 1550 nm. It is interesting that, although the first LMR is observed as a simple small dip in the transmitted power, the shape observed for the second LMR indicate the presence of the two components corresponding to the TE and TM modes. This is seen in the fact that (for the second LMR), the power decreases fast at first, then the slope changes abruptly and decreases at a slower rate until it reaches the minimum, when it begins to rise again. The same behavior is seen both at 1310 and 1550 nm for the second LMR at a

different moment during the deposition, which indicates that it was due to the overlap of two absorption peaks and not an effect of a change in the deposition rate. Another indicator of the presence of the two components in each LMR is the widening observed in the resonances when they are seen at 1550 nm compared to 1310 nm. As each component present slightly different sensitivity (to both SRI and film thickness), one of the components presents a greater shift and, as a result, the LMRs widen as the thickness increases.

The study of this fabrication process on the D-shaped fiber is of great importance for the tuning of the LMR at the desired range. However, two challenging conditions must be considered for this purpose. Firstly, the fabrication of the coating takes place with a SRI of 1, and the SRI range of characterization is above 1.33. Due to the expected high sensitivity of this LMR, the wavelength shift observed because of such SRI increase (from 1 to 1.33) is significant enough to exceed the spectral window of study. In other words, for a SRI value of 1.33, the LMR must be observed in the spectral window of study (1150-1650 nm), ideally in the lower part to maximize the range of characterization. We can denote such wavelength as $\lambda_{1.33}$. This means that for a SRI of 1 (air), which is the condition during the fabrication process, the LMR would be observed at a shorter wavelength $\lambda_1 = \lambda_{1.33} - 0.33 \cdot S_{1\text{-}1.33}$, being $S_{1\text{-}1.33}$ the sensitivity of the LMR in the 1-1.33 SRI range. Furthermore, the above-mentioned stabilization process that must be carried out for this material increases its refractive index, which shifts the LMR to a longer wavelength. These phenomena imply that the fabrication process should be designed in a way that it allows to tune the resonance at a given wavelength right at the end of the process, λ_0, considering that it will later shift to a longer wavelength after it stabilizes due to the increase on the film refractive index ($\lambda_1 = \lambda_0 + \Delta\lambda_{stabilization}$), and then it must also shift to the spectral window of study when the SRI increases from 1 to 1.33 ($\lambda_{1.33} = \lambda_1 + 0.33 \cdot S_{1\text{-}1.33} = \lambda_0 + \Delta\lambda_{stabilization} + 0.33 \cdot S_{1\text{-}1.33}$). In preliminary works with other materials, the transmission power at a wavelength of 850 nm was measured during the film fabrication process in order to effectively tune the

LMR in a SRI range close to 1.33. In the case of copper oxide, as a greater shift is expected, it was determined that measuring the optical power at a wavelength of 750 nm could be a good approach for that purpose.

The high sensitivity of the first LMR, however, can be a disadvantage for the correct tuning in the desired spectral range. As mentioned above, once a fiber has been coated and a LMR has been tuned at a given wavelength λ_0, the stabilization process can induce a shift greater than expected and, as a result, the final location of the LMR in air, λ_1, may be at a longer wavelength than it was initially intended. Then the wavelength shift caused by the increase of SRI from 1 to the range of interest starting at 1.33 may cause the LMR to end up located in a wavelength too long to be practical for a refractometer. Fig. 6.10 shows the spectra obtained with a D-shaped fiber coated with a copper oxide thin-film of 105 nm. This probe shows a LMR at a wavelength of 1,200 nm for a SRI of 1.3793. If we look at the spectrum obtained in air, we can see how a previous resonance is located at the top limit of the spectral range for SRI of 1. It is an example of the difficulties of tuning such sensitive resonances. In the case presented here, this means that the LMR tuned for this probe is not the most sensitive one. Due to the separation of the resonances, the LMR observed in air probably corresponds to one of the modes of a first order LMR (presumably the TM mode), while the one observed for SRI values above 1.3793 corresponds to a second order LMR, which presents a lower sensitivity.

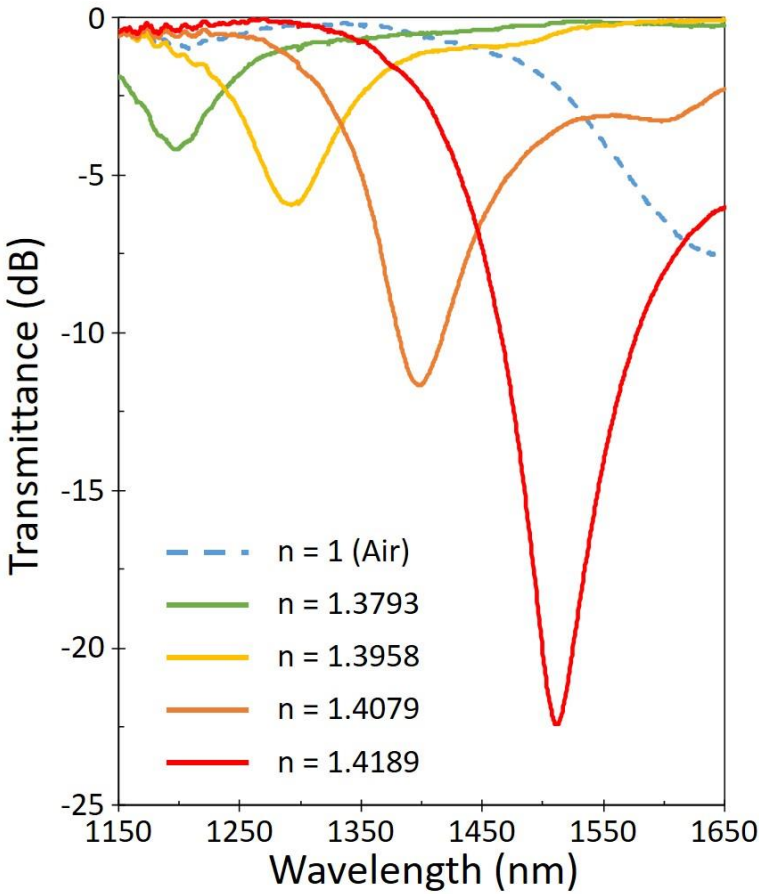

Figure 6.10: *Transmittance spectra measured on the copper oxide coated D-shaped probe for different SRI values,*

Nevertheless, this device could be characterized as a refractometer (fig. 6.11) and showed an average sensitivity of 7,932 nm/RIU. Again, as it is typical in LMR-based refractometers, the sensitivity is greater for higher SRI ranges, and in this case the maximum sensitivity achieved was 10,336 nm/RIU. The minimum FWHM for this LMR is 30 nm, which implies a FOM (figure of merit calculated as the ratio sensitivity/FWHM) is 344.5 RIU^{-1}.

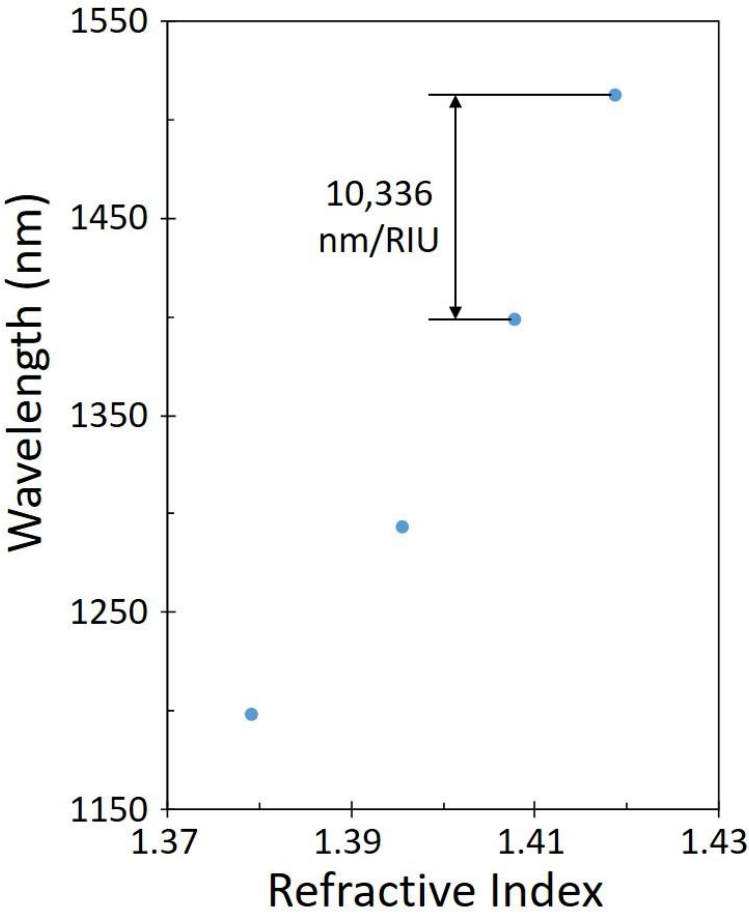

Figure 6.11: *Calibration curve of the copper oxide D-shaped probe. It achieves a maximum sensitivity of 10,336 nm/RIU.*

The performance of this sensor is good compared to that provided by devices fabricated with different coating materials. In comparison with the resonances obtained using IGZO coatings in the previous chapter, for instance, the sensitivity achieved here with copper oxide is better than the one demonstrated by the two LMRs analyzed in the 1 dB D-shaped fiber configuration described in the previous chapter, and is only surpassed by the LMR_{TM} of the 4 dB D-shaped fiber probe fabricated with IGZO. However, it must

be noted the fact that the LMR described in this chapter is not the most sensitive one. As it was seen on fig. 6.10, there is a LMR observed for lower SRI values (in air) while the one characterized as refractometer for the 1.3793-1.4189 range is a different one, probably corresponding to first and second order LMR, respectively. This implies that, if it were possible to tune properly the first LMR that is observed in air, such LMR would provide a more sensitive response. It should be noted though, that the proper tuning of the first LMR is quite challenging. The fact that this first LMR possesses such high sensitivity implies that if we want to observe for SRI values above 1.33, it cannot be observed during the coating fabrication process at a wavelength within the transmission spectrum of the fiber. The requirement of very thin films also needs a very controlled fabrication process, that ensures very homogeneous coatings. For the time being, the equipment and methods used in this study did not allow to observe a LMR of lower order fabricating copper oxide thin-films. Further optimization of the coating fabrication process is expected to allow the achievement of unprecedented sensitivities. The improvement in sensitivity caused by the use of the first LMR instead of the second one depends on the particular optical properties of the coating material. It was theoretically studied [2] that the sensitivity of the 1st order LMR compared to the 2nd order LMR is greater by a factor that depends on parameters such as the coating thickness, its refractive index, or the SRI range. Considering that behavior, we can compare the performance of copper oxide with the results obtained with other coatings. In the mentioned theoretical work, the first order LMR demonstrated a sensibility to SRI more than 3 times higher than the second order LMR. More recently, an experimental work showed that in an indium oxide coating based refractometer, the first order LMR provided a sensitivity between 5 and 7 times higher than the second order LMR [7]. If those results were extrapolated to our case, the first LMR based on copper oxide thin-films could achieve a sensitivity between 23,000 and 55,000 nm/RIU, which would exceed the performance demonstrated previously with other materials in the SRI range tested in this study.

6.4. Conclusions

The research presented here shows the possibility to fabricate high refractive index thin-films using copper oxide, and the first time this material is used for the generation of LMRs. The LMRs supported by copper oxide thin-films present a high sensitivity due to the high refractive index of this material. A CRMOF permitted to observe LMRs in the VIS-NIR range (between 450 and 1600 nm). This setup allowed to characterize as refractometer the first order LMR in two separate probes working in the VIS and the NIR range. The LMR tuned in the longer wavelength range demonstrated a greater sensitivity, as is typical in these resonances. In this probe, an average sensitivity of 5,032 nm/RIU with a maximum of 7,234 nm/RIU was achieved. Such results are comparable to the ones described previously using tin oxide, which as shown on chapter 3 is capable of provide extremely high performance.

Copper oxide thin-films were also tested on D-shaped fibers with the aim to observe the LMR corresponding to the TE and TM propagation modes and achieve a better performance in terms of sensitivity and FWHM. This configuration allowed to observe the SRI dependence of a second order LMR, which achieved a sensitivity of 10,336 nm/RIU. This sensor also achieved a FOM of 344.5 RIU^{-1}. These values show a good performance, but are not better than those provided by other materials such as tin oxide, which demonstrated an average sensitivity of 14,501 nm/RIU in a SRI range close to the water with a lower refractive index. However, the higher refractive index of copper oxide compared to other materials suggests that it should support LMRs at least as sensitive as the others, or even more sensitive. This difference is due to the fact that in the case of copper oxide the device is based on a second order LMR. The comparison between the sensitivity to SRI of the first and second order LMR studied with other materials suggests that the first LMR supported by copper oxide will provide an unprecedented sensitivity, multiplying the results shown here by a factor of 3-7 if the pattern seen in other materials is confirmed, but the

experimental procedures utilized in this research did not permit to observe such resonance. Future work should be focused on improving the fabrication setup so that the first order LMR can be effectively tuned within the range of study.

This chapter concludes the experimental study of different coating materials for the generation of LMRs. It is now necessary to understand the differences in the performance achieved with each, and the results presented previously using other materials. The following chapter will describe such analysis, adding context to the figures introduced in this thesis.

Bibliography

1. Drobny, V. F.; Pulfrey, L. Properties of reactively-sputtered copper oxide thin films. *Thin Solid Films* **1979**, *61*, 89–98, doi:10.1016/0040-6090(79)90504-2.

2. Del Villar, I.; Hernaez, M.; Zamarreño, C. R.; Sánchez, P.; Fernández-Valdivielso, C.; Arregui, F. J.; Matias, I. R. Design rules for lossy mode resonance based sensors. *Appl. Opt.* **2012**, *51*, 4298, doi:10.1364/AO.51.004298.

3. Nair, M. T. S.; Guerrero, L.; Arenas, O. L.; Nair, P. K. Chemically deposited copper oxide thin films: structural, optical and electrical characteristics. *Appl. Surf. Sci.* **1999**, *150*, 143–151, doi:10.1016/S0169-4332(99)00239-1.

4. Norambuena, G.; Patel, R.; Karau, M.; Wyles, C.; Jannetto, P.; Bennet, K.; Hanssen, A.; Sierra, R. Antibacterial and Biocompatible Titanium-Copper Oxide Coating May Be a Potential Strategy to Reduce Periprosthetic Infection: An In Vitro Study. *Clin. Orthop. Relat. Res.* **2017**, *475*, 722–732, doi:10.1007/s11999-016-4713-7.

5. Yamazoe, N.; Sakai, G.; Shimanoe, K. Oxide semiconductor gas sensors. *Catal. Surv. from Asia* **2003**, *7*, 63–75, doi:10.1023/A:1023436725457.

6. Sánchez, P.; Zamarreño, C. R.; Hernaez, M.; Del Villar, I.; Matias, I. R.; Arregui, F. J. SnO2 based optical fiber refractometers. In *OFS2012 22nd International Conference on Optical Fiber Sensors*; Liao, Y., Jin, W., Sampson, D. D., Yamauchi, R., Chung, Y., Nakamura, K., Rao, Y., Eds.; SPIE, 2012; Vol. 8421, pp. 84216B-84216B–4.

7. Fuentes, O.; Del Villar, I.; Corres, J. M.; Matias, I. R. Lossy mode resonance sensors based on lateral light incidence in nanocoated planar waveguides. *Sci. Rep.* **2019**, *9*, 8882, doi:10.1038/s41598-019-45285-x.

Chapter 7

Performance comparison of the studied materials

Previous chapters discussed the experimental use of several coating materials to develop LMR-based sensors. This chapter compares the performance achieved using tin oxide, AZO, IGZO and copper oxide thin-films. The impact of the coating material on the behavior of the LMR is also studied.

7.1. Introduction

In the previous chapters, 4 different coating materials were studied with the purpose of developing LMR-based sensors: the optimization of tin oxide thin-film in order to achieve the maximum possible sensitivity on a D-shaped fiber configuration, and the study of three new materials (AZO, IGZO and copper oxide) to demonstrate their capacity to support LMRs. Although each material is interesting on their own to develop particular sensing applications, it is also of high interest to compare their performance.

This chapter analyzes and compares the results obtained with each material, first in a CRMOF setup, and later in the D-shaped fiber configuration. AZO, IGZO and copper oxide were tested on CRMOF setups demonstrating their capacity to support LMRs, which allowed to fabricate refractometers based on them. IGZO and copper oxide (as well as tin oxide) were also used on D-shaped setups, in order to maximize the sensitivity. The comparison of their performance allows to understand the relevance and impact of the material in the design of a LMR-based refractometer.

7.2. CRMOF setup

The characterization of AZO, IGZO and copper oxide was first performed using a CRMOF setup. This setup offers the possibility to develop LMR-based refractometers at low cost with easily available materials. Its main drawback is the impossibility to separate TE and TM propagation modes, which would facilitate the observation of the LMR components separately, but that limitation can be overcome by using D-shaped fibers as it will be described in the next section.

One of the key parameters that could be compared in a CRMOF refractometer is the sensitivity. Some factors should be taken into consideration before comparing these values. First of all, the fact that the sensitivity of the LMR-based refractometers is not a

constant and they present a higher sensitivity value when the SRI increases. Another important aspect is the dependence of the sensitivity on the central wavelength of the LMR. Previous works reported the linear relationship between sensitivity and central wavelength [1]. This implies that two LMRs tuned at different wavelengths should not be compared directly.

Having those circumstances into consideration, it is interesting to analyze and compare the different average sensitivity values obtained in this research. Fig. 7.1 summarizes the performance of the refractometers reported in the previous chapters. It represents the average sensitivity obtained with each coating material as a function of the central wavelength for the lowest SRI (water). It is important to study the sensitivity in aqueous solutions because these are the media most often found in biomedical applications, which is the field where higher applicability and impact can have these LMR-based refractometers. For that purpose, the values presented in the previous chapters have been recalculated to show the average sensitivity in a limited SRI range between 1.33 and 1.36 and such figures have been plotted in the graph. Such consideration is necessary because the increase of the sensitivity for higher SRI values also implies a raise in the average sensitivity for a broader SRI range, and the comparison of sensitivity values calculated on very different SRI ranges would not be relevant.

It is important to observe that, in the case of AZO and IGZO, the superposition of modes resulted in a wider and distorted resonance that did not allow to characterize properly the LMRs of first order as refractometer. In consequence, for such materials only the second order LMRs could be studied and the plot represents their performance. In contrast, in the case of copper oxide, the plot shows the performance of a first order LMR, as in this case the resonance showed a clearer peak that allowed the unequivocal identification of its central wavelength. It can be seen that the lowest values were obtained with the AZO thin-films on the visible light range, with an average sensitivity (on a SRI range limited to

1.33-1.36) of 393 nm/RIU. Such figure rose to 742 nm/RIU when the LMR was tuned at a longer wavelength. It is interesting to compare the performance of AZO with that of IGZO. The IGZO device reported in this work presented a sensitivity of 544 nm/RIU, which is lower than the highest average sensitivity obtained with AZO. However, it should be noted that in that case, the AZO based LMR with a higher sensitivity is tuned on a longer wavelength. Provided the sensitivity keeps an almost linear tendency [1], we could extrapolate the curve presented in the graph and the IGZO based sensor would be located at a slightly higher position. That would confirm the capacity of IGZO to generate more sensitive LMRs, which can be explained by its higher refractive index in comparison to AZO. It is interesting to note that the previously observed phenomena that increasing the central wavelength of the LMR also increases its SRI sensitivity, but is not possible to stablish a concrete relationship as it is highly dependent on the optical properties of the material.

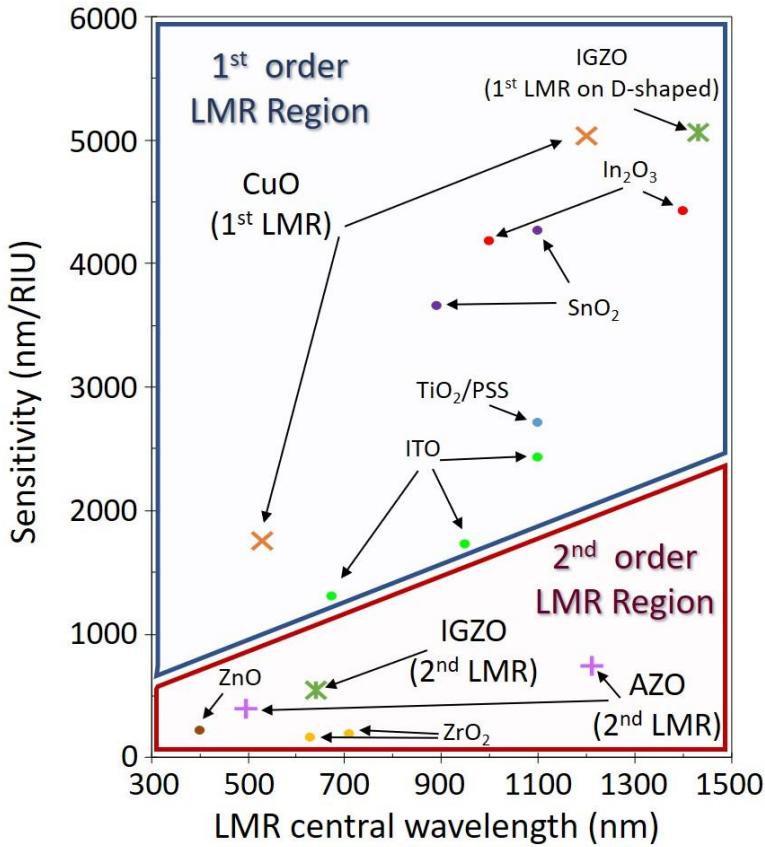

Figure 7.1: *Comparison of the average sensitivity achieved using different coating materials on a CRMOF setup in function of the central wavelength of the LMR for SRI = 1.333. The performance of the devices presented in this thesis is compared with the sensitivities reported in the literature for the sensors designed with ZnO* [2]*, ZrO_2* [3]*, TiO_2/PSS* [4]*, In_2O_3* [5,6]*, ITO* [7–9] *and SnO_2* [10,11] *coatings on CRMOF configurations. These values have been calculated with the available data in a limited SRI range of 1.33-1.36 approx.*

The graph also represents the sensitivity values obtained with copper oxide thin-films. It is easy to see that the values reported here for copper oxide differ greatly from the tendency observed in AZO and IGZO coatings. In this case the sensitivity is higher in both VIS (1,755 nm/RIU) and NIR (5,032 nm/RIU) wavelength ranges. This difference can be explained by the lower order of the LMRs in the

case of copper oxide, and the different nature of the CuO thin-film, which presents a refractive index considerably higher than AZO and IGZO (that maintain optical properties close to those of zinc oxide).

To add context to the values presented here, fig. 7.1 also represents the sensitivities achieved using zinc oxide [2], zirconium oxide [3], titanium dioxide/PSS [4], ITO [7–9], indium oxide [5,6] and tin oxide [10,11] coatings. These sensitivity values were also recalculated for a limited SRI range for a fair comparison. Note that in the values obtained from the literature the order of the LMR is not explicitly specified. However, two regions can be differentiated in the plot. One that includes the LMR that reported greater sensitivities (CuO, ITO, SnO_2, TiO_2/PSS and In_2O_3), which probably corresponds to resonances of first order. The second region includes the devices that reported considerably lower sensitivities, which are IGZO, AZO, ZnO and ZrO_2. One possibility to explain this difference in their performance compared with the one demonstrated by the materials described above could be that these resonances were LMRs of second (or higher) order, as it occurs with AZO and IGZO. It is interesting that the second order LMRs observed with AZO and IGZO coatings achieved a better performance than that shown by zinc oxide (220 nm/RIU), zirconium oxide (195 nm/RIU) and the silicon nitride film (289.5 nm/RIU).

The devices developed using TiO_2/PSS (2,709 nm/RIU), ITO (2,425 nm/RIU), SnO_2 (4,265 nm/RIU) and In_2O_3 (4,427 nm/RIU) coatings demonstrated a better sensitivity, closer to the one achieved with copper oxide. This difference could be due to the order of the LMR. As mentioned above, it could be assumed that in the case of TiO_2/PSS, ITO, SnO_2 and In_2O_3 the devices were based on first order LMR (as is the case of CuO), in contrast to the AZO and IGZO probes, which rely on second order LMRs.

Comparing the performance of copper oxide with the devices based on other materials described previously in the literature, it can be seen that it is comparatively better in the wavelength ranges where it has been studied, with a sensitivity of 1,755 nm/RIU in the VIS

range and 5,032 nm/RIU in the NIR range. It must be noted that this last device shows the highest sensitivity reported for a LMR-based refractometer in a CRMOF setup for the mentioned SRI range.

It is interesting to compare such figures with the sensitivity achieved using tin oxide thin-films of 4,265 nm/RIU at a wavelength close to 1,100 nm. As it was seen on chapter 2, this material showed an exceptional sensitivity on a D-shaped setup. Although this LMR is not exactly at the same wavelength as the one observed using copper oxide (1,200 nm), we can still make a rough comparison observing the tendencies demonstrated with each material. Considering the sensitivities reported by the copper oxide based refractometers at VIS and NIR range, it is expected that its performance would be similar or even higher than those of tin oxide at intermediate wavelengths as those where the tin oxide based LMRs are observed.

Due to the impossibility to make a straightforward comparison between LMRs of the same order between copper oxide and the rest of the materials studied in the CRMOF setup, for reference purposes, fig. 7.1 also represents the sensitivity achieved by a LMR of first order using IGZO coatings on a D-shaped setup (on the same SRI range). Note that the D-shaped setup also improves the performance of the LMR by the separation of modes but still this LMR achieved a sensitivity of 5,062 nm/RIU at a wavelength of 1,430 nm, which is almost the same sensitivity achieved using CuO thin-films on the CRMOF setup at a shorter wavelength (5,032 nm/RIU at 1,200 nm). Observing the tendency of the CuO-based sensors, a LMR observed at a longer wavelength would clearly surpass the performance seen on the first order LMR based on IGZO coatings.

This analysis indicates that the materials that showed the greatest sensitivity in this CRMOF setup correspond to those with higher refractive index, which are copper oxide, followed by tin dioxide, and indium oxide. The difference in the central wavelength of the LMR in each case make it difficult to make a direct comparison, but a slower increase is seen in the case of indium oxide for wavelengths

above 1,000 nm, probably due to its refractive index curve, which is not observed for the rest of the materials. In general terms, it can be concluded that the use of a coating material with a high refractive index and the tuning of the LMR at a longer wavelength will cause the LMR to be more sensitive to SRI variations.

7.3. D-shaped setup

The use of a D-shaped setup allows to separate the propagation modes and fully observe the LMRs corresponding to the TE and TM modes. This permits to observe LMRs of higher sensitivity, improving the performance of the sensors. This thesis has presented the experimental use of D-shaped setups using three coating materials: tin oxide, IGZO and copper oxide.

In order to better illustrate the impact of the D-shaped configuration in contrast to the CRMOF setup, fig. 7.2 shows in the same plot different spectra obtained using both setups. Fig. 7.2a shows the spectra of CRMOF and D-shaped devices based on IGZO coatings. It is clear that the D-shaped fiber causes the observation of narrower resonances, which improves the FWHM parameter of the device. It was already discussed in chapter 5 that using a 1 dB D-shaped optical fiber a FWHM of 44.8 nm could be achieved (shown on fig. 7.2a), and the use of a 4 dB fiber could decrease it up to 11.1 nm. The same behavior is observed in the devices fabricated using copper oxide (fig. 7.2b). The LMRs seen on the CRMOF setup are wider than the resonances observed on the D-shaped fiber, which reach a FWHM of 30 nm. Particularly, it is interesting to observe that the LMRs seen on the NIR region on the CRMOF setup are typically wider than at shorter wavelengths. Such effect is caused by the progressive separation of the LMR components in the CRMOF, but it is considerably compensated on the D-shaped fiber due to the isolation of modes. The observation of narrower LMRs on the D-shaped configuration indicates that this setup can optimize the performance of the LMR-based sensors. A lower FWHM will lead to a higher figure of merit (FOM, defined as sensitivity/FWHM).

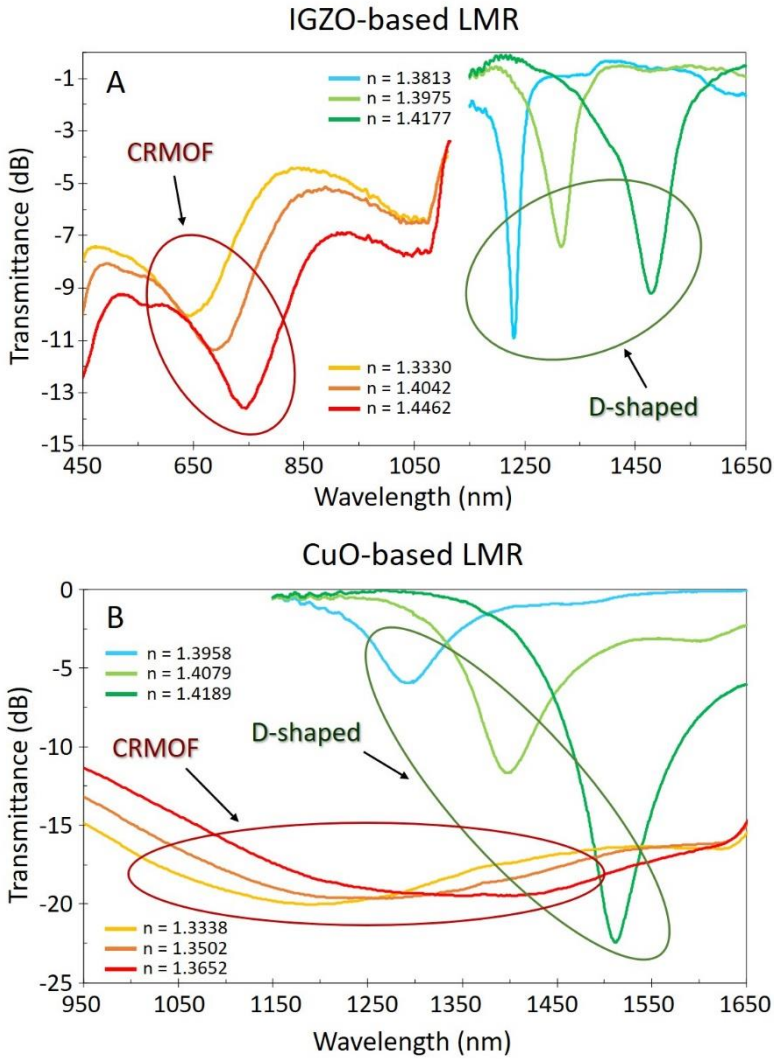

Figure 7.2: *Comparison of the spectra obtained on a CRMOF and a D-shaped setup based on (A) IGZO and (B) copper oxide thin-films.*

Considering the potential of D-shaped fibers to optimize the LMR-based refractometers, it is described in chapter 2 the use of tin oxide thin-films on a D-shaped fiber to fabricate a refractometer working on the refractive index range close to the fused silica (1.44-1.45), where it is expected that the sensitivity of the LMR-based devices

increases greatly. A sensor with an average sensitivity of 829,636 nm/RIU, with a maximum peak of 1,087,889 nm/RIU, is presented. It represents an exceptionally high sensitivity, obtained in a very limited SRI range (due to the high sensitivity and limited spectral window). Such device possesses the highest sensitivity presented in this thesis, which is also the greatest sensitivity reported in literature for LMR-based refractometers. Table 7.1 describes the performance of ITO and SnO_2 coatings on the described high SRI range. It can be seen that the sensor using tin oxide demonstrated a sensitivity 6 times greater than the probe based on ITO.

Material	Wavelength range (nm)	SRI range	Sensitivity (nm/RIU)	FOM (RIU^{-1})	Ref.
ITO	1280-1505	1.4474-1.449	136,276	N/A	[12]
SnO_2	1200-1600	1.4481-1.4486	829,636	22,483.36	Chapter 3

Table 7.1: *Comparison of the SRI sensitivities achieved by LMR-based refractometers working on a high SRI range fabricated with ITO and tin oxide coatings.*

Nevertheless, it must be noted that LMR-based sensors have been considered for biomedical applications and in such field the sensors work in a lower SRI range, close to the one of water (1.33). For that purpose, other coating materials, IGZO and copper oxide, have been tested in lower SRI ranges. As it has been discussed above, copper oxide presents a higher refractive index and such property suggests that it could support comparatively more sensitive LMRs. However, in contrast to the rest of the D-shaped probes, it was not possible to tune the first order LMR in the working wavelength range and only a LMR of second order could be characterized as refractometer. Such resonance presented an average sensitivity of 7,932 nm/RIU in a 1.3793-1.4189 SRI range, with a maximum value of 10,336 nm/RIU. These figures are not better than the ones obtained with other coating materials, but it is due to the higher order of the LMR in the case of copper oxide. It was also explained in the previous chapter that the sensitivity of the first order LMR could multiply the performance of the second one by a factor between 3 and 7 [1,13].

If such behavior is maintained on the copper oxide based probes, it is expected that the sensitivity of a first order LMR would achieve a sensitivity above 23,000 nm/RIU (table 7.2).

Material	LMR Order	Wavelength range (nm)	SRI range	Sensitivity (nm/RIU)	Ref.
CuO	2nd	1200-1500	1.3793-1.4189	7,932	Chapter 6
CuO	1st	1200-1500	1.3793-1.4189	23,000*	Chapter 6
*Theoretical					

Table 7.2: *Experimental performance of a second order LMR observed using copper oxide thin-films and the projected sensitivity expected for a LMR of first order.*

The analysis described in the previous section demonstrated that copper oxide presented a great potential to exceed the performance demonstrated with other materials, such as IGZO. It was seen on chapter 5 that IGZO coated D-shaped fibers supported LMRs, which achieved a sensitivity of 12,929 nm/RIU in a SRI range of 1.3950-1.4233. Although such performance is superior than the one experimentally obtained with copper oxide, it must be noted the higher order of the LMR tuned using copper oxide and the details explained in the previous paragraph. It seems reasonable that a LMR of first order generated using copper oxide thin-films would outstand in sensitivity, in accordance with the results demonstrated on a CRMOF setup. A conservative value of 23,000 nm/RIU could be estimated for such LMR, which would be higher than the sensitivity achieved using IGZO and ITO (8,742 nm/RIU [14]) in similar SRI ranges (see table 7.3).

The theoretical sensitivity calculated for the first order LMR of copper oxide is higher than the one demonstrated with tin oxide seen on table 7.3. However, it should be noted that they refer to separate SRI ranges and cannot be compared directly. It must also be observed that the theoretical value is an estimation and it could actually be considerably larger. For instance, an experimental work using indium oxide coatings [13] showed a 7 times greater sensitivity for a first order LMR in comparison with the second one,

which would imply a sensitivity above 55,000 nm/RIU in the case of copper oxide.

Material	Wavelength range (nm)	SRI range	Sensitivity (nm/RIU)	FOM (RIU^{-1})	Ref.
CuO (2nd LMR)	1200-1500	1.3793-1.4189	7,932	264.4	Chapter 6
ITO	1350-1650	1.365-1.38	8,742	620	[14]
IGZO	1170-1550	1.3950-1.4233	12,929	1,164.77	Chapter 5
SnO_2	1380-1480	1.321-1.326	14,501	N/A	[12]
CuO* (1st LMR)	1200-1500	1.3793-1.4189	23,000*	N/A	Chapter 6

*Theoretical 1st order LMR

Table 7.3: *Comparison of the SRI sensitivity showed by the LMRs observed using different coating materials in a D-shaped fiber configuration setup.*

7.4. Conclusions

As it has been discussed, the performance of the LMR-based sensors is highly dependent on the coating material. AZO and IGZO thin-films lead to a similar performance, with a slightly better sensitivity in the case of IGZO. The use of copper oxide coatings on a CRMOF setup achieved a better sensitivity, 4.4 and 6.7 times higher than AZO in the VIS and NIR ranges, respectively, and 3.2 times better than IGZO (on the VIS range). That performance is explained by the greater refractive index of copper oxide in comparison to the zinc oxide based coatings, as well as the lower order of the LMR. Considering the experimental works found in the literature using other materials, the best performance is achieved by copper oxide, closely followed by tin oxide and indium oxide.

In the case of the D-shaped fiber setup, the best performance was achieved with tin oxide on a high SRI range. The optimization of the fabrication process allowed to tune a LMR working in a SRI range close to the one of fused silica (1.44). An average sensitivity of 829,636 nm/RIU with a maximum peak of 1,087,889 nm/RIU was

observed in a wavelength range of 1200-1600 nm. Such value would allow to determine a refractive index variation of $9.19 \cdot 10^{-10}$ units using a OSA with a standard resolution of 1 picometer.

IGZO and copper oxide coatings demonstrated similar sensitivities, lower than the one achieved with tin oxide, despite being copper oxide the material with the highest refractive index. Here, it should be noted that in the case of copper oxide the analyzed LMR was a second order resonance, not a first order LMR like in the rest of the cases. Given the performance achieved on the CRMOF setup and considering the optical properties of copper oxide, it seems clear that copper oxide presents a great potential in the development of LMR-based sensors. It is expected that a LMR of first order based on copper oxide would achieve a considerably higher sensitivity, similar to that demonstrated using tin oxide.

The analysis performed here permits to conclude that the sensitivity of a LMR-based refractometer will greatly benefit from the choice of a thin-film with a high refractive index, the tuning of the resonance at a longer wavelength, and the observation of a LMR of lowest possible order. Therefore, copper oxide, tin oxide, indium oxide and ITO are excellent candidates for the fabrication of highly sensitive LMR-based sensors, due to their high refractive index.

It must also be considered that, apart to the response to SRI variations, there are other factors that are of high importance for evaluating the use of a given coating material. One of such parameters is the economic cost of the material for the fabrication of the probes. For instance, AZO, which led to a sensitivity slightly lower than IGZO, has a cost considerably lower, which may facilitate the research and development of sensors where a high sensitivity is not a key parameter.

Another factor to consider is the potential application of the LMR-based sensor. This thesis has focused on the refractometric response of the probes, but it must not be forgotten that this technique is the basis for the development of a number of sensing

applications. It was already mentioned, for example, that LMR-based sensors relying on zinc oxide coatings had been developed for the detection of several gases. Such feature suggests that AZO and IGZO thin films could be a good choice for the fabrication of such kind of sensors. On the other hand, tin oxide has been used several times for the fabrication of biosensors, where a high sensitivity is essential. Copper oxide, considering its antibacterial properties and its medical use on implants, can be a good candidate for biosensing applications. The great performance it demonstrated on the CRMOF setup and the fact that it presents a higher refractive index than tin oxide indicates that it may improve the performance achieved by the LMR-based sensors using tin oxide thin-films.

Bibliography

1. Del Villar, I.; Hernaez, M.; Zamarreño, C. R.; Sánchez, P.; Fernández-Valdivielso, C.; Arregui, F. J.; Matias, I. R. Design rules for lossy mode resonance based sensors. *Appl. Opt.* **2012**, *51*, 4298, doi:10.1364/AO.51.004298.

2. Paliwal, N.; Punjabi, N.; John, J.; Mukherji, S. Design and Fabrication of Lossy Mode Resonance Based U-Shaped Fiber Optic Refractometer Utilizing Dual Sensing Phenomenon. *J. Light. Technol.* **2016**, *34*, 4187–4194, doi:10.1109/JLT.2016.2585922.

3. Kosiel, K.; Koba, M.; Masiewicz, M.; Śmietana, M. Tailoring properties of lossy-mode resonance optical fiber sensors with atomic layer deposition technique. *Opt. Laser Technol.* **2018**, *102*, 213–221, doi:10.1016/j.optlastec.2018.01.002.

4. Hernáez, M.; Del Villar, I.; Zamarreño, C. R.; Arregui, F. J.; Matias, I. R. Optical fiber refractometers based on lossy mode resonances supported by TiO_2 coatings. *Appl. Opt.* **2010**, *49*, 3980, doi:10.1364/AO.49.003980.

5. Zamarreno, C. R.; Sanchez, P.; Hernaez, M.; Del Villar, I.; Fernandez-Valdivielso, C.; Matias, I. R.; Arregui, F. J. Sensing Properties of Indium Oxide Coated Optical Fiber Devices Based on Lossy Mode Resonances. *IEEE Sens. J.* **2012**, *12*, 151–155, doi:10.1109/JSEN.2011.2142181.

6. Sanchez, P.; Gonzalez, K.; Zamarreño, C. R.; Hernaez, M.; Matias, I. R.; Arregui, F. J. High-sensitive lossy mode resonance-based optical fiber refractometers by means of sputtered indium oxide thin-films. In *Smart Sensors, Actuators, and MEMS VII; and Cyber Physical Systems*; Sánchez-Rojas, J. L., Brama, R., Eds.; SPIE, 2015; Vol. 9517, p. 95171V.

7. Zamarreo, C. R.; Hernaez, M.; Del Villar, I.; Matias, I. R.; Arregui, F. J. ITO Coated Optical Fiber Refractometers Based on Resonances in the Infrared Region. *IEEE Sens. J.* **2010**, *10*, 365–366, doi:10.1109/JSEN.2009.2034628.

8. Lopez, S.; del Villar, I.; Ruiz Zamarreño, C.; Hernaez, M.; Arregui, F. J.; Matias, I. R. Optical fiber refractometers based on indium tin oxide coatings fabricated by sputtering. *Opt. Lett.* **2012**, *37*, 28, doi:10.1364/ol.37.000028.

9. Zamarreño, C. R.; Lopez, S.; Hernaez, M.; Del Villar, I.; Matias, I. R.; Arregui, F. J. Resonance-based refractometric response of cladding-removed optical fibers with sputtered indium tin oxide coatings. *Sensors Actuators, B Chem.* **2012**, *175*, 106–110, doi:10.1016/j.snb.2011.12.082.

10. Sánchez, P.; Zamarreño, C. R.; Hernaez, M.; Del Villar, I.; Matias, I. R.; Arregui, F. J. SnO2 based optical fiber refractometers. In *OFS2012 22nd International Conference on Optical Fiber Sensors*; Liao, Y., Jin, W., Sampson, D. D., Yamauchi, R., Chung, Y., Nakamura, K., Rao, Y., Eds.; SPIE, 2012; Vol. 8421, pp. 84216B-84216B–4.

11. Sanchez, P.; Zamarreño, C. R.; Hernaez, M.; Matias, I. R.; Arregui, F. J. Optical fiber refractometers based on Lossy Mode Resonances by means of SnO2 sputtered coatings. *Sensors Actuators B Chem.* **2014**, *202*, 154–159, doi:10.1016/j.snb.2014.05.065.

12. Arregui, F. J.; Del Villar, I.; Zamarreño, C. R.; Zubiate, P.; Matias, I. R. Giant sensitivity of optical fiber sensors by means of lossy mode resonance. *Sensors Actuators B Chem.* **2016**, *232*, 660–665, doi:10.1016/j.snb.2016.04.015.

13. Fuentes, O.; Del Villar, I.; Corres, J. M.; Matias, I. R. Lossy mode resonance sensors based on lateral light incidence in nanocoated planar waveguides. *Sci. Rep.* **2019**, *9*, 8882, doi:10.1038/s41598-019-45285-x.

14. Zubiate, P.; Zamarreño, C. R.; Villar, I. Del; Matias, I. R.; Arregui, F. J. J.; Del Villar, I.; Matias, I. R.; Arregui, F. J. J. High sensitive refractometers based on lossy mode resonances (LMRs) supported by ITO coated D-shaped optical fibers. *Opt. Express* **2015**, *23*.

Chapter 8

Conclusions and future work

8.1. Conclusions

The **Chapter 2** of this thesis presented a comprehensive review of sensors based on LMR. Such research was partially published as a review paper (*"A Comprehensive Review: Materials for the Fabrication of Optical Fiber Refractometers Based on Lossy Mode Resonance"* in Sensors vol. 20 (7), 1972 (2020)). This state of the art showed that a number of materials had been theoretically and experimentally studied with diverse results. It was seen that the thin-film optical properties directly affect the performance of the sensor and may provide the capacity to develop a wider range of sensing applications. The relevance of the thin-film and the broad range of materials potentially capable to support LMRs suggest the need to study coating materials of different nature to widen the possibilities of this technique.

Chapter 3 discusses the experimental work performed using a coating material that had previously proven a great potential for the development of highly sensitive refractometers: tin oxide. The optimization of the fabrication process allowed to design a sensor working in the refractive index range close to the fused silica (1.44-1.45) with unprecedented sensitivity. The use of polarized light on a tin oxide coated D-Shaped fiber permitted to observe the TE and TM propagation modes and their corresponding LMRs separately. This way, a maximum sensitivity of 1,087,889 nm/RIU with a FOM of 29,805.18 RIU^{-1} was achieved. These figures would allow to

determine a refractive index variation with a resolution of $9.19 \cdot 10^{-10}$. Such figures represent the best performance reported for a LMR based refractometer and the results presented here were published in the paper *"Is there a frontier in sensitivity with Lossy mode resonance (LMR) based refractometers?"* in Scientific Reports 7, 10280 (2017).

New materials for the design of LMR-based sensors are introduced in the following chapters. Particularly, **Chapter 4** details the development of aluminum-doped zinc oxide (AZO) coatings on a CRMOF setup. This configuration permitted to analyze several LMRs and characterize their response to SRI variations. A second order LMR tuned in a wavelength range of 1300-1340 nm achieved a maximum sensitivity of 2,280 nm/RIU in the SRI range of 1.4345-1.4471. A thinner AZO coating allowed to tune the LMR on the visible light range, which permitted to determine the SRI by observing the color of the light transmitted through the device. These results were presented in the paper *"Aluminum doped zinc oxide (AZO) coated optical fiber LMR refractometers—An experimental demonstration"* in Sensors and Actuators B: Chemical vol. 281, 698-704 (2019).

Next chapter, **Chapter 5**, described the study of IGZO (indium-gallium-zinc oxide) with the purpose of developing LMR-based sensors. These thin-films showed a refractive index higher than that of previous materials, which indicated the potential capacity to support higher sensitive LMRs. IGZO thin-films permitted to achieve a maximum sensitivity of 1,666 nm/RIU in a SRI range of 1.4346-1.4462 using a CRMOF setup on a LMR observed between 720 and 740 nm. IGZO coatings were also used on D-Shaped fibers with a different polishing degree to analyze the effect of such parameter on the performance of the sensors. It was determined that the polishing degree does not affect significantly on the sensitivity to SRI, but it does have an indirect impact on the figure of merit (FOM) as the amplitude and shape of the resonances and, therefore, the FWHM varies with a deeper polishing. Using a fiber with a deeper

polishing a sensitivity of 12,929 nm/RIU was achieved, with a FOM of 396.20 RIU^{-1}. Such probe worked on a SRI range of 1.3950-1.4233 with a LMR observed in a wavelength range between 1170 and 1550 nm. A fiber with a lower polishing degree may provide a lower FOM with a similar sensitivity, which could be a better choice depending on the setup, as the LMRs obtained this way present a smoother shape that may facilitate the determination of the central resonance wavelength. The results of this research were published on the article *"Lossy mode resonance optical sensors based on indium-gallium-zinc oxide thin film"* in Sensors and Actuators A: Physical vol. 290, 20-27 (2019).

The last material analyzed in this research was copper oxide in **Chapter 6**. The preliminary work performed with this material was presented in a poster presentation at the Eurosensors 2018 conference (*"Development of copper oxide thin film for lossy mode resonance-based optical fiber sensor"* in Proceedings 2(13), 893 (2018)). Copper oxide presents a refractive index comparatively higher than the rest of the materials considered previously. That is an important feature as the refractive index of the coating material is directly related to the sensitivity of the LMR. The use of copper oxide thin-films on a CRMOF setup allowed to fabricate a refractometer with a sensitivity of 7,234 nm/RIU for a SRI range of 1.3558-1.3652, based on a LMR observed in the 1280-1360 nm range. The work presented in this thesis allowed to tune a second order LMR in a wavelength range of 1200-1500 nm using a copper oxide coated D-shaped fiber. Such probe achieved an average sensitivity of 7,932 nm/RIU in a SRI range of 1.3793-1.4189. Such figures suggest that, as seen on the work performed with different materials, an adequate tuning of the first LMR by means of the optimization of the film fabrication process would allow to improve the sensitivity achieved in this work. Particularly, an improvement of the sensitivity by a factor between 3 and 7 is suggested, which would yield a sensitivity of 23,000-55,000 nm/RIU.

Finally, **Chapter 7** compares the results presented previously with each coating material and analyzes their performance. The study of the different coating materials presented in this work revealed the impact that the material chosen for the thin-film fabrication has on the performance of the LMR-based sensors. It concluded that a coating material with a high refractive index permits to achieve highly sensitive LMRs. The sensitivity of the resonances will also increase if the LMR is observed at a longer wavelength, if it works in a higher SRI range and if the LMRs are of lower order. The availability of a variety of materials for the design of sensors permits to obtain more appropriate parameters for a target application. It also represents a demonstration of the versatility of the LMR-based technique and may facilitate a broader study of this phenomenon.

8.2. Future work

The study presented in this thesis suggests the continuation of the research in various fields. In the first place, the optimization of the copper oxide thin-film fabrication process should be carried out so that the first order LMR can be tuned in a D-shape configuration and its performance maximized.

Another research line is the study of the combination of two or more layers with different optical properties and the impact such structure has on the behavior of the LMR. Some studies indicate that the combination of different deposition techniques for the fabrication of the coatings could facilitate the tuning of the LMR at the desired wavelength at the time that the combination of the coatings improves the sensitivity.

Finally, although this thesis is focused on the study of LMR supporting coatings, it is also of high of interest for the optimization of LMR-based sensors the study of the combination of LMR with novel optical fiber structures. For instance, tilted fiber Bragg gratings (TFBG) allow to couple to the optical fiber cladding certain modes propagating at selected wavelengths. Such property

combined with the fabrication of LMR supporting coatings on the TFBG may lead to the development of very interesting devices.

Appendix I

Scientific Contributions

I.1 Publications on scientific journals directly related to this thesis

[1] *Is there a frontier in sensitivity with Lossy mode resonance (LMR) based refractometers?* A. Ozcariz, C. R. Zamarreño, P. Zubiate, F. J. Arregui. Scientific Reports 2017, 7, 10280, doi:10.1038/s41598-017-11145-9.

[2] *Aluminum doped zinc oxide (AZO) coated optical fiber LMR refractometers—An experimental demonstration.* A. Ozcariz, D. A. Piña-Azamar, C. R. Zamarreño, R. Dominguez, F. J. Arregui. Sensors and Actuators B: Chemical 2019, 281, 698–704, doi:10.1016/j.snb.2018.10.158.

[3] *Lossy mode resonance optical sensors based on indium-gallium-zinc oxide thin film*. A. Ozcariz, M. Dominik, M. Smietana, C. R. Zamarreño, I. Del Villar, F. J. Arregui. Sensors and Actuators A: Physical 2019, 290, 20–27, doi:10.1016/j.sna.2019.03.010.

[4] *A Comprehensive Review: Materials for the Fabrication of Optical Fiber Refractometers Based on Lossy Mode Resonance*. A. Ozcariz, C. R. Zamarreño, F. J. Arregui. Sensors 2020, 20, 1972, doi:10.3390/s20071972.

I.2 Other publication on scientific journals

[5] *Generation of lossy mode resonances with different nanocoatings deposited on coverslips.* O. Fuentes, J. Goicoechea, J. M. Corres, I. Del Villar, A. Ozcariz, I. R. Matias. Optics Express 2020, 28, 288, doi:10.1364/OE.28.000288.

[6] *Micro and Nanostructured Materials for the Development of Optical Fibre Sensors*. C. Elosua, F. J. Arregui, I. Del Villar, C. R. Zamarreño, J. M. Corres, C. Bariain, J. Goicoechea, M. Hernaez, P. J. Rivero, A. B. Socorro, A. Urrutia, P. Sanchez, P. Zubiate, D. Lopez-Torres, N. De Acha, J. Ascorbe, A. Ozcariz, I. R. Matias. Sensors 2017, 17, 2312, doi:10.3390/s17102312.

[7] *Electric discharge detection and localization using a distributed optical fiber vibration sensor*. I. B. V. da Costa, G. H. Weber, D. F. Gomes, J. R. Galvão, M. J. da Silva, D. R. Pipa, A. Ozcáriz, C. R. Zamarreño, C. Martelli, J. C. Cardozo da Silva. Optical Fiber Technology 2020, 58, 102266, doi:10.1016/j.yofte.2020.102266.

I.3 Oral communications on international conferences directly related to this thesis

[8] *Experimental use of IGZO thin film for optical fibre sensors*. A. Ozcariz, M. Dominik, M. Smietana, C. Ruiz Zamarreño, I. Del Villar; F. J. Arregui. XIV Conference on optical chemical sensors and biosensors EUROPT(R)ODE 2018, March 25-28, Naples, Italy.

I.4 Other oral communications on international conferences

[9] *Micro and Nano structured Coatings for the Development of Optical Fibre Sensors*. C. Elosua, F. J. Arregui, I. Del Villar, C. R. Zamarreño, J. M. Corres, C. Bariain, J. Goicoechea, M. Hernaez, P. J. Rivero, A. B. Socorro, A. Urrutia, P. Sanchez, P. Zubiate, D. Lopez, N.

De Acha, J. Ascorbe, A. Ozcariz, I. R. Matias. 6th International Conference on Materials and Applications for Sensors and Transducers, September 27-30, 2016, Athens, Greece.

I.5 Poster contributions on international conferences directly related to this thesis

[10] *Development of copper oxide thin film for lossy mode resonance-based optical fiber sensor*. A. Ozcariz, I. Martinez, C. R. Zamarreño, F. J. Arregui. XXXII Eurosensors 2018, September 9-12, 2018, Graz, Austria.

I.6 Other poster contributions on international conferences

[11] *Considerations for the development of LMR-based optical fiber sensors for gas sensing applications*. U. J. Dreyer, A. Ozcariz, P. Zubiate, C. Martelli, J. C. C. da Silva, C. R. Zamarreño. Advanced Photonics: OSA Optics & Photonics Congress, July 2-5, 2018, Zurich, Switzerland.

[12] *Gas Detection Using LMR-based Optical Fiber Sensors*. U. J. Dreyer, A. Ozcariz, J. Ascorbe, P. Zubiate, I. Vitoria, C. Martelli, J. C. C, da silva, C. R. Zamarreño. XXXII Eurosensors 2018, September 9-12, 2018, Graz, Austria.

[13] *DNA optical fiber biosensor based on Lossy Mode Resonances (LMRs)*. P. Zubiate, C. R. Zamarreño, A. Ozcariz, I. del Villar, A. Urrutia, M. A. Ramos-Arroyo, M. Moreno-Igoa, B. Hernández-Charro, I. R. Matias, F. J. Arregui. XIV Conference on optical chemical sensors and biosensors EUROPT(R)ODE 2018, March 25-28, Naples, Italy.

Glossary

α-Fe@Sn CS: α-Fe_2O_3 nanoparticles and SnO_2 Core-Shell nanostructure

ALD: Atomic Layer Deposition

AZO: Aluminum-Doped Zinc Oxide

CuO: Cupric Oxide

CRMOF: Cladding-Removed Multimode Optical Fiber

CuO: Cupric Oxide

CVD: Chemical Vapor Deposition

EDX: Energy-Dispersive X-ray Spectroscopy

FOM: Figure Of Merit

FWHM: Full Width at Half Maximum

GNR: Gold Nanorods

GO: Graphene Oxide

IGZO: Indium-Gallium-Zinc Oxide

In_2O_3: Indium Oxide

ITO: Indium Tin Oxide

LbL: Layer-by-Layer

LMR: Lossy Mode Resonance

LMR_{TE}: Lossy Mode Resonance on the TE mode

LMR_{TM}: Lossy Mode Resonance on the TM mode

LOD: Limit Of Detection

LSPR: Localized Surface Plasmon Resonance

MCM: Multimode-Coreless-Multimode

MIP: Molecularly Imprinted Polymer

MMF: Multimode Fiber

NPs: Nanoparticles

NRs: Nanorods

OSA: Optical Spectrum Analyzer

PAA: Polyacrylic Acid

PAH: Polyallylamine Hydrochloride

PECVD: Plasma-Enhanced Chemical Vapor Deposition

PEI: Poly(ethyleneimine)

PMMA: Poly(methyl methacrylate)

PSS: Poly(sodium 4-styrenesulfonate)

PVD: Physical Vapor Deposition

RH: Relative Humidity

RI: Refractive Index

RIU: Refractive Index Unit

SEM: Scanning Electron Microscope

SLED: Super Luminescent Emitting Diode

SMF: Single Mode Fiber

SnO_2: Tin Oxide

SPR: Surface Plasmon Resonance

SRI: Surrounding Refractive Index

TCO: Transparent Conductive Oxide

TE: Transverse Electric

TiO_2: Titanium Dioxide

TM: Transverse Magnetic

WDM: Wavelength Division Multiplexer